



MONASH University

***Structural and Functional Analysis of
Chemokine Receptor CCR2 and its
Cognate Chemokines***

Zil E Huma
B.Sc., M.Sc., M.Phil.

Submitted in total fulfilment of the requirements of the degree of
Doctor of Philosophy

*Department of Biochemistry and Molecular Biology
Faculty of Medicine, Nursing and Health Sciences
Monash University*

Copyright notice

© Zil E Huma (2017).

I certify that I have made all reasonable efforts to secure copyright permissions for third-party content included in this thesis and have not knowingly added copyright content to my work without the owner's permission.

Table of Contents

Abstract	VII
Declaration	IX
Publications during enrolment	X
Thesis including published works declaration	XI
Acknowledgements	XIII
List of general abbreviations	XV
Chapter 1. Introduction	1
1.1. Inflammation and Leukocyte Trafficking	2
1.2. Chemokines	3
1.2.1. Classification	5
1.2.2. Chemokine Tertiary Structure	6
1.2.3. Quaternary Structure	8
1.3. Chemokine Receptors	10
1.3.1. GPCR Structure and Signalling	10
1.3.2. Chemokine Receptors as Drug Targets	14
1.4. The Chemokine Network	15
1.4.1. Chemokine-Receptor Interaction	15
1.4.2. Two-step, Two-site Model of Receptor Interactions	15
1.5. CCR2 and its Ligands	19
1.5.1. CCR2	19
1.5.2. Monocyte Chemoattractant Protein -1 and MCP-3	20
1.5.3. Disease Relevance of CCR2/MCPs	21
1.6. Modulation of Signalling Pathways	22
1.6.1. Partial Agonism	22
1.6.2. Biased Agonism	23
1.7. Tyrosine Sulfation	25
1.8. Hypotheses, Project Aims and Thesis Outline	29
1.8.1. Hypotheses	29
1.8.2. Project Aims	29
1.8.3. Thesis Outline	31
Chapter 2. Materials and Methods	33
2.1. Materials	34
2.2. Buffers, Media and Solutions	34
2.3. Bacterial Strains	35
2.4. Plasmids	36
2.5. DNA Analyses	37

2.5.1. Preparation of Competent Cells	37
2.5.2. Bacterial Transformation	37
2.5.3. Plasmid DNA Preparation.....	37
2.5.4. Synthesis of Gene Constructs by PCR.....	38
2.5.5. Site-directed Mutagenesis	38
2.5.6. Agarose Gel Electrophoresis.....	40
2.5.7. DNA Sequencing	40
2.6. Production and Purification of Recombinant Proteins in a Bacterial Expression System.....	40
2.7. Protein Analysis	42
2.7.1. SDS-PAGE Gel Electrophoresis.....	42
2.7.2. Silver Staining.....	42
2.8. Nuclear Magnetic Resonance (NMR).....	42
2.9. Homology Modelling of CCR2:Chemokine Complexes.....	42
2.10. Design and Selection of the Receptor Mutants.....	43
2.11. Construction and Expression of CCR2 Mutants.....	43
2.12. Mammalian Cell Line and Culture	43
2.13. Generation of Stable Cell lines	44
2.14. Cell Based Assays.....	44
2.14.1. Cell Surface Receptor Expression: Whole Cell (Enzyme-Linked Immunosorbent Assay (ELISA).....	44
2.14.2. Membrane Preparation and Radioligand Binding Assays	45
2.14.3. β -Arrestin 2 Recruitment Using a BRET-Based Assay.....	46
2.14.4. Inhibition of Forskolin-induced cAMP	46
2.14.5. ERK 1/2 Phosphorylation Assay	47
2.15. Data Analysis and Statistics.....	47
Chapter 3. NMR Characterisation of Cooperativity: Fast Ligand Binding Coupled to Slow Protein Dimerisation.....	51
3.1. Preface to Chapter 3.....	52
Chapter 4. Characterisation of Critical Regions of MCP-1 and MCP-3 that Direct Partial Agonism	59
4.1. Introduction.....	60
4.2. Selection of Signalling Readouts.....	62
4.3. MCP Chemokines have Different Efficacies and Affinities at CCR2.....	65
4.4. Design of Chimeric Chemokines	72
4.5.2. Protein Production and Purification.....	74
4.5.3. 1D NMR Comparison of Chimeric Chemokines to Parent Chemokines	78
4.6. Assessment of Receptor Binding and Activation	78
4.6.1. Radioligand Binding.....	78
4.6.2. β -arrestin 2 Recruitment by Chemokine Chimeras.....	82
4.6.3. Induction of ERK 1/2 Phosphorylation by Chemokine Chimeras.....	82
4.6.4. Receptor Internalisation.....	83
4.7. Discussion.....	83
4.7.1. Interpretation of Data within the 2-Site Model.....	86

Table of Contents

4.7.2. The Chemokine N-terminal Tail is a Major Determinant of Affinity and Efficacy	87
4.7.3. Background Dependence of Chimeras.....	87
Chapter 5. Identification of Key CCR2 Elements that Interact with the N-terminal Region of Cognate Chemokines	89
5.1. Introduction.....	90
5.2. Design of CCR2 Mutants.....	93
5.3. Determination of Receptor Expression Levels	93
5.4. Effects of CCR2 Mutations on Binding and Activation by Wild type Chemokines	96
5.5. Discussion.....	101
Chapter 6. General Discussion.....	107
6.1. Chemokine:Receptor Interactions.....	108
6.2. Existing 2-Site, 2-Step Model.....	108
6.3. Elaboration of the Existing Model.....	108
6.3.1. Fitting Dimerisation into the Two-Site Model.....	108
6.3.2. The Structural Interactions of the Chemokine:Receptor Pair	112
6.3.3. Extensions of the 2-Step Model for Partial Agonists.....	115
6.4. Future Studies of Differential Agonism.....	117
6.5. Biophysical Studies of Receptor Activation and Dynamics.....	118
6.6. Cellular and Physiological Outcomes of Differential Agonism	119
6.7. Conclusion	119
References.....	121
Appendices.....	143
Appendix I	144
Appendix II	145
Appendix III.....	151
Appendix IV.....	157
Appendix V	161

Abstract

Chemokine receptors are G protein-coupled receptors (GPCRs) that regulate the movement of leukocytes during normal immune surveillance and inflammation. CCR2, a major chemokine receptor on monocytes and macrophages, binds to several CC chemokine ligands and plays key roles in atherosclerosis, obesity and type 2 diabetes. The major ligands of human CCR2 include monocyte chemoattractant protein-1 (MCP-1; systematic name CCL2), MCP-2 (CCL8) and MCP-3 (CCL7).

The interactions of chemokine receptors with their cognate chemokine ligands can be regulated by a wide variety of mechanisms. This thesis describes our investigations of two such mechanisms – the ability of receptors to regulate the equilibrium between active (monomeric) and inactive (dimeric) states of a chemokine and the ability of chemokines to differentially activate a shared receptor.

Most chemokines exist in equilibrium between monomeric and dimeric (or higher order oligomeric) forms. Monomeric MCP-1 can activate CCR2, whereas dimeric MCP-1 cannot. A previous study showed that both monomeric and dimeric MCP-1 can bind to peptides from the N-terminal region of CCR2. However, binding of the dimer to receptor peptides appeared to destabilise the dimer promoting dissociation to the active monomeric state. The first aim of this thesis involved a study of the energetics of this novel mechanism of chemokine regulation, as described in Chapter 3. A theoretical framework was developed for the analysis of 2D NMR spectra to evaluate the cooperativity between a fast process (such as ligand binding) and a slow process (such as dimerisation). This approach is applicable to any system in which NMR spectra show separate resonances for the two slow-exchanging species (e.g. monomer and dimer). NMR data were collected for titration of wild type MCP-1 with N-terminal peptides from CCR2. These data were fit to the theoretical model to simultaneously provide information about the coupled equilibria of chemokine dimerisation and receptor peptide binding.

It has been established that different chemokines instigate different responses at the same receptor. In comparison to MCP-1, MCP-2 and MCP-3 are partial agonists of their shared receptor CCR2. In Chapters 4 and 5, we have extended previous results showing that MCP-1, MCP-2 and MCP-3 have distinct potencies and efficacies of signalling at CCR2 and we have identified structural features of both the chemokines and receptor contributing to these differences.

In Chapter 4, using a series of chemokine chimeras constructed by swapping the three main receptor recognition regions between MCP-1 and MCP-3, we have identified structural elements of MCP chemokines responsible for differences in receptor activation. We found that the chemokine N-

Abstract

terminal region is the primary determinant of the binding and signalling selectivity of these two chemokines at CCR2. The affinities of the chemokine chimeras for CCR2 also confirmed that the N-terminal region makes a significant contribution to receptor binding by these two chemokines.

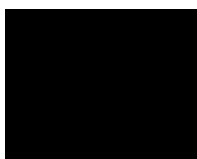
In Chapter 5, using a series of CCR2 mutants, we have identified elements of CCR2 that interact preferentially with the chemokines. The affinity of chemokine binding and the potency of MCP-1 and MCP-3 were determined for each receptor mutant. Four of the mutants, Y120F, R206A, I263A/N266A and Y259F displayed differential effects on the affinity of MCP-1 relative to MCP-3. These mutated residues are clustered together in the transmembrane region of the receptor. This analysis has shown that the chemokine N-terminus interacts with the major subpocket in the transmembrane helices of the CCR2. We conclude that this region of the receptor plays a major role in distinguishing between the two cognate chemokines, apparently by differential interactions with the N-terminal regions of the chemokines.

Overall, our investigation has yielded significant new information on chemokine receptor binding and signalling. We have described a novel approach to interpretation of 2D NMR data for cooperativity between ligand binding and protein dimerisation. Our method yields the cooperativity between dimerisation and ligand binding with substantially higher precision than previous approaches. By using MCP-1/-3 chimeras and CCR2 receptor mutants, we have identified the structural determinants of differential receptor activation. These results will help guide the future development of small molecules inhibitors to target the major subpocket of the receptor.

Declaration

This thesis contains no material which has been accepted for the award of any other degree or diploma at any university or equivalent institution and that, to the best of my knowledge and belief, this thesis contains no material previously published or written by another person, except where due reference is made in the text of the thesis.

Signature:



Name: Zil E Huma

Date: 25/05/2017

Publications during enrolment

Huma Z.E., Ludeman J.P., Wilkinson B.L., Payne R.J., Stone M.J., NMR Characterisation of Cooperativity: fast ligand binding coupled to slow protein dimerisation. *Chem Sci.* 2014; 5:2783-8; DOI: 10.1039/c4sc00131a.

Stone M.J., Hayward J.A., Huang C., **Huma Z.E.**, Sanchez J., Mechanisms of Regulation of the Chemokine-Receptor network. *Int. J. Mol. Sci.* 2017, 18, 342; DOI: 10.3390/ijms18020342.

Huma Z.E., Sanchez J., Lim H.D., Bridgford J.L., Parker B.J., Pazhamalil J.G., Porebski B.T., Pflieger K.D.J., Lane J.R., Canals M., Stone M.J., Key Determinants of Selective Binding and Activation by the Monocyte Chemoattractant Proteins at the Chemokine Receptor CCR2, *Sci. Signal.* 2017, 10, 480. DOI: 10.1126/scisignal. aai8529.

Thesis including published works declaration

I hereby declare that this thesis contains no material which has been accepted for the award of any other degree or diploma at any university or equivalent institution and that, to the best of my knowledge and belief, this thesis contains no material previously published or written by another person, except where due reference is made in the text of the thesis.

This thesis includes 1 original papers published in peer reviewed journals. The core theme of the thesis is chemokine receptor interactions. The ideas, development and writing up of all the papers in the thesis were the principal responsibility of myself, the student, working within the Department of Biochemistry and Molecular Biology under the supervision of Associate Professor Martin Stone. The inclusion of co-authors reflects the fact that the work came from active collaboration between researchers and acknowledges input into team-based research.

In the case of Chapter 3 my contribution to the work involved the following:

- Expression and purification of the MCP-1
- Collection of the NMR data
- Analysis of the NMR data
- Development of the mathematical algorithm
- Involved in manuscript preparation, figure generation and writing of the first draft

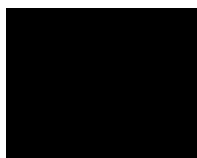
Thesis Chapter	Publication Title	Status	Extent of Contribution (%)	Co-author name, Nature, % of Co-author's contribution	Co-author(s), Monash student?
3	NMR Characterisation of Cooperativity: fast ligand binding coupled to slow protein dimerisation	Published	45%	1. Justin Ludeman, collection of the NMR data, editing of the manuscript, 10% 2. Brendan Wilkinson, synthesis of receptor peptides, 5% 3. Richard Payne, design of the sulfopeptides, 5%	No No No

Declaration

				4. Martin Stone, Overall project direction, supervision of the data analysis, finalisation of the manuscript, 35%	No
--	--	--	--	---	----

I have not renumbered sections of submitted or published papers in order to generate a consistent presentation within the thesis.

Student signature:



Date: 25/05/2017

The undersigned hereby certify that the above declaration correctly reflects the nature and extent of the student's and co-authors' contributions to this work. In instances where I am not the responsible author I have consulted with the responsible author to agree on the respective contributions of the authors.

Main Supervisor signature:



Date: 25/05/2017

Acknowledgements

First, I would like to thank GOD, the creator of this universe for being my companion at each and every step of my life, for giving me strength to gain this knowledge and for making me realise my hidden potentials through this journey which I have not known before.

I would like to thank my supervisor, Associate Professor Martin Stone for his invaluable support, guidance and supervision throughout this PhD project. Your continuous encouragement has persuaded me to work hard and in keeping my moral high. Thank you for helping me and guiding me through the tough times when nothing seemed to be working right.

I would like to express my gratitude to Dr. Meritxell Canals for her expertise, supervision and encouragement during this PhD project. Thanks a lot Meri for personally guiding me and teaching me all the cell-based work. Thank you for your patience for all the time I annoyed you in the DDB lab.

I would also like to thank Dr. Rob Lane for his guidance and valuable time and for all the ideas and contributions to the result discussions.

I am also thankful to Dr. Richard Payne, Dr. Kevin Pflieger and Dr. Brenden Wilkinson for their invaluable contribution towards this PhD project.

I would also like to acknowledge my PhD committee, Dr. Sheena McGowan, Dr. Ashley Buckle, Dr. Natalie Borg, Dr. Jackie Wilce and Dr. Mibel Aguilar for their guidance and support at all the milestones and their encouragement and motivation throughout my candidature.

Lots of thanks to all the people in the DDB lab (especially Dr. Holly Yeatman and Dr. Herman Lim) who have provided help during my signalling work. A big thankyou to all the people who have contributed in any way to our research papers.

I am thankful to all my lab fellows past and present (especially Enzo Huang, Julie Sanchez and Jenni Hayward) and my friends from B109 office (Nathan Habila and Baydaa Hirmiz) for their continuous moral and intellectual support. Life at the office couldn't have been much better than it has with you people. Thank you for your friendship and suggestions throughout this journey. A big thanks to all my friends who have helped me during this PhD.

An immense thank you to my parents for being there whenever I needed them. Thank you for your endless support and prayers. Lots of thanks to my siblings too for all their love and the tension-relieving chats through this tough task. I am forever grateful to you guys.

Finally, I am thankful to my husband Dr. Jamshaid Ahmad for encouraging me to go ahead in pursuing my dreams. Thanks for all the encouragement and continuous help throughout this thesis.

Acknowledgements

And lastly, I dedicate this thesis to my daughters, Amna and Fatima for making my life beautiful with their love, enduring the stress with me and being a motivation which kept me going whenever I wanted to quit.

List of general abbreviations

δ H	Chemical shift in 1 H dimension
δ N	Chemical shift in 15 N dimension
β -arr 2	β -arrestin 2
bp	Base pair
BRET	Bioluminescence resonance energy transfer
BSA	Bovine serum albumin
cAMP	Cyclic adenosine monophosphate
CCR2	CC chemokine receptor 2
CCR2 (18-31)	Peptide corresponding to residues 18-31 of the CCR2 N-terminus
cDNA	Complementary DNA
Da	Dalton
dNTPs	Deoxynucleotide triphosphates
DMEM	Dulbecco's Modified Eagle Medium
DNA	Deoxyribose nucleic acid
DSS	4,4-dimethyl-4-silapentane-1-sulfonic acid
E. coli	Escherichia coli
EC ₅₀	Chemokine concentration which induces 50% of the maximum response
ECL	Extra-cellular loop
ELISA	Enzyme linked immunosorbent assay
ERK	Extra-cellular regulated kinase
FBS	Foetal bovine serum
Fsk	Forskolin
GAG	Glycosaminoglycan
GPCR	G protein-coupled receptor
GRK	G protein kinase
h	Hour
HBSS	Hanks' Balanced salt solution
HEK293	Human Embryonic Kidney 293 cell line
HIV-1	Human immunodeficiency virus
HSQC	Hetero-nuclear single quantum correlation
ICL	Intra-cellular loop

Abbreviations

IL	Interleukin
IP3	Inositol triphosphate
K _D	Dissociation constant
LB	Luria-Bertani
MAPK	Mitogen activated protein kinases
MCP	Monocyte chemoattractant protein
MCP-1(P8A)	MCP-1 with a Pro8→Ala substitution
MCP-1(T10C)	MCP-1 with a Threonine→Cysteine substitution
NMR	Nuclear magnetic resonance
OD	Optical density
PCR	Polymerase chain reaction
PBS	Phosphate buffer saline
pEC ₅₀	-log ₁₀ EC ₅₀
pERK	Phosphorylated ERK
pIC ₅₀	-log IC ₅₀ where IC ₅₀ is the concentration of compound required for 50% inhibition
pK _i	-log ₁₀ K _i , where K _i is the concentration of chemokine required for half maximal inhibition of ¹²⁵ I-MCP-1 binding
Rcf	Relative centrifugal force
Rluc	Renilla luciferase
SDS	Sodium dodecyl sulphate
SDS-PAGE	Sodium dodecyl sulphate polyacrylamide gel electrophoresis
SEM	Standard error of the mean
SFM	Serum free media
TBS	Tris-buffered saline
TE	Trypsin / EDTA
Tet	Tetracycline
TM	Trans-membrane
TPST	Tyrosylprotein sulfotransferase
TREx	Tetracycline-regulated expression
v/v	Volume per volume
w/v	Weight per volume
WT	Wild type
YFP	Yellow fluorescent protein

Chapter 1. Introduction

1.1. Inflammation and Leukocyte Trafficking

Inflammation is an integral part of our innate immunity as it is a way of self-protection adapted by the body to get rid of any harmful irritants. The standard expressions of inflammation (redness, swelling, heat, pain and loss of function) are the outcome of different concealed biochemical processes, which are initiated by an infection by any foreign particle or tissue damage [1]. The inflammation triggers the movement of different leukocytes from blood into affected tissues. These leukocytes work as the initial host defence and initiate the tissue repair process.

Inflammation can be a sudden response of the body towards an infection, which leads to rapid movement of leukocytes to the site of infection, known as acute inflammation; or can be chronic if it remains for a prolonged period, leading to various diseases such as atherosclerosis, diabetes, asthma and cancer.

Generally, inflammation is a protective mechanism however, sometimes the immune system gets triggered automatically resulting in deterioration of the normal healthy tissues, leading to auto-immune diseases like lupus, psoriasis, rheumatoid arthritis and multiple sclerosis.

Leukocyte trafficking is a composite process that involves different physiological events. It involves several groups of adhesion molecules which help in the migration of the leukocytes from the blood into the damaged tissue because of inflammation. The movement of these leukocytes is mediated by an array of small proteins known as “chemokines”. The chemokines are secreted in response to a variety of inflammatory signals, directing leukocytes along the chemotactic gradient.

The appearance and retention of the chemokines on the surface of endothelial cells is mediated by glycosaminoglycans (GAGs), cell surface polysaccharides [2]. These interactions are very important as they provide a mechanism for keeping high concentration of chemokines confined to the production site, which works as an indication for leukocytes to the source of chemokine secretion [3]. Leukocytes, during their usual immune-surveillance process, roll along endothelium. The selectins (a group of adhesion molecules) on the endothelium interact with the mucin counter-receptors on the walls of the leukocytes resulting in slowing and induces rolling of the leukocyte along the endothelial surface [4]. In the next step, the GAG-bound chemokines (or chemokines released from GAGs) interact with their G protein-coupled receptors present on leukocyte walls. These interactions trigger another set of adhesion molecules on the walls of leukocytes, integrins, which bind to integrin receptors on the endothelium wall. Integrin activation on the leukocytes leads to tight adhesion of the leukocytes to the endothelial surface [5, 6] (Fig 1.1). Some cytoskeletal changes also occur within the leukocytes, allowing cell movement across the endothelial surface to the site of inflammation [7] (Fig 1.1). In addition to its role in inflammatory responses, constitutively expressed chemokines also play

an important role in directing leukocytes to perform their homeostatic functions in normal immune surveillance [8, 9].

1.2. Chemokines

Chemokines or chemotactic cytokines are small signalling proteins (8-10 kDa; ~70-80 amino acids) secreted by a variety of cells, including endothelial cells. The human genome and other mammalian genomes each encodes approximately 50 different chemokines [10]. These chemokines play important roles in immunity, acting mainly on lymphocytes, monocytes, neutrophils, basophils and eosinophils. The sequence identity between chemokines varies from 20-90%. The first chemokine discovered was CXCL4 (platelet factor 4), but their proper recognition as chemotactic molecules came after the detailed study of CXCL8 (IL-8) in 1987 [11].

There is a high level of sequence conservation among homeostatic CC chemokines from fish to higher vertebrates, which emphasises the need of these genes for carrying out normal physiological function [12].

Chemokines bind to their receptors, which are G protein-coupled receptors, present in the membranes of leukocytes, and initiate complicated signal transduction pathways [13]. Receptor activation leads to a variety of downstream effects, including degranulation, protease release, the respiratory burst and apoptosis to resolve the abnormal cellular pathology [14]. The response may be terminated due to receptor desensitisation and internalisation [3].

In addition to binding to their receptors, chemokines have also been found to bind to cell surface GAGs [15]. Demonstrating the importance of GAG binding, Proudfoot et al. [16] studied mutants of three chemokines that were defective in GAG-binding but retained the ability to induce chemotaxis *in vitro*. These mutants did not show cell migration *in vivo*, whereas the corresponding wild type chemokines displayed significant recruitment of leukocytes. Chemokine-GAG interactions play a tremendous role in cellular localisation, both in normal physiological processes as well as processes like inflammation and cancer. It has been reported that changes in the structure of the tumor cell surface GAGs critically effect the growth kinetics of tumor cells and also affects the metastasis potential [3, 17, 18]. Further it has been observed that GAG-binding and chemokine oligomerisation (described below) are functionally coupled [3]. Upon binding to GAGs, chemokines show an increase in dimerisation, which is important for their function.

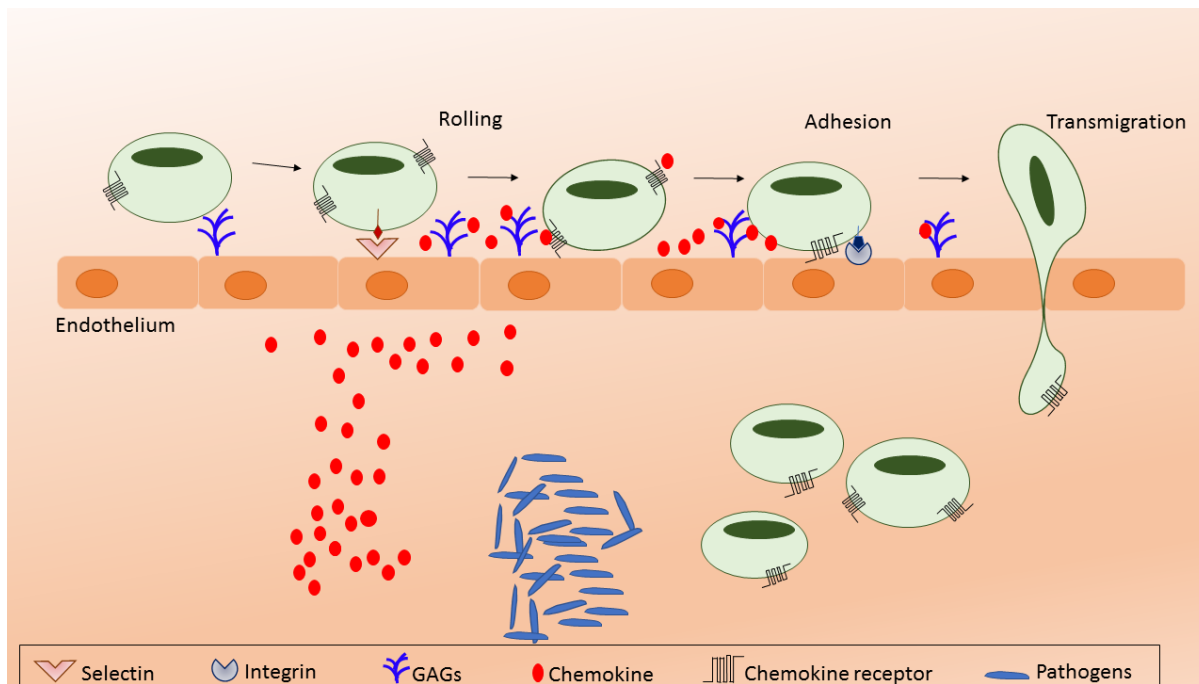


Figure 1.1. Illustration of leukocyte trafficking. Steps that occur in migration of leukocytes from blood to tissue in response to chemokine production.

Cellular chemotaxis is the most prominent function of chemokines [19]. Inappropriate or excessive expression [20] of either chemokines or receptors can lead to inflammatory diseases like asthma/allergic inflammation, rheumatoid arthritis, cardiovascular diseases, neuro-inflammation, cancer and transplant rejection [14, 21]. In addition, chemokines perform key roles in cancer progression/spreading, promoting metastasis and possibly angiogenesis at secondary sites [22, 23]. The possible mechanism involved in this process is that tumor cells secrete cytokines which in turn recruit leukocytes, in particular tumor associated macrophages (TAMs) and neutrophils [24]. These leukocytes become a rich source of cytokines, growth factors and other associated proteases. The angiogenic chemokines then start promoting vascularisation and the metalloproteases start remodelling the extracellular matrix proteins that in turn facilitates metastasis; however, the exact mechanism still needs to be investigated [24].

1.2.1. Classification

Chemokines are classified into two major subfamilies (CC and CXC) and two minor subfamilies (CX₃C and XC) based on the spacing of conserved cysteine residues approximately 10 residues from the N-terminal end of the peptide chain. Four consistent cysteine residues that are involved in formation of disulfide bonds characterise chemokines. The first cysteine in the chain links with the third and the second cysteine joins with the fourth to form disulfide bonds.

CXC or α -chemokines have one amino acid between the first two cysteines; CC or β -chemokines have the two cysteines beside each other. The genes for α -chemokines are present on chromosome 4 while the genes for β -chemokines are present on chromosome 17 [25]. The small class, CX₃C or the δ -chemokines possess three residues between the first two cysteines. The only member of this family is CX₃CL1 (fractalkine). The CX₃C chemokine is different as it is part of a cell surface receptor. The fractalkine forms the N-terminal domain of the receptor CX₃CR1. The γ -chemokine or C-subclass is an exception to the four-cysteine criteria as it has only two cysteine residues. Both members of this sub-family are encoded by the same gene and are different in only two amino acids [19].

Chemokines are designated per their subfamily classification by systematic names composed of a prefix (CCL, CXCL, CX₃CL or XCL; 'L' signifies a ligand as opposed to a receptor) followed by an identifying number. However, most chemokines also have common or historical names relating to their earliest characterised functions. Herein, we have used the systematic names for all the chemokines (mentioned in this thesis), except MCP chemokines, which have been used with their common names throughout this thesis (except in Fig 1.6. which shows human chemokine receptor

network). However, at the first point of mention their systematic names have been given in parenthesis. (A table is given in appendix I which shows both the systematic and common names of the chemokines used in this thesis).

Chemokines can be classified on their function as well as structures. Based on their functions, chemokines are grouped into two subsets. There are pro-inflammatory chemokines which control the engagement of leukocytes in cases of inflammation, tumour or tissue injury to the site of infection [26, 27]. Homeostatic chemokines are responsible for steering leukocytes in general immune surveillance of healthy tissues (tissue maintenance) and during induction of adaptive immune responses in lymph nodes, spleen and Peyer's patches (PPs) [27]. However, recent studies suggest that most of the chemokines perform a "dual function".

1.2.2. Chemokine Tertiary Structure

Different techniques like X-ray crystallography and/or NMR spectroscopy have been used to determine the three-dimensional (3D) structures of many chemokines. The tertiary structure of all chemokines is highly conserved (Fig 1.2). The chemokines consist of a long N-terminus that is present before the first cysteine. After the first two cysteines, is a loop of approximately 10 residues, which is often followed by one turn of a 3_{10} -helix. The region between the second cysteine and the 3_{10} -helix is known as the N-loop and plays very important role in chemokine function. The single turn 3_{10} -helix is followed by three β -strands and a C-terminal α -helix. The β -strands are oriented antiparallel to each other and form a β -pleated sheet. The C-terminal α -helix is packed against one face of the β -sheet, via hydrophobic interactions.

The secondary structural units are connected by turns known as the 30s, 40s and 50s loops, which are based on the residue numbering. The 30s and 50s loops also possess the third and fourth cysteines in the sequence. Disulfide bonds from these to the first two cysteines (in the CC or CXC motif) limit the flexibility of the N-terminus [19]. It has been shown by NMR studies that the N-loop is the most flexible region of the protein (excluding the N- and the C-termini). This flexibility is important in chemokine receptor binding and/or activation [19, 28, 29].

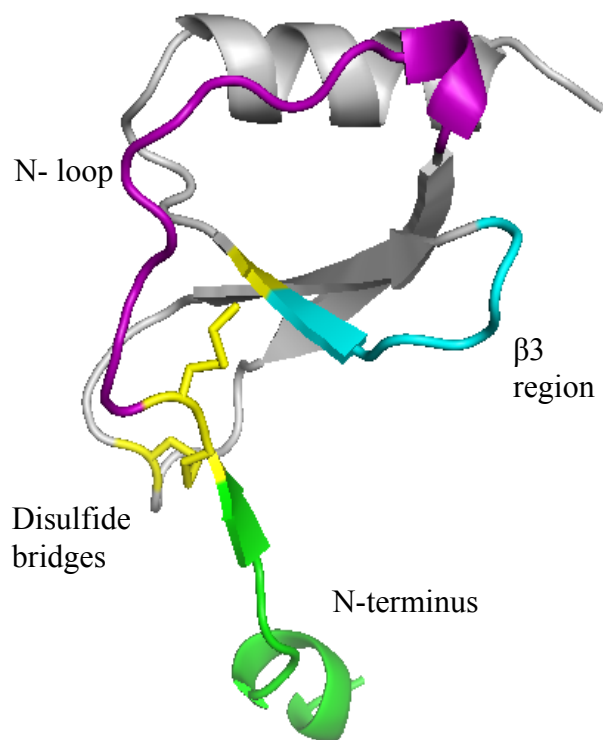


Figure 1.2. Tertiary Structure of a typical CC chemokine (MCP-1/CCL2) [PDB ID: 1DOK]. N-terminus, N-loop and $\beta 3$ regions are important for binding and interaction. The disulfide bridges are shown as yellow sticks.

1.2.3. Quaternary Structure

Structural studies have revealed that most chemokines form dimers or high order oligomers [30]. The dimers of different sub-families adapt different quaternary conformations. The dimers belonging to CXC and CX₃C chemokines are more globular in structure while CC chemokines join to form elongated dimers. An exception is MCP-1 (CCL2), a CC chemokine that crystallises as a tetramer [20] (Fig 1.3).

Chemokines oligomerise at high concentrations, or in the presence of GAGs such as heparin. Most chemokines can form dimers or higher order oligomers and can exist in equilibrium between different oligomeric states in solution [16]. Therefore it is a point of interest for scientists to identify the chemokine state responsible for receptor binding and activation [31]. Different structures solved by X-ray crystallography and NMR spectroscopy has proven that chemokines exist as dimers [19, 25, 32, 33]. However, because the dissociation constants of dimerisation for many chemokines are in the low micromolar range, it was hypothesised that chemokines exist as monomer in the human body and that the monomeric form of chemokines is the biological active form [34]. Some *in vitro* experiments done on chemokine mutants (obligate monomers) of MCP-1, CXCL8 (IL-8) and CCL4 (MIP-1 β) supported this hypothesis. These mutants showed binding with receptors, stimulated intracellular signalling and induced chemotaxis of leukocytes in *in vitro* experiments [35-37]. However, several studies done later have revealed that these obligate monomeric constructs of MCP-1 and CCL4 and CCL5 (RANTES) could not recruit leukocytes *in vivo* in mice [16]. This led to the conclusion that the monomeric state is very important for receptor binding and activation, but dimerisation is essential for different *in vivo* physiological functions. For example, dimerisation is required to bind to GAGs present on endothelial surfaces with high affinity. As these interactions are very important to regulate the localised chemokine concentration to avoid their accelerated dissemination in the bloodstream [38-40].

Further research has shown that CXC dimers can bind to their receptors (CXCL8 was studied as an example) as after dimerisation their receptor-binding surfaces are still exposed [31], whereas CC dimer formation obstructs the receptor binding site [41], which results in inability of CC dimers to bind to their receptors, so these dimers must dissociate to allow receptor activation [38, 42].

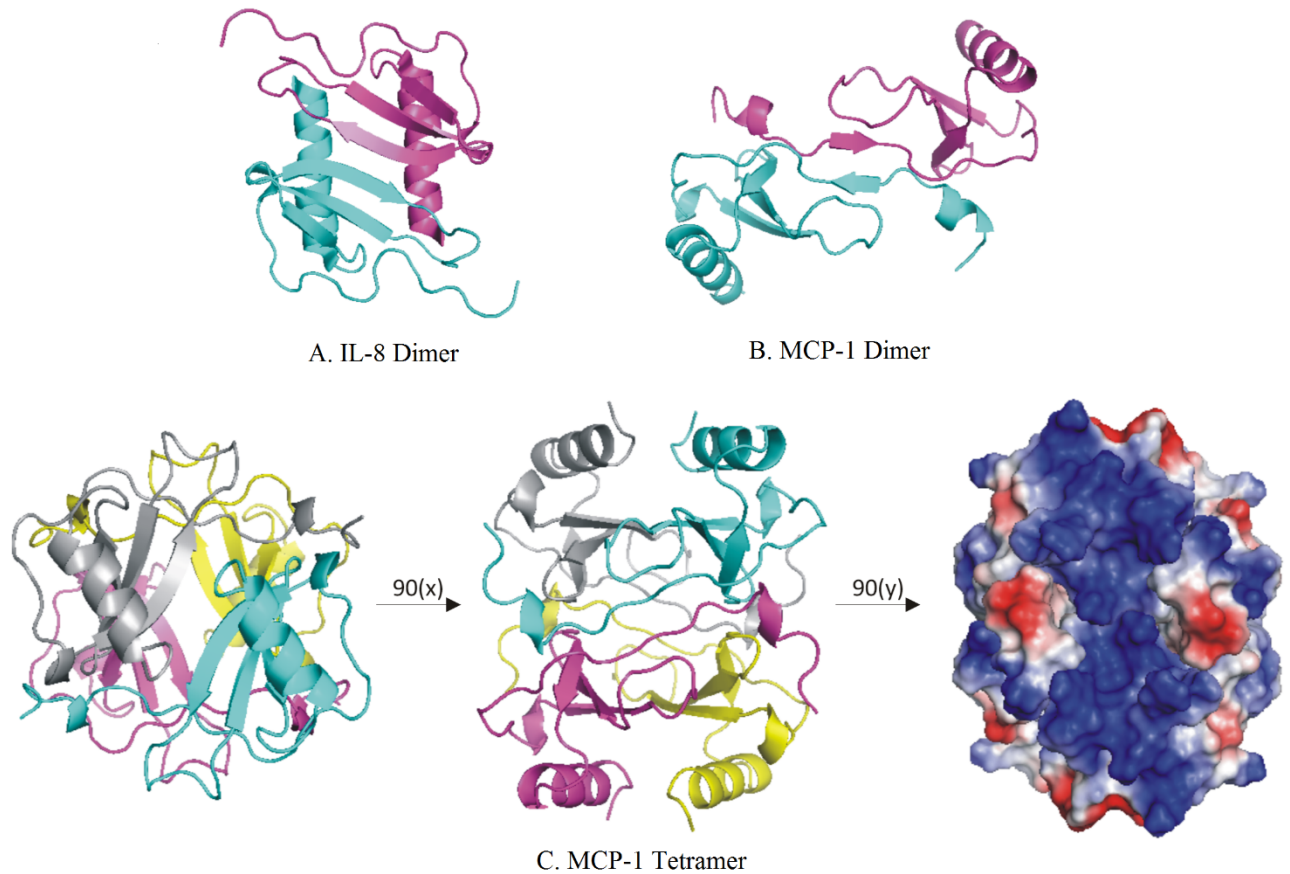


Figure 1.3. [42] Oligomeric structures of chemokines. (A, B) Dimer structures of (A) IL-8/CXCL8 and (B) MCP-1/CCL2, highlighting the distinct dimer interfaces for CXC and CC chemokines, respectively. (C) Tetramer structure of MCP-1/CCL2, highlighting: (left) the CXC-type dimer interfaces (cyan to grey and magenta to yellow protomers); (center) the CC-type dimer interfaces (cyan to magenta and yellow to grey protomers); and (right) the highly electropositive (dark blue) surface involved in GAG binding.

1.3. Chemokine Receptors

Chemokine receptors belong to the large family of class A G protein-coupled receptors (GPCRs), showing close resemblance to rhodopsin [43]. Chemokine receptors, like all GPCRs, contain seven transmembrane α -helices (TM 1-7) which alternate in their orientation across the membrane. The N-terminus is extracellular while the C-terminus is cytoplasmic and the seven transmembrane domains are joined by three extracellular loops (ECLs) and three intracellular loops (ICLs) [13, 44-46] (Fig 1.4). The first chemokine receptor to be cloned was the IL-8 receptor in 1991 and now more than 25 receptors are known [11]. The chemokine receptors are classified based on the chemokines with which they interact. For example, receptors designated ‘CCR’ interact predominantly with CC chemokine ligands. However, there are also some atypical receptors, like Duffy antigen receptor for chemokines (DARC) and D6, which have a structure similar to the chemokine receptors, but upon binding to the chemokines they fail to couple to G proteins [47]. However, they do signal and internalise via β -arrestins [48, 49].

1.3.1. GPCR Structure and Signalling

Guanine nucleotide binding protein (G protein)-coupled receptors (GPCRs) constitute the largest family of integral cell surface receptors. There are more than 800 members of this superfamily which respond to a variety of stimuli. They play important roles in a wide range of biological processes and respond to different hormones, neurotransmitters, metabolites, chemokines, odorants and ions, as well as photons [50, 51].

Human GPCRs are generally classified on the basis of sequence similarity into 5 main classes, called rhodopsin, glutamate, adhesion, frizzled and secretin [52, 53]. Those receptors for which ligands or physiological function are still unknown are termed as orphan receptors [54, 55].

All GPCRs share a common structural topology, having an extracellular N-terminus and intracellular C-terminus; with seven trans-membrane helices (TM 1-7), which are connected with each other by three extracellular loops (ECLs) and three intracellular loops (ICLs). A disulfide bridge present at the top of ECL2 and TM3, is a conserved feature of GPCRs and contributes to receptor stability [56]. Although, the binding pocket is very diverse as these receptors are activated by a variety of ligands, there are some features conserved within each class of GPCRs. The first reported crystal structure of a GPCR was of bovine rhodopsin [57].

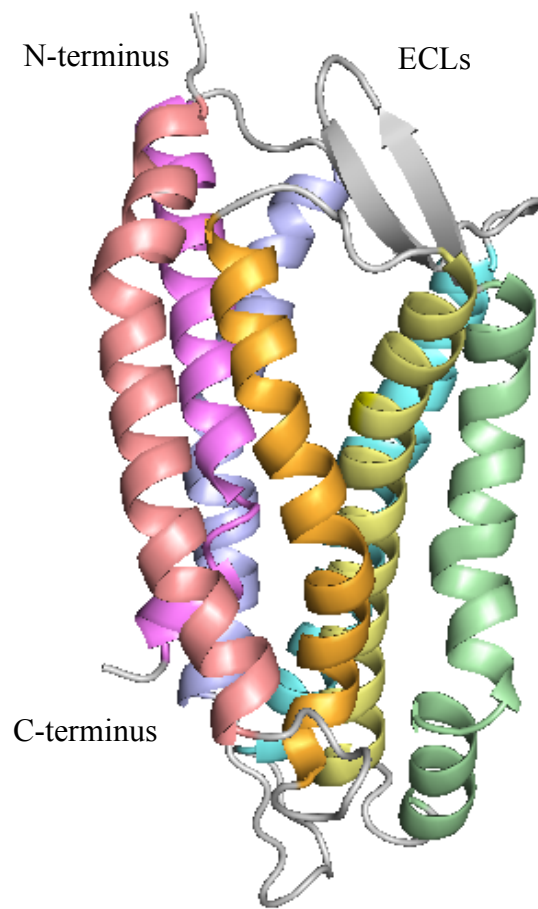


Figure 1.4. Typical structure of a chemokine receptor: Homology model of CCR2, transmembrane helices are coloured salmon (TM1), orange (TM2), pale yellow (TM3), pale green (TM4), aquamarine (TM5), light blue (TM6) and violet (TM7); other receptor residues are in grey.

G proteins are heterotrimeric proteins made up of three subunits, alpha (α), beta (β) and gamma (γ) [58]. Once the ligand interacts with the receptor, the receptor undergoes conformational changes due to rearrangement of TM helices. This activates the associated G proteins, promoting exchange of guanosine diphosphate (GDP) with guanosine triphosphate (GTP) [59]. The activated G protein dissociates into the α -subunit and the $\beta\gamma$ complex. Both can then activate an independent set of effectors, ultimately leading to generation of secondary messengers, which direct and activate intracellular processes [58, 60] (Fig 1.5).

$G\alpha$ subunits are generally classified, based on their sequence and function, into 4 classes ($G\alpha_s$, $G\alpha_{q/11}$, $G\alpha_{i/o}$ and $G\alpha_{12/13}$), which activate specific signalling pathways [61]. Most of the receptors couple to a subset of $G\alpha$ subunits. The $G\alpha_s$ subunits activate adenylyl cyclase (AC) which eventually lead to increased levels of 3', 5'-cyclic adenosine monophosphate (cAMP) [62]. However, the other $G\alpha_{i/o}$ subunits lead to inhibition of cAMP production by negative regulation of AC [63]. The most important target of cAMP is cAMP dependent protein kinase A (PKA) which further interacts with various targets to implement the effects of cAMP signalling [64]. $G\alpha_{q/11}$ is involved in controlling the release of intracellular Ca^{2+} , which is important for regulating several critical cellular processes [65]. $G\alpha_{q/11}$ activates the enzyme, phospholipase C which catalyzes cleavage of phosphatidylinositol 4,5-biphosphate (PIP_2), a membrane lipid, into two secondary messengers, 1,2-diacylglycerol (DAG) and inositol 1,4,5-triphosphate (IP_3) [66]. DAG remains in the membrane and activates protein kinase C (PKC). IP_3 binds to intracellular receptors present on smooth endoplasmic reticulum resulting in release of Ca^{2+} into cytoplasm. Among other effects, Ca^{2+} activates PKC, which further promotes phosphorylation of other cytoplasmic proteins, resulting in various cellular outcomes [67, 68]. $G\alpha_{12/13}$ are directly involved in activation of Rho signalling which is responsible for cytoskeletal rearrangements necessary for cell growth [69].

After dissociation from $G\alpha$, the $G\beta\gamma$ complex also participates in a variety of signalling events. It has been reported that it activates certain ion channels [70] and is also involved in phosphorylation of the extracellular signal-regulated kinases (ERK 1/2) via the protein kinase C/protein kinase A pathway [71, 72]. According to classical model of GPCR activation, the $G\beta\gamma$ complex is involved in bringing G protein-coupled receptor kinases (GRKs) from cytoplasm to the cell surface membrane, after activation of the receptor [73]. GRK phosphorylates specific residues of the receptor [74]. This leads to recruitment of β -arrestins as the phosphorylated receptor has increased affinity for β -arrestins, which ultimately results in internalisation of the receptor in clathrin coated pits [75].

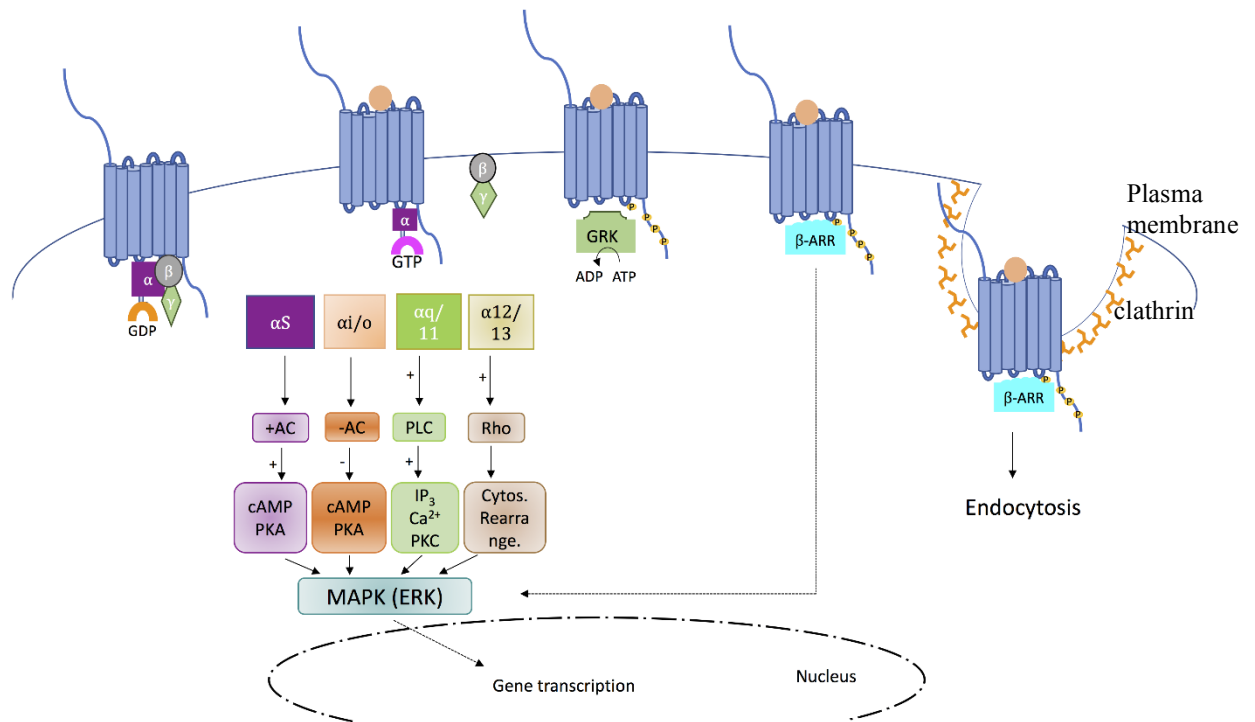


Figure 1.5. GPCR signalling pathways. GPCR's conformation determines the associating activation of the G proteins. The major pathways that can be adopted depends on the $G\alpha$ subunit involved or the involvement of β -arrestin. β arrestin recruitment leads to internalisation of the receptor in clathrin coated pits.

However, in addition to their G $\beta\gamma$ -dependent signalling, it is now known that arrestins can also signal independently of G proteins in response to GPCR activation [76]. It has been shown by Eichel et al. that β -arrestins can promote ERK pathways from endosomes [77]. In addition, β -arrestins have been found to play roles in activation of several other pathways establishing their role as capable of G protein independent signalling [78-83].

1.3.2. Chemokine Receptors as Drug Targets

Chemokine receptors are critical in controlling inflammatory responses and are possible targets for therapeutic intervention in some diseases. Most of the chemokine receptors are involved in various diseases. CXCR4 and CCR5 have been of interest to researchers due to their involvement as co-receptors for cellular fusion by the HIV virus [84, 85]. It was reported by Liu et al. that individuals with an inherited defective (32 bp deleted) allele of CCR5 are resistant to HIV infection [86]. It was further reported that a protein gp120 present on the surface of the HIV is responsible for interaction with the chemokine receptors [87]. This has led to the idea of small molecule CCR5 (or CXCR4) antagonists which can be used to block the receptors thus preventing viral entry into the cell; or stimulating receptor internalisation so it is not available on the cell surface [88, 89]. Two small molecule antagonists have been approved for therapeutic purposes to date. The first chemokine receptor antagonist which was recognised in 2007 for therapeutic use was Maraviroc, which is an inhibitor of CCR5 used to control HIV [90]. The other CXCR4 antagonist was approved in 2008, Mozobil (Plerixafor), which is used in cancer patients for hematopoietic stem cell mobilisation [91]. Another CCR9 inhibitor, CCX-282 is in phase 3 clinical trials and is showing promising future for patients with Crohn's disease [92].

There are (and have been) a large number clinical trials of other drugs that target chemokine receptors, but the results are not very promising. This is probably partly related to the redundancy found among the chemokine:receptor interactions, as multiple chemokines bind to the same receptor and multiple receptors respond to the same chemokines [92]. Most of these drugs are not highly efficacious which is accredited to redundancy of the chemokine system [92]. However, recent research suggests that the chemokine system is not redundant but there are subtle structural differences in each chemokine:receptor interaction, which are responsible for fine tuning of leukocyte response [27, 93]. Thus, there is an ongoing endeavour in understanding the chemokine:receptor interactions, which will help guide development of better therapeutics.

1.4. The Chemokine Network

1.4.1. Chemokine-Receptor Interaction

As described above, almost 50 chemokines and 25 chemokine receptors have been identified. The large number of chemokine receptors bind to more than one chemokine and a single ligand can bind to several different receptors. Most leukocytes also express multiple chemokine receptors, so if one ligand or receptor is impaired another chemokine or receptors could potentially induce a similar cellular response [94]. Receptors that interact with multiple chemokines do so only with chemokines of the same sub-family [95]. Antagonistic binding for receptors across sub-families can sometimes occur [19, 94]. A detailed chart showing human chemokines and their receptors is presented in Fig 1.6. These multiple ligand-receptor interactions are considered responsible for lots of redundancy among the chemokine family.

1.4.2. Two-step, Two-site Model of Receptor Interactions

A general two-site model has been proposed by various researchers to describe the chemokines' interaction with their receptors [96]. In the first step, the chemokine recognises and binds to the N-terminal region of its receptor (site 1). In the next step, the flexible N-terminus of the chemokine binds to the extracellular loops and transmembrane helices of the receptor (site 2), causing some conformational changes (Fig 1.7). These conformational changes ultimately lead to receptor activation [97].

Mutational studies have shown that the N-terminal domain of the chemokine receptor is important for ligand binding. Chemokine receptor N-termini have a negative charge and their binding to the chemokine is mainly enhanced by the electrostatic and hydrophobic interactions [98-101]. The results from NMR studies carried out with isotope-labelled chemokines in the presence of peptides derived from the N-termini of chemokine receptors have distinguished a groove marked by the chemokine N-loop and the β -sheet as the receptor N-terminus binding site [102]. This binding site contains a conserved highly hydrophobic region [102]. The electrostatic interactions between the positively charged core of chemokine and negatively charged N-terminus of the chemokine receptor help in stabilisation of the chemokine-receptor complexes. However, the chemokine N-terminus has generally not been considered important for binding but plays a critical role in receptor activation and signalling [101, 103, 104].

Recent structural studies by Qin et al. [105] and Burg et al. [106] have validated some key features of the two-site model. The crystal structure of the chemokine receptor CXCR4 in covalent

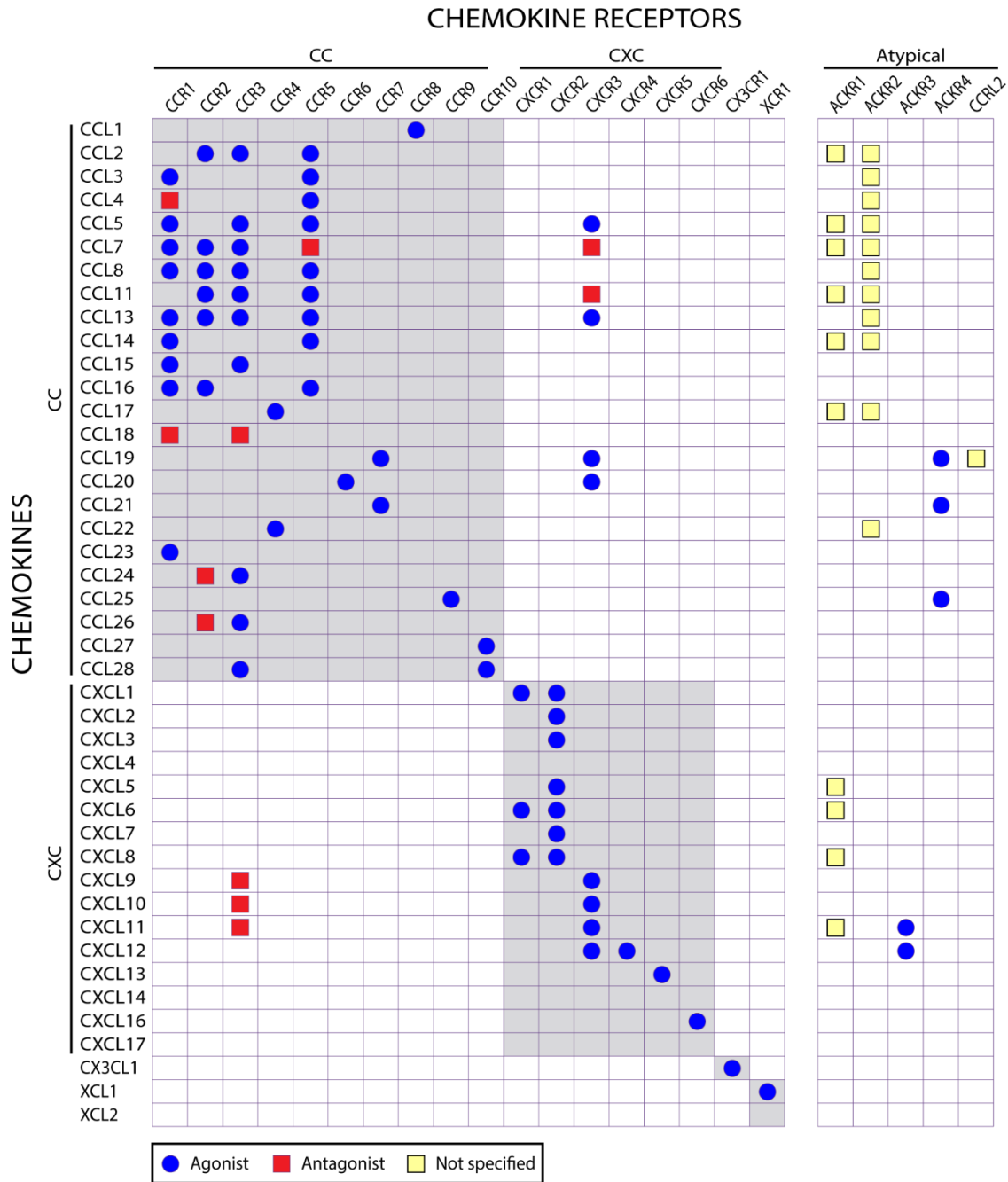


Figure 1.6. [42] Human chemokine-receptor network. Human chemokines and receptors are listed with symbols indicating whether they are specified as agonists or antagonists (or not specified) in the IUPHAR database

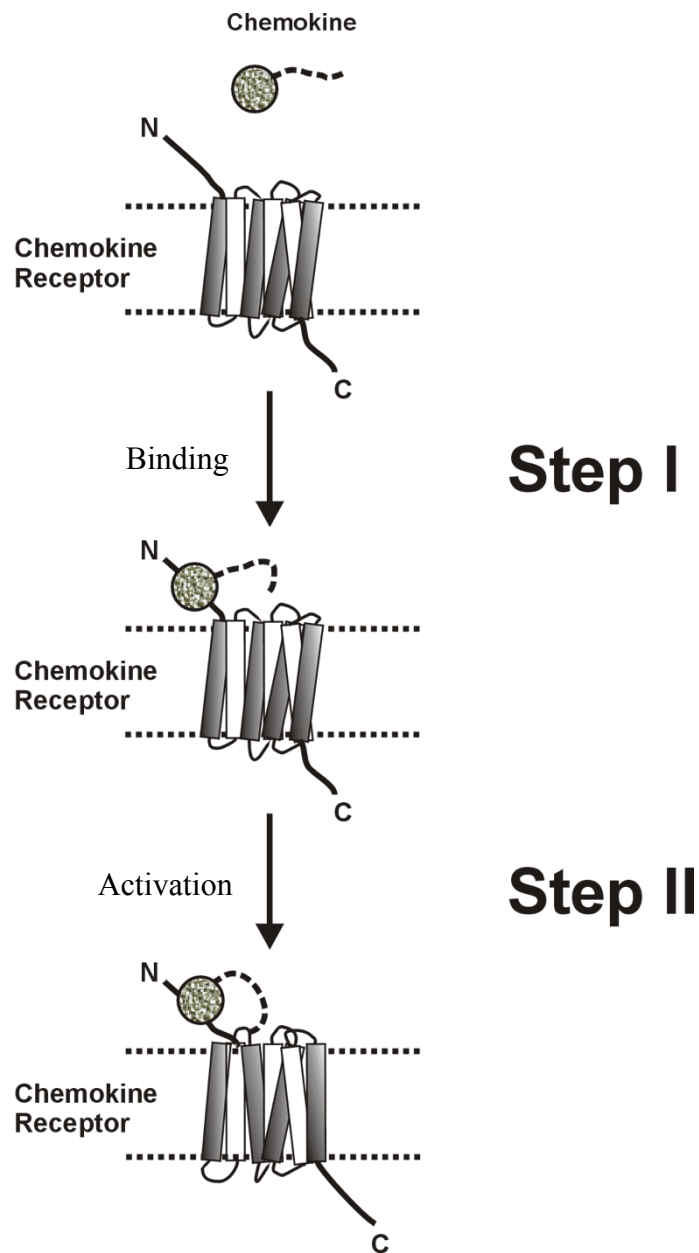


Figure 1.7. A schematic representation of two-site model of chemokine receptor activation: In the **first step** the chemokine core binds to the receptor N-terminus; while in the **second step** the chemokine N-terminus interacts with the receptor TM helices resulting in receptor activation.

complex with a viral chemokine antagonist vMIP-II has been reported by Qin et al., whilst Burg et al. have characterised a complex between human cytomegalovirus GPCR US28 and the chemokine CX₃CL1. Both models have identified receptor “site 2” residues that interact with the chemokine. However, Qin et al. have suggested that there is no clear borderline between site 1 and 2 reported by the previous researchers, and have therefore defined an intermediate site (“site 1.5”). Kleist et al. have also reported a similar “site 1.5” within the CXCL12: CXCR4 complex [107].

This model is quite widely accepted as it is consistent with many mutational studies. However, independence of the two sites is a difficult question that is still not clear and further effort is needed to fully understand the mechanism of chemokine recognition by receptors. The site 2 interaction could contribute to the binding affinity, which is not explained by the two-site model, as it explains the interactions as independent of each other. Further interactions at site 1 could vary depending on the presence of post-translational modifications (see section 1.7.) and these interactions could indirectly influence the subsequent interactions of the chemokine N-terminus at site 2. Furthermore, the model doesn’t consider the role of ECLs. As it has been reported by different mutational studies that ECLs do play a part in receptor activation [108, 109].

An additional concern about the two-site model is that it does not consider dimerisation of the receptor. Previously it was believed that chemokine receptors exist as monomers, but recent studies have demonstrated that they can exist either as homodimers or heterodimers [110]. As reported by Springael et al. [111], some chemokine receptors form homodimers and heterodimers. However, these dimers can bind only one chemokine with high affinity. That leads to a few more questions that either binding of a chemokine to one protomer within a dimer could sterically inhibit the binding to the other protomer. Binding of a chemokine to one protomer within a receptor dimer could indirectly influence the conformation of the other protomer (via the receptor dimerisation interface) and thereby alter interactions of the second protomer with chemokine ligands. These observations have added more complexity to the chemokine receptor structure and function. Future studies are required to explain the molecular basis of this allosteric behaviour of receptor dimers [110-112].

In summary, the two-site model has provided a basic frame work for many years, but considering the recent research and advancement in the field of GPCRs and signal transduction, it is not sufficient to explain all the details involved in chemokine:receptor interaction [113]. Thus, this two-site model can be used to guide future experiments but it should not be considered rigorously correct in all the details.

1.5. CCR2 and its Ligands

1.5.1. CCR2

CCR2 is a major chemokine receptor on monocytes and macrophages, cells that play important roles in atherosclerosis, obesity and type-2 diabetes. It is a receptor for all four human MCP chemokines. It has also been found to be expressed on dendritic cells, activated T lymphocytes and basophils, playing an important role in the immune system [114, 115].

There are multiple chemokines which activate CCR2 including MCP-1 (CCL2), MCP-2 (CCL8), MCP-3 (CCL7), MCP-4 (CCL13), CCL11 and CCL16 [116]. However, the most studied agonist of CCR2 is MCP-1, which is highly potent. These chemokines play important roles in cell physiology however any increase in their level leads to various inflammatory diseases.

CCR2 has been recognised as a promising drug target because of its role in various inflammatory and metabolic diseases [117]. CCR2 has also been identified as a co-receptor for some HIV-1 strains, which increases interest in CCR2 as a drug target [118]. There has been a continual effort to produce CCR2 antagonists, which can be used to control CCR2-mediated response. Several companies have tried different strategies to target CCR2 and have designed small molecule antagonists to block CCR2 signalling. INCB3344 is reported as a potent antagonist of CCR2, which shows a 100-fold selectivity of CCR2 over other homologous receptors [119]. It has a binding IC_{50} of 5.1 nM and efficiently displaces MCP-1 in binding assays. It can also block chemotaxis with an IC_{50} of 3.8 nM [119]. INCB3344 has been found effective in lowering macrophage level in target disease mouse models of multiple sclerosis and obesity and a rat model of inflammatory arthritis [120]. However, later it was reported that INCB3344 does not contribute to reducing atherosclerotic lesions in mice [121]. Another novel antagonist reported for CCR2 is TLK-19705, which is found to prevent the progression of albuminuria and atherosclerosis in mice [122]. Several companies, including Millennium, Incyte, ChemoCentryx, BMS, Merck and Pfizer, have developed and reported several other small molecule antagonists, which are still under different phases of clinical trials [123]. Most of these have been discontinued after phase 2 trials, which is often attributed to the lack of efficacy [124]. However, there is an ongoing search for new antagonists which will assist for future development of better therapeutics.

Different studies have shown that the N-terminal region of CCR2 contains a motif (D²⁵Y²⁶D²⁷Y²⁸) which gets sulfated at the tyrosine residues. Preobrazhensky et al. have demonstrated that the residue Tyr-26 in this motif is sulfated by using a ³⁵SO₄²⁻-labelled CCR2 [125]. They expressed the radiolabelled receptors on cells, immuno-precipitated and then ran on SDS-PAGE. The

sulfated receptor was detected by measuring radioactivity. A mutation of Tyr-26 resulted in a reduction in sulfation, a ten-fold loss of binding affinity and gross deactivation in response to MCP-1. Charge potential also regulates the interactions of CCR2 with the MCP-1. Tan et al. have also shown that sulfation of the N-terminal residues of CCR2 is responsible for enhanced binding affinity of MCP-1 [126]. These *in vitro* studies have provided good evidence that post-translational sulfation has the ability to change the interactions of CCR2 with its chemokine ligands, however, the *in vivo* outcomes of CCR2 sulfation are still under evaluation [126].

CCR2 exists in two isoforms, CCR2A and CCR2B which are formed by alternative splicing of a single gene [127]. They differ from each other in their carboxyl terminus. The major part of the CCR2A is present in the cytoplasm, while the CCR2B is most abundant on the cell surface. The CCR2B found in the cytoplasm is mainly internalised receptors [128]. Tanaka et al. have shown that overall total expression of CCR2B is ten-fold higher than CCR2A in monocytes [128]. However, differentiation of monocytes to macrophages reduces the level of both CCR2A and CCR2B [129]. Most previous studies of CCR2 function have focused on the CCR2B isoform. In the current study we have also exclusively used CCR2B. The sequence of CCR2B (P41597-2) was obtained from Uniprot.

1.5.2. Monocyte Chemoattractant Protein -1 and MCP-3

MCP chemokines are members of the β -chemokine (CC) subfamily. MCP-1 is the third chemokine purified after platelet factor-4 and interleukin (IL-8) [130]. There are four human MCPs (1-4); they have less than 40% sequence identity with other CC chemokines and 56-71% sequence identity with each other.

The intact MCP-1, -2 and -3 forms consists of 76 amino acids. MCP-2 and MCP-3 show a sequence homology of 62% and 71% respectively with MCP-1 [131]. MCP-4 shows a sequence identity of 56-61% with other MCPs. Other than four cysteine residues, only seven residues are conserved in all human CC chemokines and almost 42 amino acids are conserved among MCPs. MCP-1 is usually found in two forms because of different O-glycosylation with molecular weights of 9 and 13 kDa [131].

In the amino-terminal region of MCP-1, residues 1-6 are essential and Asp-3 is considered to play a major role in chemoattraction [132]. The amino acid at position 1 is significant for formation of secondary structure and for direct receptor binding, while residues 7-10 are necessary for receptor desensitisation [132]. The complete 10 residue N-terminus before the first cysteine takes part in receptor binding and activation. Insertion of three extra amino acids at the N-terminus of MCP-3

leads to loss of activity in monocyte chemotaxis in comparison with a normal MCP-3, confirming the importance of amino terminal region of chemokines for biological activity [133].

MCP-1 dimerises by forming a 2-stranded antiparallel β -sheet using residues near the N-terminus as is the case with CC chemokine subfamily in general. However, it has also been shown that MCP-1 binds and activates CCR2 as a monomer form [38]. The quaternary structure of MCP-1 dimer matches CCL5 and CCL4 as the shape of the protein is quite elongated.

MCP-1 is secreted by endothelial cells, fibroblasts, monocytes, T-cells and other cells that are involved in the recruitment of immune cells to the inflammation site. High expression of MCP-1 has been observed in inflammatory diseases, including atherosclerosis, arthritis and cancer [134]. MCP-2 is secreted from normal fibroblasts and mononuclear cells and from carcinoma and osteosarcoma cells along with MCP-1, although its production level is ten times lower than MCP-1 [135, 136]. MCP-3 is expressed along with MCP-1 in mononuclear cells and osteosarcoma cells [137, 138]. It is normally produced by mononuclear leukocytes and fibroblasts. At transcriptional level the expression of MCP-1 is regulated by TNF- α , interferon gamma (IFN- γ), platelet derived growth factor (PDGF) and stress factors, while retinoic acid, glucocorticoids and oestrogens have found to inhibit MCP-1 expression [139].

All MCP chemokines are known to interact with CCR2 [131]. However, other than CCR2, MCP-1 interacts with CCR3 and CCR5. MCP-3 also interacts with CCR1 and CCR3 while MCP-2 engages CCR1, CCR3 and CCR5 therefore, it has the most extensive range of action as compared to MCP-1 and -3 [133]. In line with this receptor selectivity, human MCP-1, -2, -3 are active on multiple leukocyte populations [131]. Both MCP-1 and MCP-3 activate monocytes, T-cells and basophils. However, MCP-3 activates a vast variety of cells other than these like dendritic cells, lymphocytes, natural killer cells, eosinophils and neutrophils [137]. MCP-2 activates basophils and eosinophils like MCP-3 [140]. MCP-4 show activities on eosinophils, basophils and monocytes induced in allergic and non-allergic inflammation [141]

1.5.3. Disease Relevance of CCR2/MCPs

Chemokines and their receptors play important roles in several inflammatory and autoimmune disorders including obesity, diabetes, asthma, atherosclerosis, psoriasis, rheumatoid arthritis and multiple sclerosis. Their overexpression can lead to severe inflammatory responses, leading to chronic outcomes [96, 142, 143]. In addition, chemokine or chemokine receptor overexpression has also been implicated in angiogenesis and metastasis [144].

MCP-1 is expressed in a variety of inflammatory conditions, including human coronary diseases, myocardial infarction, lung injury, liver and renal ischemia [145]. It has been found that

synovial fluids contain high levels of MCP-1 in arthritis patients. Elevated MCP-1 levels are found in asthma patients too [146]. MCP-1 has also been found to induce angiogenesis. Some studies have also shown that MCP-1 is overexpressed in many tumours, including ovarian, breast and oesophagus cancer [134]. Animal models and knock-out mice have clearly shown the involvement of chemokines in atherosclerosis [147]. In a rodent model of atherosclerosis, the mice deficient in both LDL receptor and MCP-1 had 83% less lipid deposition in aortas and fewer macrophages in their aortic walls than controls which were fed on a high cholesterol diet. Atherosclerotic lesions are much lower in CCR2 $-/-$ mice than in wild type mice [3, 131, 147, 148]. MCP-1 and its receptor CCR2 are the most involved chemoattractants in atherosclerosis [149]. Hypertension and hypercholesterolemia induces release of MCP-1 from vascular endothelial cells [147], which in turn motivates the movement of CCR2 bearing monocytes into sub-endothelium where they differentiate into macrophages and settle down. Ingestion of lipids and cholesterol changes them into foam cells, adding to fatty deposition inside the arterial walls, which ultimately causes thickening of the vessel wall. This continuous process of cellular infiltration then becomes the major cause of cell wall thickening, thus promoting atherosclerosis [3].

MCP-3 along with MCP-1 has been found in higher levels in systemic sclerosis patients, both in fibroblasts and skin lesions [150]. Higher levels of MCP-3 have been found in lung biopsies of patients suffering from interstitial pneumonia, bronchiolitis and other lung diseases [151]. Maddaluno et al. have reported about the role of MCP-3 in atherosclerosis [152]. Finally, both MCP-1 and -3 have been found to aid in HIV transmission by activating the immune system [151].

1.6. Modulation of Signalling Pathways

1.6.1. Partial Agonism

It has been observed that GPCRs do not respond identically to all agonists. Different ligands can induce stronger or weaker signals via the same receptor by inducing different populations of activated receptor. This simplest type of differential signalling is termed “partial agonism”, where, even if two ligands are added in the same concentration, one can induce maximal response (full agonist) as compared to the other which induces a lower response (partial agonist). It should be noted that partial agonism is a relative phenomenon; a partial agonist is always compared with the standard set by the full agonist [153].

Partial agonism can be detected by measuring the populations of signalling molecules coupled directly to the receptor (non-amplified signals, such as direct G protein activation or β -arrestin recruitment). However, the downstream signals (e.g. generation of second messengers, Ca^{2+} levels

and activation of kinases) are often highly amplified; therefore, the maximal effect of full and partial agonists can become indistinguishable.

Berchiche et al. [154] have shown that cognate chemokines for CCR2 display differences in their efficacies of activation of both β -arrestin and G protein-mediated signalling pathways [154]. MCP-1 acts as a full agonist at CCR2, while MCP-2, -3 and -4 activate CCR2 as partial agonists. Chapters 4 and 5 of this thesis describe our investigation of the structural basis of partial agonism by MCP chemokines at CCR2.

1.6.2. Biased Agonism

Previously it was believed that GPCRs act as simple on/off switches, existing either in activated or non-activated states [155-157]. However, recent studies have shown that GPCRs can exist in different activated conformational states [158] that are linked to different signalling pathways. Different ligands may selectively bind to different receptor conformations, thus leading to different signalling pathways [159]. This phenomenon, known as biased agonism, functional selectivity or pluridimensional efficacy, has now been reported for many GPCRs [160] (Fig 1.8).

It has been reported that each receptor has a specific conformation for a particular ligand [161]. These results are generally deduced from the fact that there are different signals reported by different ligands. Although this is the simplest way to explain biased agonism, there are other possible explanations such as differences in ligand binding kinetics and kinetics of different signalling pathways which also play an important role in biased agonism [162].

The first reported case of biased agonism was of an acetylcholine receptor to pilocarpine and carbachol [163]. After that biased agonists have been identified for several therapeutically important GPCRs [164]. The few examples include μ -opioid receptors [165, 166], β 2 adrenergic receptor [167, 168], 5-HT₂ and 5HT_{1A} serotonin receptors [169, 170], dopamine D_{2L} and D₁ receptors [171, 172], melanocortin MC₄ receptor [173] and angiotensin type 1A (AT_{1A}) receptor [174, 175].

Whereas biased agonism for these previously studied GPCR was observed with the synthetic agonists, for chemokine receptors the biased agonism has been observed with natural chemokine ligands. For example, CCR7 has shown biased agonism with CCL19 and CCL21, where both the agonists activate the G protein activation and calcium mobilisation but only CCL19 is able to promote receptor desensitisation which is mediated by recruitment of β -arrestins [176].

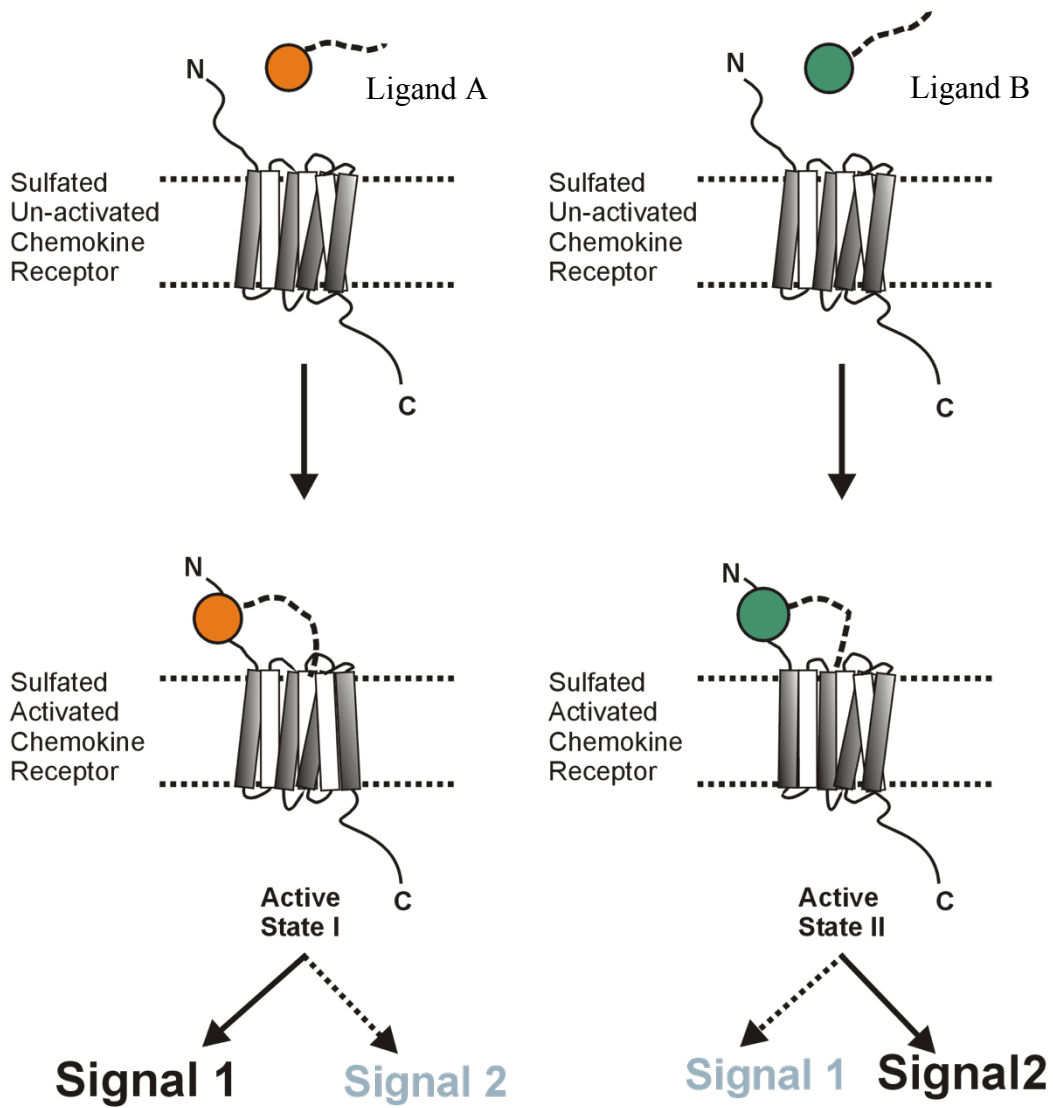


Figure 1.8. A schematic example of biased agonism at chemokine receptor. Different ligands stabilise different active conformations of the same receptor that engage different set of intracellular effectors, ultimately leading to different set of signalling pathways.

Kohout et al. [176] have also shown that CCL19 favours ERK 1/2 phosphorylation around 4-fold higher compared to CCL21 and this kinase activation was found to be β -arrestin dependent. Recently, there have been two systematic studies of biased agonism at chemokine receptors. Rajagopal et al. [159] have reported a study of G protein-mediated response versus a β -arrestin mediated response for three CC and three CXC chemokine receptors. All the chemokine receptors were tested against their endogenous ligand chemokines, mentioned in parentheses. CCR1 (CCL3, CCL5, CCL14, CCL15 and CCL23), CCR10 (CCL27, CCL28) and CXCR3 (CXCL9, CXCL10 and CXCL11) are found to exhibit significant level of signalling bias. Whereas CCR5 (CCL3, CCL3L1, CCL4, CCL8 and Met-CCL5), CXCR1 (CXCL1, CXCL6, CXCL8) and CXCR2 (CXCL1, CXCL2, CXCL3, CXCL5, CXCL6 and CXCL8) failed to show any bias with their respective chemokine ligands [159]. Likewise, Corbisier et al. [177] did a comparative study of G protein activation using several $G\alpha$ subtypes as well as β -arrestin 2, cAMP and Ca^{2+} signalling [177]. They have reported some levels of signalling bias for CCR2 (CCL2, CCL7, CCL8 and CCL13) and CCR5 (CCL3, CCL4, CCL5, CCL8 and CCL13) further indicating that signalling bias does exist at chemokine receptors [177]. CCR2 signalling is studied in Chapters 4 and 5 and has not been found to support biased agonism.

In summary, it is now understood that the phenomena of partial agonism and biased agonism may enable chemokines to fine tune inflammatory responses by differentially influencing different signalling pathways via chemokine receptors [178].

1.7. Tyrosine Sulfation

Tyrosine sulfation is a post-translational modification of secreted proteins that occurs extensively in multicellular eukaryotic organisms [125, 179]. It occurs in the trans-Golgi network and involves the addition of a sulfate (SO_4^-) group from 3'-phosphoadenosine 5'-phosphosulfate (known as PAPS) to an exposed hydroxyl group of a tyrosine side chain to form a tyrosine O4-sulfate ester (Fig 1.9). In mammalian cells, two enzymes called tyrosylprotein sulfotransferases-1 and -2 (TPST-1 and TPST-2) catalyse tyrosine sulfation [180, 181]. TPSTs consist of a short 8-residue N-terminal cytoplasmic domain, a 17-residue transmembrane domain and a luminal catalytic domain [182-184]. The different expression patterns for TPST1 and TPST2 in different tissues suggests that the two enzymes have distinct (possibly overlapping) functions and protein targets [185].

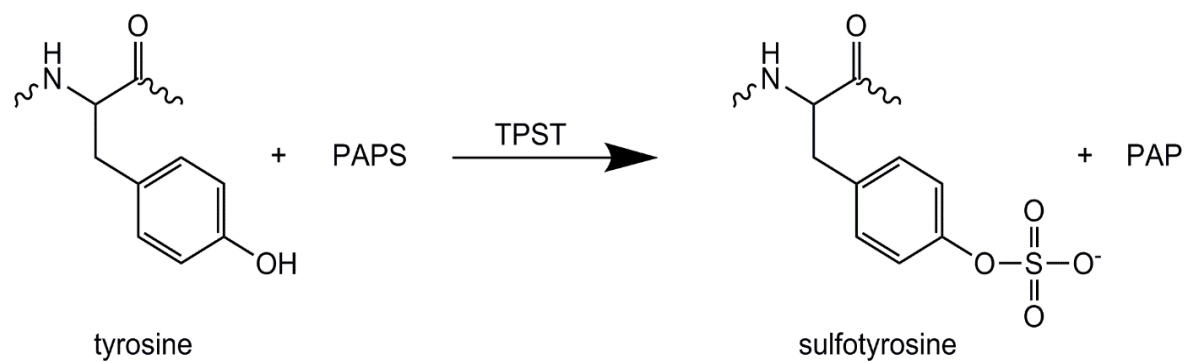


Figure 1.9. General schematics of tyrosine sulfation. PAPS is the sulfate provider and the reaction is catalysed by TPSTs.

Although there is no simple way to predict which tyrosine residues will be sulfated, there are some general sequence features that make a tyrosine residues more likely to be sulfated. The susceptible tyrosines are the ones near acidic residues and sulfation studies of different synthetic peptides have confirmed the presence of acidic residues in the surroundings of a sulfated tyrosine to be a structural requirement [184]. In comparison, basic residues, glycosylated asparagine and phenylalanine are not found near sulfotyrosines as they inhibit sulfation [186] (Table 1.1).

Huttner et al. have found that tyrosine sulfation sites have strong turn-inducing amino acids (glycine or proline) or weaker turn-inducing residues (aspartic acid, serine or asparagine) within seven amino acid positions from the sulfated tyrosine [179, 187].

Tyrosine sulfation was first studied on fibrinopeptide B in 1954 [188]. P-Selectin glycoprotein ligand (PSGL-1) was the first membrane protein shown to be altered by tyrosine sulfation [189, 190]. The flexible N-terminus of PSGL-1 contains both sulfotyrosines and adjoining O-glycosylation. More recently, tyrosine sulfation has been identified in a wide variety of proteins, including peptide hormones, enzymes, extracellular matrix proteins, anticoagulants and GPCRs [184].

Most chemokine receptors contain one or more likely tyrosine sulfation sites in their N-terminal regions. Several have been shown to be sulfated [125, 191-193] (Table.1.1) and sequence analysis also predicts sulfation in most other chemokine receptors [194]. Delocalisation of electrons over the highly polarisable sulfate and phenyl groups makes sulfotyrosine fit to be accommodated by a conserved positively charged pocket at the surface of the ligands [195-198]. Thus, these amino-terminal sulfotyrosines are very important for binding of the chemokines. The amino-terminal regions of many chemokine receptors carry multiple tyrosine residues, but their post-translational sulfation may not be equally important for ligand recognition. It has been reported by Simpson et al. [199] that sulfation of two different tyrosine residues can have different effects on the binding affinities. Sulfation of a CCR3 N-terminal derived peptide at Tyr-17 increases CCL11 binding by ~7 fold, while the sulfation of Tyr-16 amplifies it by ~28 fold [199]. Jen and Leary in 2010 have shown that a single tyrosine sulfation increases the affinity of MCP-3 for CCR2 by ~4 fold, while a double sulfation enhances it by ~36 fold [200]. Tan et al. have demonstrated that sulfation of a single tyrosine residue can enhance the affinity of MCP-1 to CCR2 by 4- to 30- fold [126].

Recent structural modelling and NMR studies suggested that all chemokines contain a conserved sulfotyrosine binding pocket, which provides a molecular evidence for sulfotyrosine conservation among chemokine receptors [194]. The presence of these sulfotyrosine binding pockets has been experimentally shown for different chemokines from different families i.e. XCL1, CCL5,

Chapter 1. Introduction

Receptor	Chemokine Ligands ¹	Receptor N-terminal Amino Acid Sequence ²	Key Findings	References
CCR2	CCL2/MCP-1 CCL7/MCP-3 CCL8/MCP-2 CCL11/eotaxin-1 CCL13/MCP-4 CCL16/HCC-4/LEC	<u>1</u> MLSTSRSRFIRNTN <u>ESG</u> <u>EEVTTFFD</u> <u>YDY</u> GAPC ₃₂	<ul style="list-style-type: none"> • Y26 is sulfated • Y26A mutant has reduced receptor binding/activation • Mutation of D25 reduces sulfation 	[125, 201]
CCR5	CCL3/MIP-1 α CCL4/MIP-1 β CCL5/RANTES CCL8/MCP-2 CCL11/eotaxin-1 CCL14/HCC-1 CCL16/HCC-4/LEC	<u>1</u> MD <u>Y</u> QVSSPI <u>YD</u> IN <u>YYT</u> SEPC ₂₀	<ul style="list-style-type: none"> • CCR5 is Tyr-sulfated • Sulfated Tyr residues contribute to binding of MIP-1α, MIP-1β and HIV-1 surface proteins 	[191]
CCR8	CCL1/I-309 CCL4/MIP-1 β CCL16/ HCC-4/LEC CCL17/TARC	<u>1</u> MD <u>Y</u> TLDL SVTTVT <u>DY</u> <u>YY</u> PDIFSSPC ₂₅	<ul style="list-style-type: none"> • N-terminal Tyr residues are sulfated • Sulfated Tyr residues contribute to binding of I-309 	[202]
CXCR3	CXCL9/Mig CXCL10/IP-10 CXCL11/I-TAC	<u>1</u> MVLEVSDHQVLNDAE VAALLENFSS <u>YDY</u> GE NESDSC ₃₇	<ul style="list-style-type: none"> • Y27 and Y29 or CXCR3 are sulfated • Mutation of Y27 or Y29 reduces binding and activation by CXCL9-11 	[203, 204]
CXCR4	CXCL12/SDF-1	<u>1</u> MEGIS <u>Y</u> TSDN <u>Y</u> TEEM GSGD <u>Y</u> DSMK <u>EP</u> C ₂₈	<ul style="list-style-type: none"> • N-terminal Tyr residues are sulfated • Mutation of N-terminal Tyr residues reduces SDF-1 binding 	[205]
CX ₃ CR1	CX ₃ CL1/fractalkine	<u>1</u> MDQFP <u>ES</u> VTENFE <u>YDD</u> LAEAC <u>Y</u> IGD <u>IV</u> ₂₇	<ul style="list-style-type: none"> • Mutation of N-terminal Tyr residues or sulfatase treatment reduces fractalkine binding affinity 	[192]
DARC	Many CC and CXC chemokines	<u>1</u> MGNCLHRAELSPSTEN SSQLDF <u>ED</u> VWNSS <u>Y</u> GV NDSFPD <u>GD</u> <u>Y</u> DANLEAA APCHSCNLLD <u>DS</u> ₆₀	<ul style="list-style-type: none"> • Y30 and Y41 are sulfated • Mutation of Y30 and Y41 reduces binding to different chemokines • Mutation of Y41 reduces binding to <i>Plasmodium vivax</i> Duffy binding protein 	[193]

¹Chemokine ligands are those listed in [194]

²Potentially sulfated Tyr residues are shown in bold; acidic residues are underlined

³Ligand and Receptor Nomenclature according to Alexander et al. 2001.

Table.1.1. [185]. Chemokine receptors known to be sulfated and their cognate chemokines³

CXCL12, CX₃CL1 and CCL11 [102, 194, 206]. The structure of CXCL12 bound to three different variants of N-terminal sulfopeptides from receptor CXCR4 (with different combinations of sulfotyrosine residues sulfated) has been solved by Veldkamp et al. [207]. The different sulfotyrosine residues bind to different residues of CXCL12, suggesting the presence of distinct binding sites. However, the binding site for the tyrosine that contributes most to chemokine binding (Tyr-21) is a conserved sulfopeptide binding site present within a shallow cleft on chemokine surface. This same binding site was identified in our laboratory's structure of a sulfated CCR3 fragment bound to CCL11 [102].

In addition to the importance of chemokine receptor sulfation for chemokine binding, sulfation of the receptor CCR5 [191, 198] enhances the ability of CCR5 to act as a co-receptor for HIV-1, a critical step in the invasion of host cells by the virus [191].

1.8. Hypotheses, Project Aims and Thesis Outline

As discussed above, the activation of chemokine receptor CCR2 with the MCP chemokines is critical to the recruitment of monocytes (which differentiate to macrophages) in several inflammatory diseases. Our laboratory is investigating several aspects of chemokine recognition by CCR2. In this thesis, I describe two different aspects of these studies, specifically focusing on the structural basis of chemokine recognition by the sulfated receptor and the ability of different MCP chemokines to activate CCR2 leading to differential outcomes.

1.8.1. Hypotheses

- a. The N-terminal region of chemokine receptor CCR2 allosterically influences dimerisation of MCP-1.
- b. Interactions between specific residues in MCP chemokines and CCR2 are responsible for full versus partial agonism.

1.8.2. Project Aims

1. To characterise the thermodynamics of MCP-1 dimerisation and binding to CCR2 sulfopeptides

The Stone lab has shown that both monomeric and dimeric MCP-1 bind to sulfated peptides derived from the receptor CCR2 [38]. However, binding to the dimeric form caused some conformational changes in those parts of the N-terminus of the chemokine, which were involved in dimer formation. This conformational change destabilised the dimer interface, resulting in its dissociation to the active monomeric state [126], which indicated that the sulfated receptor promotes

dimer dissociation and chemokine activation.

This aim involved the study of the energetics of this important allosteric mechanism using N-terminal peptides from CCR2 that were sulfated at different positions. NMR was used to characterise the dynamic properties of MCP-1 monomer and dimer in coupled equilibria. Data were collected for the titration of wild type (WT) MCP-1 with different sulfopeptides. Furthermore, we developed a mathematical model to account for spectral changes and to describe the thermodynamics of the dimerisation. In addition, a computational algorithm was devised for simulation of observable NMR parameters and to fit these data to get the equilibrium constants for our thermodynamic model. Finally, the equilibrium dissociation constant and cooperativity values were determined by fitting the titration data using the algorithm. This novel approach gave us information simultaneously about coupled equilibrium, dimerisation and ligand binding.

2. To identify the structural elements of MCP-1 and MCP-3 involved in interactions with receptor CCR2 that define full versus partial agonism

Although, human MCP-1 and MCP-3 have 71% sequence identity, when bound to their shared chemokine receptor CCR2, they activate it with different maximal effects. In this aim we focused on determining the essential sequence differences between the two chemokines which cause such functional outcomes. As previous data indicated that the N-loop and $\beta 3$ region are important for binding to the N-terminus of the receptor [102], we hypothesized that by altering these regions of the chemokines, we could identify the structural elements responsible for full versus partial agonism. Thus, we created several MCP-1/MCP-3 chimeras and tested their interactions (binding and activation) with the CCR2 receptor.

3. To identify the key receptor site 2 interactions responsible for differential agonism and their dependence on site 1 interaction

CCR2 receptor mutants were used to identify site 2 residues of the receptor that differentially interact with chemokine ligands. Recent structures of two receptor complexes [105, 106] have shown that the N-terminal region of the chemokine penetrates and interacts with the residues lining the transmembrane helices of their receptors. As we know that MCP chemokines activate CCR2 differentially, we hypothesised that one ligand interacts more favorably with some residues within CCR2 as compared to other ligands. CCR2 mutants (with different transmembrane mutations) were expressed in stable cell lines and their binding affinity and activation profile were studied with wild type MCP-1 and MCP-3, to answer these questions.

1.8.3. Thesis Outline

The results from Aim 1 have been published as an Edge article in *Chemical Science* (2014). Therefore, the published paper is included as Chapter 3. The supplementary material from the paper has been added in the appendix II.

The outcomes of Aim 2 and 3 are presented as Chapters 4 and 5 in the thesis. A paper describing the results and conclusions from these Aims has been published by *Science Signalling* (2017).

Chapter 2. Materials and Methods

2.1. Materials

Oligonucleotides were purchased from Geneworks (Australia). Deoxynucleotide triphosphates (dNTPs) and all the enzymes required for cloning were purchased from NEB (Ipswich, MA) and Promega (Madison, WI, USA).

Dulbecco's Modified Eagle Medium (DMEM) and Hanks's balanced salt solution (HBSS) were from Invitrogen. Blastocidin and HygroGold were from InvivoGen (San Diego, CA). Foetal bovine serum (FBS) was from In Vitro Technologies (Noble Park, VIC, Australia). Polyethyleneimine was from Polysciences, Inc. (Warrington, PA). Coelenterazine h was from NanoLight (Pinetop, AZ). 5 mL HisTrap HP nickel affinity column and HiLoad 16/60 Superdex 75 preparative grade size exclusion column (PSEC) were from GE Healthcare. Unless otherwise noted, all other chemicals/reagents were purchased from Sigma-Aldrich.

2.2. Buffers, Media and Solutions

Ampicillin: 50 mg/mL in milliQ H₂O

Kanamycin: 30 mg/mL in milliQ H₂O

Inclusion body storage buffer: 20 mM Tris.HCl, pH 8.0, 150 mM NaCl, 0.02% (w/v) NaN₃

Lysis Buffer: 20 mM Tris.HCl, pH 8.5, 500 mM NaCl, 5 mM imidazole, 0.02% (w/v) NaN₃

Inclusion body wash buffer: 20 mM Tris.HCl, pH 8.5, 500 mM NaCl, 5 mM imidazole, 0.5% (v/v) TX-100, 2 mM DTT and 0.02% (w/v) NaN₃

His Trap column buffers

Buffer A: 20 mM Tris.HCl, pH 8.0, 500 mM NaCl, 20 mM imidazole

Buffer B: 20 mM Tris.HCl, pH 8.0, 500 mM NaCl, 200 mM imidazole

Thrombin cleavage buffer: 20 mM Tris.HCl, pH 8.5, 400 mM NaCl, 2.5 mM CaCl₂

Anion exchange Buffer A: 20 mM Bis-Tris (pH 6.5), pH 8.0

Anion exchange Buffer B: 20 mM Bis-Tris (pH 6.5), 1 M NaCl, pH 8.0

Cation exchange Buffer A: 20 mM Tris.HCl, pH 8.0

Cation exchange Buffer B: 20 mM Tris.HCl, 2 M NaCl/1 M NaCl

Superdex 75 16/60 Gel filtration buffer: 10 mM HEPES, pH 7.4, 150 mM NaCl

Running gel buffer: 1.5 M Tris.HCl, pH 8.8

Stacking gel buffer: 0.5 M Tris.HCl, pH 6.8

10 x Tank buffer: 0.25 M Tris.HCl, glycine (1.92 M), 10 g SDS

Gel drying buffer: 40 mL glycerol, 300mL EtOH, 660 mL milliQ H₂O

2 x R Loading Dye: 0.5 M Tris.HCl, pH 6.8, 2.5 mL Glycerol, 0.5% (w/v) bromophenol blue, 10% (w/v) SDS, 0.5 mL β -ME

2 x NR loading Dye: As above omitting the β -ME

His Trap stripping buffer: 20 mM NaH_2PO_4 , 0.5 M NaCl, 50 mM EDTA

LB media/per litre: 10 g tryptone, 5 g yeast extract, 10 g NaCl, 1 mL 1M NaOH

LB plates: 17.5 g agar/LB

Refolding buffer: 20mM Tris. HCl, pH 8.0, 400 mM NaCl, 2.0 mM/ 0.5 mM GSH/GSSG, 0.02% w/v NaN_3

Ni-NTA denaturing load buffer: 6 M guanidine HCl, 20 mM Tris, pH 8.0, 20 mM imidazole and 20 mM β -ME

Ni-NTA denaturing elution buffer: 6 M guanidine HCl, 20 mM Tris, pH 8.0 200mM imidazole, 20 mM β -ME

Fixing solution: 40% methanol, 13.5% formalin

Developing solution: 3% Na_2CO_3 , 0.05% formalin, 0.000016% $\text{Na}_2\text{S}_2\text{O}_3$

Phosphate buffered saline (PBS): 137 mM NaCl, 2.7 mM KCl, 10 mM Na_2HPO_4 and 2 mM KH_2PO_4 , pH 7.4

TAE buffer: 2 M Tris, 5.71% (v/v) glacial acetic acid and 50 mM EDTA (pH 8.0)

TBS: 50 mM Tris (pH 7.5), 150 mM NaCl

Primary antibody buffer: TBS/0.1% BSA

Blocking buffer: 0.1 M NaHCO_3 (pH 8.6) + 1% fat free milk

2.3. Bacterial Strains

The genotypes of competent cells (Invitrogen™) used in this study are as follows

1. DH5 α ™ - Φ 80*lacZ* Δ M15 Δ (*lacZYA-argF*) U169 *recA1 endA1 hsdR17* (rK $^-$, mK $^+$) *phoA supE44* λ - *thi-1 gyrA96 relA1*
2. BL21 (DE3) - *ompT hsdSB* (rB $^-$, mB $^-$) *gal dcm* (DE3)

2.4. Plasmids

Plasmid	Antibiotic Resistance	Source
pET11a + MCP-3	Ampicillin	Stone Laboratory
pET28a	Kanamycin	Stone Laboratory
pcDNA5/FRT/TO + CCR2	Ampicillin, Hygromycin, Blasticidin	Canals Laboratory
CCR2-Rluc8	Hygromycin, Blasticidin	Pfleger Laboratory
β -arrestin2-YFP	Hygromycin, Blasticidin	Pfleger Laboratory
pET28a + MCP-1	Kanamycin	This thesis
pET28a + MCP1-311	Kanamycin	This thesis
pET28a + MCP1-131	Kanamycin	This thesis
pET28a + MCP1-113	Kanamycin	This thesis
pET28a + MCP1-133	Kanamycin	This thesis
pET28a + MCP1-333	Kanamycin	This thesis
pET28a + MCP3-133	Kanamycin	This thesis
pET28a + MCP3-313	Kanamycin	This thesis
pET28a + MCP3-331	Kanamycin	This thesis
pET28a + MCP3-311	Kanamycin	This thesis
pET28a + MCP3-111	Kanamycin	This thesis
pcDNA5/FRT/TO (K34A)	Hygromycin, Blasticidin	This thesis
pcDNA5/FRT/TO (Y120F)	Hygromycin, Blasticidin	This thesis
pcDNA5/FRT/TO (V187A/V189A)	Hygromycin, Blasticidin	This thesis
pcDNA5/FRT/TO (N199A/T203A)	Hygromycin, Blasticidin	This thesis
pcDNA5/FRT/TO (R206A)	Hygromycin, Blasticidin	This thesis
pcDNA5/FRT/TO (Y259F)	Hygromycin, Blasticidin	This thesis
pcDNA5/FRT/TO (I263A/N266A)	Hygromycin, Blasticidin	This thesis
pcDNA5/FRT/TO (E270A/F272A)	Hygromycin, Blasticidin	This thesis
pcDNA5/FRT/TO (D284A)	Hygromycin, Blasticidin	This thesis
pcDNA5/FRT/TO (E291A)	Hygromycin, Blasticidin	This thesis

Table 2.1. List of all the plasmids used/generated during this thesis

2.5. DNA Analyses

2.5.1. Preparation of Competent Cells

A colony from a plate of freshly grown cells [DH5 α /BL21 (DE3)] was selected and transferred into 5 mL Luria-Bertani (LB) media. Cells were grown at 37 °C overnight. Two mL of this overnight culture was used to inoculate 200 mL LB in a 500 mL flask. The cells were grown shaking at 37 °C to OD₆₀₀ ~0.3-0.35. The cells were harvested by centrifugation at 3,000 x g for 5 minutes at 4 °C. The pellet was resuspended gently in 50 mL of 0.1 M CaCl₂ (sterile, filtered and chilled to 4 °C in ice-bath), followed by incubation on ice for 20 minutes. Cells were harvested by centrifugation at 3,000 x g for 5 minutes. The pellet (cells) was resuspended in 4 mL of ice-cold 0.1 M CaCl₂. Sterile-filtered 75% glycerol was used to make the freezer stock of competent cells (15% final glycerol concentration). Aliquots (50 μ L) were stored at -80 °C until needed.

2.5.2. Bacterial Transformation

A 50 μ L aliquot of competent *E. coli* was transformed with 1-5 μ L of DNA and incubated on ice for 30-45 minutes. Cultures were then heat shocked at 42 °C for 45 seconds and placed on ice for 1-2 minutes. Subsequently, 450 μ L of LB broth was added and the cultures incubated in a shaker at 37 °C for 60 minutes. Cultures were spread onto LB agar plates containing selection antibiotic and incubated overnight at 37 °C.

2.5.3. Plasmid DNA Preparation

Single colonies were picked from plates of transformed DH5 α *E. coli* and used to inoculate 5 mL cultures of LB broth containing selection antibiotic. Cultures were incubated overnight shaking at 37 °C for 17 hour (h). Plasmid DNA was isolated from the cells using a QIAprep Spin Miniprep Kit (QIAGEN) according to manufacturer's instructions. The concentration of the plasmid DNA was determined by spectrophotometric analysis of the sample. 5 μ L of eluted DNA sample was diluted with 495 μ L autoclaved water and the OD₂₆₀ and OD₂₈₀ were measured. The concentration of DNA in the original sample of eluted plasmid was calculated using the formula:

$$[\text{DNA}] (\mu\text{g}/\mu\text{L}) = \text{OD}_{260} \times 5 \quad (\text{Equation 1})$$

The purity of the DNA was estimated from the ratio of OD₂₆₀/OD₂₈₀. In general, ratios in the range of 1.65-1.85 were considered acceptable for DNA sequencing reactions. Higher values indicated RNA contamination, whereas lower values indicated protein contamination. The samples

were stored at -20 °C for further use.

2.5.4. Synthesis of Gene Constructs by PCR

Genes encoding all the chemokine chimeras were synthesised using recursive polymerase chain reaction (PCR). The primers were obtained from *Geneworks* (Australia) and dissolved to stock concentrations of 100 pmol/μL. Fig 2.1 explains the PCR scheme involved in the process. One full length gene construct was synthesised from six overlapping oligonucleotides. Firstly, oligonucleotides 3 and 4 prime against each other and are extended to create the first PCR product. In the next step, oligonucleotides 2 and 5 prime against the first PCR product and extension yields a second PCR product. In the last step, oligonucleotides 1 and 6 prime against the second PCR product to extend and amplify the product.

Recursive PCR reactions (total volume 50 μL) contained: oligonucleotides 3 and 4 (0.02 μM/μL each), 2 and 5 (0.1 μM/μL each) and 1 and 6 (1 μM/μL each); dNTPs (0.2 mM each); pfu buffer and Pfu polymerase (0.204 U/μL, Promega, Madison, WI, USA). Reactions were started at 95 °C for 5 minutes and then subjected to 30 cycles of 1 min at 95 °C (melting), 1 min at 60 °C (annealing) and 2 min at 72 °C (extension) using a Minicycler™ (MJ Research). The PCR products were purified by using a QIAquick PCR purification kit (QIAGEN) according to manufacturer's instructions then digested and ligated into the *NcoI/XhoI* (MCP-1 background) or *NcoI/BamHI* (MCP-3 background) restriction sites of the pET28a plasmid and transformed into DH5α (*E. coli*) cells. The colonies were further screened using colony PCR and 2% agarose gel electrophoresis (detail in section 2.5.6). Recombinant plasmids were prepared using the miniprep procedure (described in 2.5.3). (List of oligonucleotides used for chimeras and mutants is given in appendix III A and B. The protein and nucleotide sequences of all the chimeras have been given in appendix IV)

2.5.5. Site-directed Mutagenesis

Mutant clones for CCR2 were prepared by site-directed mutagenesis using the Quikchange protocols (Agilent technologies). The primers were diluted to storage stock concentrations of 100 pmol/μL. Working stocks were prepared by diluting to obtain the final concentration of 0.3 pmol/μL. Mutagenesis reactions (total volume 50 μL) contained: the starting plasmid (pcDNA5/FRT/TO-CCR2, ~200 ng/μL); two complementary oligonucleotide primers containing the desired mutation (0.3 pmol/μL each); dNTPs (1 mM each); Pfu buffer; and Pfu polymerase (3 U/μL). Reactions were incubated at 95 °C for 30 seconds and then subjected to 26 cycles of 30 seconds at 95 °C, 1 min at 55 °C and 15 min at 68 °C using a Minicycler™ (MJ Research). The PCR sample was treated with

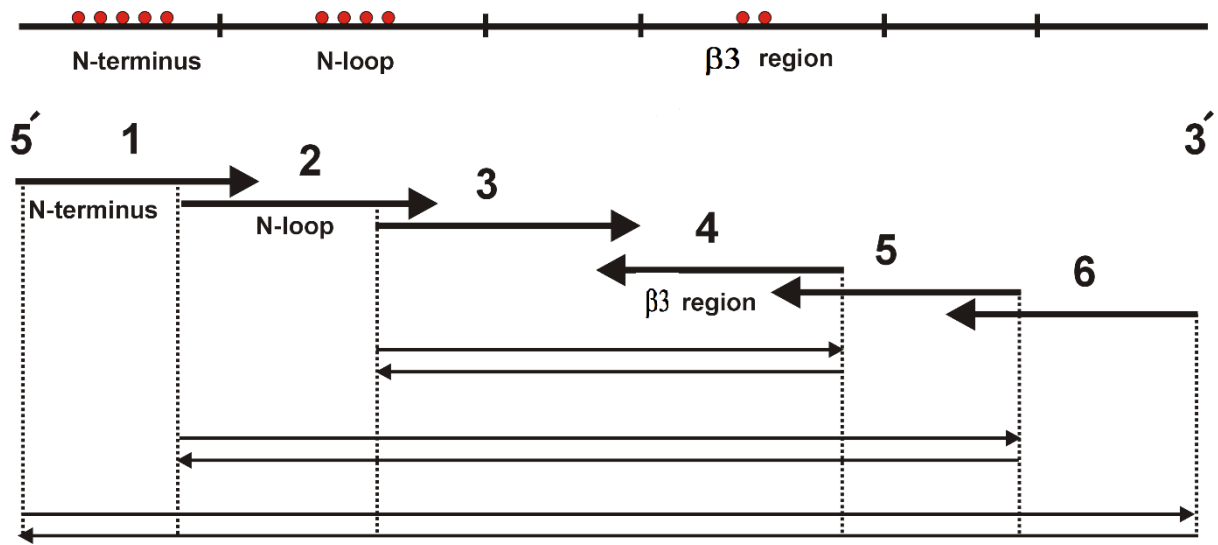


Figure 2.1. Schematics of recursive PCR process. Oligonucleotide 3 and 4 prime to form the first PCR product followed by priming of oligonucleotide 2 and 5 against the first product forming a second PCR product. And in final step oligonucleotide 1 and 6 prime with the second PCR product to extend.

DpnI (2 U/ μ L, New England Biolabs) for 1.5 h to digest the parental DNA, then 5 μ L was used to transform DH5 α cells (as described in 2.5.2).

2.5.6. Agarose Gel Electrophoresis

The TAE agarose gel electrophoresis was used throughout the cloning process. Agarose gels were prepared by dissolving 2% (w/v) agarose in 1x TAE buffer through heating. 1 x RedSafe Nucleic Acid staining solution (iNtRON Biotechnology) or ethidium bromide was added into the dissolved agarose solution. Samples were combined with 10 x loading dye. DNA Ladder (Promega) 1kb was used for molecular weight comparisons. A 1 x TAE buffer was used as the running buffer with electrophoresis performed at 100 V for ~50-60 minutes.

2.5.7. DNA Sequencing

Miniprep DNA samples (5 μ L of ~200 ng/ μ L) were sent to *Micromon, Monash University* for sequencing. Sequence analysis was performed using the software *Sequence Scanner 2.0* (Applied Biosystems).

2.6. Production and Purification of Recombinant Proteins in a Bacterial Expression System

The following procedure was used for production of all wild type and chimeric chemokines. BL21 (DE3) competent cells were transformed with the expression plasmid for the chemokine and were screened for best colony expression. A well isolated single colony was used to inoculate the starter culture, 50 mL of LB media containing kanamycin (30 μ g/mL) or ampicillin (50 μ g/mL). The culture was grown overnight in a shaker incubator at 37 °C at 180 rpm. For large-scale growth, four 2 L flasks, each containing 1 L of LB/antibiotic media, were inoculated with 10 mL of the overnight starter culture and left to grow at 37 °C, 180 rpm until an optical density (OD₆₀₀) of ~0.6-0.7 was reached. Next the expression of the chemokine was induced by addition of 1 mL of 1 M isopropyl β -D-1-thiogalactopyranoside (IPTG) to each flask. The flasks were left in the shaker incubator at 37 °C, 180 rpm overnight to continue protein expression.

Cells were harvested via centrifugation (Sorvall Evolution RC-SLC 6000 rotor, 5000 rpm, 15 minutes, 4 °C). The resultant pellet was resuspended in lysis buffer (60 mL) and hen egg white lysozyme (2 mL of 10 mg/mL) was added, followed by sonication of the cells with 6 x 30 seconds' bursts at 10 Ampere with 30 second to 1 minute incubations on ice between bursts (MSE Soni prep 150 plus). The insoluble fractions were separated by centrifugation and resuspended in lysis buffer along with DNase I to degrade the genomic DNA. The inclusion bodies (IBs) were washed four times

with lysis buffer and inclusion body wash buffer and left to denature overnight in the Ni-NTA denaturing load buffer. These denatured inclusion bodies were purified by immobilised metal affinity chromatography (IMAC) using Ni-NTA agarose (QIAGEN/Sigma; ~10 mL wet volume) and were refolded by dropwise dilution (0.1 mL/min) into refolding buffer (2 L) over 4-5 h. The solution was left overnight at 4 °C to ensure that refolding equilibrium has been attained. Refolded protein solution was filtered and degassed using a SPARMAX pump then loaded onto a 5 mL HisTrap nickel affinity column attached to a GE AKTA purifier chromatography system. The column was washed with HisTrap buffer A and the purified proteins were eluted at 5 mL/min using a stepwise isocratic elution with HisTrap buffer B. The fractions showing UV absorbance were further analysed on SDS-PAGE under reducing and non-reducing conditions.

As the expressed proteins have an N-terminal His₆-tag which is followed by a modified thrombin cleavage site (Leu-Val-Pro-Arg*-Gln¹-Pro², in which Gln¹-Pro² is the N-terminus of both MCP-1 and MCP-3), cleavage at Arg* releases the N-terminus of the required protein. Therefore, eluted proteins were dialysed against thrombin cleavage buffer overnight at room temperature using snakeskin dialysis tubing (3500 Da molecular weight cut off (MWCO)). The UV absorbance (280 nm) of the protein sample was measured. The mass of protein in the sample was measured using Beer-Lambert's Equation:

$$\text{mass} = A / \epsilon l \times M_w \times V \quad (\text{Equation 2})$$

Where A is the observed UV absorbance (280 nm); ϵ is the molar absorptivity coefficient for protein (8730 M⁻¹.cm⁻¹); l is the length of the cuvette (1 cm); M_w is the molecular weight of the protein to cleave and V is the volume of the sample.

Dialysis was followed by incubation with thrombin (10 U/mg of protein) overnight at 37 °C to cleave the protein at the thrombin cleavage site and remove the N-terminal His₆-tag. To halt the thrombin cleavage reaction phenylmethanesulfonylfluoride (PMSF) (final concentration 200 μM) was used after 24 h. The protein was again loaded on the 5 mL His-trap column to remove the His₆-tag and any uncleaved protein if still present at this stage. The flow-through containing the cleaved protein was collected, concentrated to 2 mL and loaded onto a Hi-load 16/60 Superdex 75 prep grade size exclusion chromatography (SEC) column attached to a GE AKTA purifier FPLC system. The proteins were eluted with HEPES buffer at 0.3 mL/min. The fractions containing the correct protein were pooled and concentrated. Protein purity was evaluated by SDS-PAGE.

2.7. Protein Analysis

2.7.1. SDS-PAGE Gel Electrophoresis

A 15 % polyacrylamide running gel was prepared and polymerisation initiated with 0.1% ammonium persulfate (APS), stabilised by 0.01% TEMED. This was immediately poured between the plates of a Mini-Protean II SDS-PAGE apparatus (Bio-Rad®). When the running gel had polymerised, a 4% stacking gel was prepared with 0.1% APS, 0.01% TEMED and poured on top of the running gel. A comb was added into the top of the stacking gel to form wells, and the gel allowed to polymerise.

Once the gel had polymerised, samples were boiled for 5 minutes and then loaded into the wells alongside protein markers and electrophoresed at 200 V in a Mini-Protean II assembly (Bio-Rad®) with SDS-PAGE running Tank buffer until the dye front migrated off the bottom of the gel.

2.7.2. Silver Staining

For silver staining, the running gel was incubated at room temperature for 10 minutes in fixing solution, followed by washing with milliQ water, 1 minute in 0.02% Na₂S₂O₃, followed by washing again with milliQ water, and then 10 minutes in 0.1% silver nitrate solution. The gel was then washed twice with milliQ water and incubated in developing solution (approx. 1-3 minutes) until protein bands were visible. Citric acid (2.3 M) was used to stop the reaction and the gel was then washed a further 3 times in milliQ water.

2.8. Nuclear Magnetic Resonance (NMR)

NMR experiments were conducted at 25 °C on a Bruker Avance 600 MHz spectrometer equipped with a triple-resonance cryoprobe. Chemical shifts were referenced to internal or external 4, 4-dimethyl-4-silapentane-1-sulfonic acid (DSS). All the samples were exchanged into NMR buffer (20 mM sodium acetate-d₄, 5% D₂O, 0.02% NaN₃, pH 7.0). 1D ¹H experiments were recorded with 128 scans using gradient water suppression. NMR data was processed using Bruker TopSpin 3.0.

2.9. Homology Modelling of CCR2:Chemokine Complexes

A structural model of CCR2 bound to MCP-1 was produced by Bradyn Parker (Stone lab) through homology modelling based on the structure of CXCR4 in complex with a viral chemokine vMIP-II (PDB code: 4RWS) [105]. Using Bio python, the two receptors were aligned using a dynamic alignment algorithm. The alignment was then used to produce a series of models with the program

Modeller. Subsequently, the chemokine was aligned to vMIP-II to give the CCR2:MCP-1 complex models.

2.10. Design and Selection of the Receptor Mutants

The model of CCR2 bound to MCP-1 was used to identify residues within RS2, which could potentially influence the interactions differentially with different ligands. The target residues were selected based on orientation within RS2 and each chosen residue was analysed in PyMOL to determine where mutations are structurally allowable. Although most of the residues were mutated to alanine, the target tyrosine residues were mutated to phenylalanine, as they are in the center of the RS2, and an alanine mutation was most likely to destabilise the structure.

2.11. Construction and Expression of CCR2 Mutants

Individual CCR2 residues or pairs of residues were selected for mutation based on their locations and orientations in the predicted chemokine binding site on the interior of the TM helical bundle. The wild type c-Myc-FLAG-CCR2 construct in pcDNA5/FRT/TO [38] was used as a template for Quikchange site-directed mutagenesis to generate CCR2 mutants. Wild type and mutant c-Myc-FLAG-CCR2 constructs were transfected in HEK293 FlpIn TReX cells using Lipofectamine (Invitrogen™) (details in section 2.13). Cells were selected and maintained at 37 °C in 5% CO₂ humidified incubators. Receptor expression was induced 24 h prior to each experiment by addition of 10 µg/mL tetracycline.

2.12. Mammalian Cell Line and Culture

In all cell culture experiments, we used human embryonic kidney 293 (HEK 293) cells stably transfected with the vector FlpIn™ TREx™ 293 (Invitrogen™) into which we had sub-cloned the sequence encoding c-Myc-FLAG-CCR2 (see above). The FlpIn expression system ensures that the receptor transgene will be incorporated into the same position of the genome in each cell, maintaining equal receptor expression levels across cells. The TREx (tetracycline-regulated expression) system places the receptor gene under transcriptional control of the tetracycline-repressor gene, thereby activating transcription only in the presence of tetracycline. The cells were grown and maintained in full media comprised of Gibco™ DMEM supplemented with 5% (w/v) tetracycline-free foetal bovine serum (FBS) 5 µg/mL blasticidin (Invitrogen) to maintain selection of cells stably transfected with the tet-repressor gene, and 200 µg/mL Hygromycin B (Invitrogen) to maintain selection of cells stably transfected with the gene of interest.

Cells were grown and maintained at 37 °C in 5% CO₂ in 175 cm² flasks and were detached from the flask by washing with versene (PBS/EDTA), followed by incubation in versene for 5 minutes. The receptor expression was induced 24 h prior to each experiment by addition of 10 µg/mL tetracycline to cell media.

2.13. Generation of Stable Cell lines

Correctly sequenced plasmids were used to generate stable cell lines. 2.5 x 10⁶ HEK293 Flp-In TRex cells were plated in a T25 flask. The DNA (10 µg total: 1 µg pcDNA5/FRT/TO-GOI + 9 µg pOG44) was diluted in 625 µL of reduced serum media (Opti-MEM). 25 µL Lipofectamine 2000 (Invitrogen™) was mixed with 600 µL Opti-MEM and incubated at room temperature for 5 minutes and then was added to the DNA tubes, which were then incubated for 20 minutes at room temperature. The old media from the cells was replaced by Opti-MEM. This was followed by the addition of (1.25 mL) complexes (Lipofectamine and DNA) to the cells and plates were left at 37 °C. The media was changed after 4-6 h to Dulbecco's Modified Eagle Medium (DMEM) supplemented with 5% (v/v) tetracycline-free foetal bovine serum (FBS). Cells were split 48 h post-transfection. Selection of the cells was started using the media containing Hygromycin (200 µg/mL) and blasticidin (5 µg/mL). The cells were fed with the selective medium every 3-4 days till foci were visible. This practice was continued till stable cell-lines were achieved.

2.14. Cell Based Assays

2.14.1. Cell Surface Receptor Expression: Whole Cell (Enzyme-Linked Immunosorbent Assay (ELISA))

Cells were plated at 2 x 10⁵ cells per well in a poly-D-lysine coated 48 well clear bottom plate. Cells were grown in full media containing 10 µg/mL tetracycline in 5% CO₂ at 37 °C overnight. After 24 h the media was removed and cells were fixed with 4% paraformaldehyde at room temperature for 30 minutes. Cells were washed once with TBS. Cells which required permeabilisation were incubated with 0.5% (v/v) IGEPAL[®] CA-630 in TBS for 30 minutes at room temperature. Cells which did not require permeabilisation were incubated with TBS for the same time. Cells were washed with TBS to remove traces of the IGEPAL[®] CA-630 NP-40 and blocked with blocking buffer for 4 h at room temperature on a shaker to reduce the non-specific binding. It was then replaced with the primary antibody, anti-c-Myc (9E10, Sigma) diluted 1:2000 in TBS/0.1% (w/v) BSA and plates were left on a shaker overnight at 4 °C.

To remove traces of primary antibody, cells were washed three times with TBS and incubated on the shaker with secondary antibody, anti-mouse-IgG-horseradish peroxidase diluted 1:2000 in blocking buffer. Cells were washed three times with TBS and then treated with SIGMAFAST™ OPD substrate solution, which is used to detect the level of peroxidase activity. The reaction was stopped by adding 3 M HCl as soon as a clear colour difference was visible between positive and negative controls. The OD was determined by reading the absorption at 490 nm (OD₄₉₀) on PerkinElmer EnVision 2103 multilabel plate reader. Data were normalised as the ratio of OD₄₉₀ of the mutants over the OD₄₉₀ of the wild type CCR2. For internalisation experiments, cells were stimulated with 100 nM of chemokine in full media and incubated for 1 h at 37 °C, and rinsed with DMEM at pH 2.5 prior to fixation [208]. All experiments were carried out in triplicate and repeated independently three times.

2.14.2. Membrane Preparation and Radioligand Binding Assays

Cell membranes were prepared by detaching the cells from the flasks, centrifugation at 1500 x g for 3 minutes and resuspension in ice-cold 50 mM MOPS buffer with 5 mM MgCl₂ and 0.1% 3-[(3-cholamidopropyl)-dimethylammonio]-1-propanesulfonic acid (CHAPS), pH 7.4. The lysates were homogenised by sonication and centrifuged at low speed for 5 minutes. Membrane and cytosolic fractions were separated by centrifugation of the supernatants at relative centrifugal force (rcf) of 40,000 x g for 30 minutes at 4 °C. The membrane pellet was resuspended in MOPS buffer with 5 mM MgCl₂ and 0.1% CHAPS, pH 7.4 and stored at -20 °C. Protein concentrations were measured using a BCA protein determination assay [209].

Competitive radioligand binding assays were performed as described by Zweemer et al. [210] using ¹²⁵I-CCL2 (product no. NEX332005UC) purchased from PerkinElmer (Australia). It was stored for a week before usage. Briefly, binding assays were performed in a 100 µL reaction volume containing 50 mM MOPS buffer (pH 7.4), 5 mM MgCl₂, 0.1% CHAPS, 5-20 µg of membranes, increasing concentrations of chemokines and 45 pM ¹²⁵I-MCP-1. Membranes were incubated for 120 minutes at 37 °C. Nonspecific binding was determined in the presence of 10 µM INCB3344. Binding was terminated by dilution with ice-cold 50 mM MOPS buffer supplemented with 0.05% CHAPS and 0.5 M NaCl followed by rapid filtration through a 96-well GF/C filter plate precoated with 0.5% polyethyleneimine using a PerkinElmer Filtermate-harvester (PerkinElmer, Groningen, The Netherlands). Filters were washed 3 times with ice-cold wash buffer, dried at 50 °C, and 25 µL of MicroScint-O scintillation cocktail (PerkinElmer) was added to each well. Radioactivity was determined by using a MicroBeta² LumiJET 2460 Microplate Counter (PerkinElmer). The average

data were plotted and fitted by non-linear regression analysis to competitive binding equation of One site-Fit K_i using GraphPad Prism v.6.0 software.

2.14.3. β -Arrestin 2 Recruitment Using a BRET-Based Assay

Recruitment of β -arrestin-2 to CCR2 was assessed in HEK293 Flp-In TRex transiently transfected with CCR2-RLuc8 and β -arrestin-2-YFP [211]. Cells were plated in petri plates (approximately 2.5×10^6 cells per plate) and allowed to grow for 48 h in full media at 37 °C in 5% CO₂. The plasmids encoding CCR2-RLuc8 and β -arrestin-2-YFP were diluted in 150 mM NaCl at a receptor:arrestin ratio of 1:4 and added to an equal volume of Polyethyleneimine (PEI) in 150 mM NaCl. A 1 μ g:6 μ g ratio of DNA:PEI was used and, after mixing, the tube was vortexed quickly for 3-5 seconds. This transfection mixture was incubated for 10 minutes at room temperature then added to the cells dropwise and plates were swirled to ensure even mixing. After 24 h, the media was changed to fresh full media and replated to poly-D-Lysine (PDL)-coated white 96 well white opaque CulturePlates (PerkinElmer). Next day, the cells were rinsed once and incubated in HBSS to a total volume of 80 μ L per well for approximately 30 minutes at 37 °C (in absence of 5% CO₂). Coelentrastazine h was diluted in HBSS (final concentration 5 μ M) and added to each well and further incubated for 10 minutes followed by the addition of the chemokines. Cells were incubated for an additional 10 minutes in the dark at 37 °C. RLuc and YFP signals were then detected on a PHERAstar plate reader (BMG Labtech, Ortenberg, Germany) that allows for sequential integration of the signals detected at 475 ± 30 and 535 ± 30 nm, using filters with the appropriate band pass. Data are presented as a ligand-induced BRET ratio (YFP:RLuc). The data were normalised by subtracting the BRET ratio of vehicle treated cells. All experiments were carried out in triplicate and repeated independently three times.

2.14.4. Inhibition of Forskolin-induced cAMP

The ability of ligands to inhibit forskolin-induced cAMP production was assessed in c-Myc-FLAG-CCR2 HEK293 FlpIn TRex cells transiently transfected to express the CAMYEL cAMP BRET biosensor [208]. Cells were grown overnight in white poly-D-Lysine-coated 96-well Culturplates (PerkinElmer).

Transient transfection was performed using PEI at a 6:1 ratio of DNA. 48 h after transfection cells were rinsed and pre-incubated in HBSS for 30 minutes at 37 °C. Cells were then incubated with the RLuc substrate Coelenterazine h, final concentration 5 μ M, for 5 minutes. It was followed by a further 5 minutes incubation with increasing concentrations of the chemokine. Forskolin was then added to a final concentration of 10 μ M. After 5 minutes the YFP and the RLuc emissions were

measured using a LumiSTAR Omega (BMG Labtech, Ortenberg, Germany) that allows for sequential integration of the signals detected at 475 ± 30 and 535 ± 30 nm, using filters with the appropriate band pass. BRET ratio was calculated as the ratio of YFP to RLuc signals, and data are expressed as the percentage of the forskolin-induced signal. All experiments were carried out in triplicate and repeated independently three times.

2.14.5. ERK 1/2 Phosphorylation Assay

Phosphorylation of ERK 1/2 was measured using the AlphaScreen® SureFire® p-ERK 1/2 (Thr202/Tyr204) Assay Kit (PerkinElmer, TGR biosciences) following the manufacturer's instructions. 4×10^5 cells/well were seeded in a poly-D-Lysine-coated 96-well plate in full media containing 10 µg/mL tetracycline. After 6 h incubation at 37 °C in 5% CO₂ cells were washed twice with PBS and serum starved overnight to minimize basal levels of phosphorylation by incubation in serum (FBS)- free media (SFM) containing 10 µg/mL tetracycline. The cells were stimulated with chemokines in SFM to an aggregate volume of 100 µL per well. Initial time-course experiments determined that peak levels of ERK 1/2 phosphorylation were achieved 3-5 minutes after the addition of chemokines. In subsequent concentration response experiments cells were stimulated with chemokine for 3 minutes at 37 °C. The reaction was stopped 3 minutes after stimulation with the chemokines by removal of media and replacement with 100 µL of SureFire lysis buffer to each well. Lysis of cells was assisted by stirring the plate on a plate shaker at 600 rpm for 5 minutes. Next 5 µL of lysate from each well was transferred to a white 384-well Proxiplate™ and 8 µL of SureFire AlphaScreen detection mix (240:1440:7:7 (v/v) dilution of SureFire Activation buffer: SureFire Reaction Buffer: AlphaScreen Acceptor Beads: AlphaScreen Donor Beads) was added to each well in low-light or green light conditions. This detection mix contains antibodies that form complexes with phosphorylated ERK 1/2. AlphaScreen donor and acceptor beads are brought closer by binding the antibody complexes, allowing energy transfer from the donor to the acceptor bead, which increases the fluorescence of the acceptor beads with increasing pERK 1/2. The plate was incubated in the dark for 1.5 h at 37 °C and the AlphaScreen signal was read on an *Envision*® plate reader (PerkinElmer). The data were normalised between the fluorescence emitted without chemokine (0% response) and in the presence of 10% (v/v) FBS (100% response). All experiments were performed in triplicate and replicated at least three times independently.

2.15. Data Analysis and Statistics

All data points represent the mean and error bars represent the standard error of the mean (SEM) of at least three independent experiments. The results were analyzed using Prism 6.0

(GraphPad Software Inc., San Diego, CA). All data from concentration-response curves for β -arrestin 2 and ERK phosphorylation were normalised as outlined above and fitted using the following three parameter equation (equation 3)

$$Y = bottom + \frac{top - bottom}{1 + 10^{(\log EC_{50} - \log[A])}} \quad (\text{Equation 3})$$

in which *top* and *bottom* represent the maximal and minimal asymptote of the concentration–response curve, $[A]$ is the molar concentration of agonist and EC_{50} is the molar concentration of agonist required to give a response half way between *bottom* and *top*. Concentration–response data were also fitted to the following form of the operational model of agonism [212] to allow the quantification of biased agonism

$$Y = basal + \frac{(E_m - basal) \left(\frac{\tau}{K_A} \right)^n [A]^n}{[A]^n \left(\frac{\tau}{K_A} \right)^n + \left(1 + \frac{[A]}{K_A} \right)^n} \quad (\text{Equation 4})$$

in which E_m is the maximal possible response of the system, *basal* is the basal level of response, K_A represents the equilibrium dissociation constant of the agonist (A) and τ is an index of the signalling efficacy of the agonist that is defined as R_T/K_E , where R_T is the total number of receptors and K_E is the coupling efficiency of each agonist-occupied receptor, and n is the slope of the transducer function that links occupancy to response. The analysis assumes that the transduction machinery used for a given cellular pathway are the same for all agonists, such that the E_m and transducer slope (n) are shared between agonists. Data for all chemokines for each pathway were fit globally, to determine values of K_A and τ . Biased agonism was quantified as previously described [213]. In short, to exclude the impact of cell-dependent and assay-dependent effects on the observed agonism at each pathway, the $\log(\tau/K_A)$ value of a reference agonist, in this case MCP-1 WT, is subtracted from the $\log(\tau/K_A)$ value of the other chemokines to yield $\Delta\log(\tau/K_A)$. The relative bias can then be calculated for each chemokine at the two different signalling pathways by subtracting the $\Delta\log(\tau/K_A)$ of one pathway from the other to give a $\Delta\Delta\log(\tau/K_A)$ value, which is a measure of bias. A lack of biased agonism will result in values of $\Delta\Delta\log(\tau/K_A)$ not significantly different from 0 between pathways. To account for the propagation of error associated with the determination of composite parameters, the following equation was used:

$$Pooled_SEM = \sqrt{(SEj1)^2 + (SEj2)^2} \quad (\text{Equation 5})$$

Where pooled_SEM is the calculated difference in the error and SEj1 and SEj2 is the individual uncorrelated/random error values used to propagate the pooled SEM value.

For radioligand binding, the concentration of agonist that inhibited half of the ^{125}I -MCP-1 binding (IC_{50}) was determined using the following equation:

$$Y = \frac{Bottom + (Top - Bottom)}{1 + 10^{(X - \log IC_{50})n_H}} \quad (\text{Equation 6})$$

in which Y denotes the percentage-specific binding, *Top* and *Bottom* denote the maximal and minimal asymptotes, respectively, IC_{50} denotes the X-value when the response is midway between *Bottom* and *Top*, and n_H denotes the Hill slope. For ^{125}I -MCP-1 homologous competition-binding experiments, estimates of affinity (K_d) were obtained using the equation:

$$IC_{50} = [Hot] + K_d \quad (\text{Equation 7})$$

For all other chemokines IC_{50} values obtained from the inhibition curves were converted to K_i values using the Cheng and Prusoff equation [214].

All affinity (pK_i), potency (pEC_{50}) and transduction ratio ($\log(\tau/K_A)$) parameters were estimated as logarithms. Christopoulos et al. have previously demonstrated that the logarithm of the measure is approximately Gaussian [215] and, as the application of t-tests and analyses of variance assume Gaussian distribution, estimating the parameters as logarithms allows valid statistical comparison.

Multiple T test comparison with Holm-Sidak correction or one way ANOVA were used as stated in figure legends. Significance is defined as * for $p < 0.05$, ** for $p < 0.01$ and *** for $p < 0.001$ for the comparison graphs.

***Chapter 3. NMR
Characterisation of
Cooperativity: Fast Ligand
Binding Coupled to Slow
Protein Dimerisation***

3.1. Preface to Chapter 3

It has been discussed in the Introduction and in our recent review article [42] that chemokine:receptor interactions can be regulated at many different levels, including: the post-translational sulfation of chemokine receptors; and oligomerisation of the chemokines.

In a previous study, the Stone lab has shown that an obligate MCP-1 dimer (T10C) is inactive, whereas a previously characterised form, the obligate monomeric MCP-1 (P8A) is active [36, 38]. MCP-1 (T10C) was evaluated against both wild type MCP-1 and MCP-1 (P8A) in cell based binding and activation assays, which showed that MCP-1 (T10C) is unable to bind and activate CCR2 (up to $\sim 1 \mu\text{M}$) [38].

In a subsequent study by Tan et al. [126] the lab investigated the interactions of both monomeric and dimeric forms, as well as wild type MCP-1, with sulfated peptides derived from the N-terminus of CCR2 [126]. They reported that both forms of MCP-1 bind to the receptor peptides. However, the monomer binds more tightly than the dimeric form, ($\sim 3\text{-}10$ fold, depending on the sulfation state). Correspondingly, they also reported that the sulfated peptides appeared to induce dissociation of the wild type dimer (inactive state) into wild type monomer (active state) [126].

These latter results suggested that binding of the receptor N-terminus to the chemokine is thermodynamically coupled to dimerisation of the chemokine (or dimer dissociation). Rigorous characterisation of such coupled equilibria is experimentally challenging. However, the data reported by Tan et al. [126] suggested that it would be possible by careful analysis of 2D NMR data. For this reason, we undertook the study described in this chapter to develop a mathematical model, which can describe the thermodynamics of the dimerisation coupled to ligand binding.

This chapter is comprised of a published manuscript (**Huma Z.E.**, Ludeman J.P., Wilkinson B.L., Payne R.J., Stone M.J., NMR Characterisation of Cooperativity: fast ligand binding coupled to slow protein dimerisation. Chem Sci. 2014; 5: 2783-8, DOI: 10.1039/c4sc00131a.) in which we described this theoretical approach and applied it to characterising the coupled dimerisation and receptor peptide binding by MCP-1. The supplementary data is included as Appendix II. The results have been reprinted with permission from the journal. (© The Royal Society of Chemistry 2014)

NMR characterization of cooperativity: fast ligand binding coupled to slow protein dimerization†

Cite this: *Chem. Sci.*, 2014, 5, 2783Zil E Huma,^a Justin P. Ludeman,^a Brendan L. Wilkinson,^b Richard J. Payne^c and Martin J. Stone*^a

We describe a general approach for analysis of 2D NMR spectra to evaluate the cooperativity of ligand binding and protein dimerization in coupled systems. The approach is applicable to systems in which NMR spectra display separate resonances for monomeric and dimeric species but each resonance shifts in response to ligand binding. Three experimental parameters (monomer chemical shift, dimer chemical shift and relative monomer–dimer peak intensity) are fitted globally, as a function of ligand concentration, to yield equilibrium constants for dimerization, monomer–ligand binding and dimer–ligand binding as well as the cooperativity between ligand binding and dimerization. We have applied the approach to characterise a system in which dimerization of the chemokine monocyte chemoattractant protein-1 (MCP-1/CCL2) is coupled to binding of peptides derived from the chemokine receptor CCR2. The global fitting approach allowed evaluation of cooperativity with higher precision than is possible by alternative methods.

Received 13th January 2014
Accepted 24th April 2014

DOI: 10.1039/c4sc00131a

www.rsc.org/chemicalscience

Introduction

Dimerization is a common property of proteins and frequently influences interactions with binding partners, including proteins, nucleic acids, polysaccharides, lipid membranes, metal ions and small molecules.^{1,2} A fundamental thermodynamic characteristic of such proteins is cooperativity between protein dimerization and ligand binding, defined as the factor by which dimerization enhances (or reduces) the ligand binding affinity. The classical approach to characterize the cooperativity in such coupled systems is to analyze the influence of ligand concentration on the position of the monomer–dimer equilibrium and/or the influence of the total protein concentration on the apparent ligand binding affinity.^{3–9} This typically requires an extensive series of experiments; the analysis is further complicated if both monomeric and dimeric species bind to the ligand. In such coupled systems it would be advantageous to measure ligand binding using a technique that simultaneously reports on the dimerization state of the protein. Herein, we show that 2D NMR can achieve this because different features of NMR spectra are sensitive to ligand binding and dimerization. We present a novel theoretical framework for analysis of such

2D NMR data and we demonstrate application of this approach to characterizing the interactions of a chemokine with fragments of a chemokine receptor.

Chemokines are soluble proteins that activate G protein-coupled receptors in leukocyte membranes, thereby inducing leukocyte trafficking in both inflammation and normal immune surveillance.^{10,11} Most chemokine receptors contain sulfated tyrosine residues in their extracellular N-terminal regions, the site of initial binding by chemokine ligands, and receptor tyrosine sulfation enhances chemokine binding affinity.^{12,13} Many chemokines dimerize weakly, although members of the two major chemokine families (CC and CXC) have distinct dimer structures.^{13,17} Although the monomeric form is sufficient for receptor binding and activation, the dimeric forms of some CC and CXC chemokines are also able to bind to the N-terminal regions of their receptors;^{12,18,19} the dimeric forms of certain CXC chemokines can even activate their receptors.^{20–24} Here, we analyze the interactions of sulfated N-terminal peptides derived from the chemokine receptor CCR2 with both monomeric and dimeric forms of the chemokine monocyte chemoattractant protein-1 (MCP-1/CCL2).

Results and discussion

NMR observation of coupled equilibria

Wild type human MCP-1 has been shown previously to dimerize with a dissociation equilibrium constant (K_{MD}) in the low micromolar range.^{14–16} The 2D ¹⁵N-¹H NMR spectrum (¹⁵N-HSQC) of MCP-1 displays peaks corresponding to both monomeric and dimeric species, indicating that the rate of

^aDepartment of Biochemistry and Molecular Biology, Monash University, Clayton, VIC 3800, Australia. E-mail: martin.stone@monash.edu

^bSchool of Chemistry, Monash University, Clayton, Victoria 3800, Australia

^cSchool of Chemistry, The University of Sydney, Sydney, New South Wales 2006, Australia

† Electronic supplementary information (ESI) available: Experimental, data analysis and fitting methods and the iterative computational algorithm used for simulation of NMR parameters. See DOI: 10.1039/c4sc00131a

exchange between these two forms is slow in comparison to the minimum frequency difference between corresponding monomer and dimer peaks, *i.e.* slower than $\sim 100 \text{ s}^{-1}$. Upon addition of sulfated N-terminal peptides derived from chemokine receptor CCR2, we observe that both monomer and dimer peaks in the ^{15}N -HSQC of MCP-1 shift monotonically until saturation is reached but they remain as separate resonances (Fig. 1 and S1†).

This indicates that (1) both the monomeric and dimeric species are binding to the peptide; (2) the rate of exchange between the free and bound forms of the monomer (or of the dimer) is fast in comparison to the frequency differences between free and bound resonances (faster than $\sim 100 \text{ s}^{-1}$); and (3) the rate of exchange between the bound monomer and bound dimer species remains slow in comparison to the monomer–dimer frequency differences. However, in addition to undergoing frequency changes in response to ligand binding, the relative intensities of the monomer and dimer peaks also change, indicating that ligand binding alters the position of the monomer–dimer equilibrium. Thus, the spectra contain independent parameters [change in monomer chemical shift (m); change in dimer chemical shift (d); and the ratio of monomer to dimer peak intensity (r_{MD})] that report on each of the three equilibrium processes [monomer–peptide binding; dimer–peptide binding; and monomer–dimer equilibrium, respectively]. In theory, these three parameters can be used to fully characterize the thermodynamics of the coupled equilibrium system, including cooperativity.

Thermodynamic model of coupled equilibria

The simplest thermodynamic model to explain these data is the set of coupled equilibria shown in Fig. 2. This model contains five equilibrium constants of which only three are independent (coloured red in Fig. 2); the others are mathematically related to

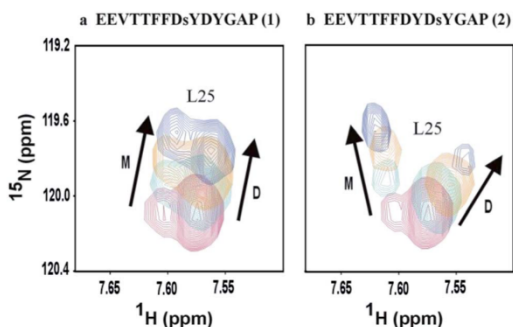


Fig. 1 Binding of MCP-1 to sulfopeptides corresponding to a fragment of the CCR2 extracellular domain [CCR2 (18–31)]. A detailed region (Leu-25 NH resonances) of the ^{15}N -HSQC spectrum is shown for 50 μM MCP-1 alone (red) and in the presence of 20 μM (cyan), 50 μM (orange) and 150 μM (blue) of CCR2 sulfopeptides: (a) 1 and (b) 2, whose amino acid sequences are shown at the top (sY = sulfotyrosine); the sulfopeptides have free N-termini and C-terminal amide moieties. Sulfopeptide-induced shifts of monomer (M) and dimer (D) resonances are indicated by arrows.

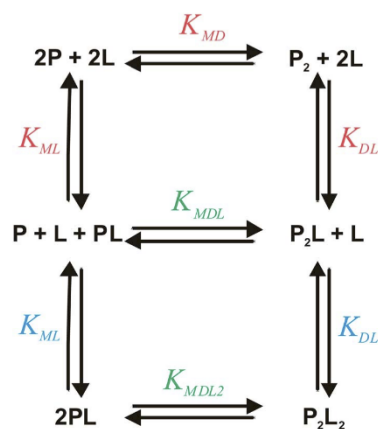


Fig. 2 Thermodynamic model of coupled equilibria. Ligand binding by monomeric and dimeric protein (K_{ML} and K_{DL} , respectively) is coupled to protein dimerization (K_{MD} , K_{MDL} and $K_{\text{MDL}2}$).

the first three. The equilibrium between the protein monomer (P) and dimer (P_2) is characterized by the equilibrium dissociation constant K_{MD} ,

$$K_{\text{MD}} = \frac{[\text{P}]^2}{[\text{P}_2]} \quad (1)$$

The monomer can bind to a single molecule of ligand (L) with equilibrium dissociation constant K_{ML} , defined as:

$$K_{\text{ML}} = \frac{[\text{P}][\text{L}]}{[\text{PL}]} \quad (2)$$

whereas the dimer is assumed to bind independently to two molecules of ligand with equilibrium dissociation constant K_{DL} , defined as:

$$K_{\text{DL}} = \frac{[\text{P}_2][\text{L}]^2}{[\text{P}_2\text{L}_2]} = \frac{[\text{P}_2\text{L}][\text{L}]}{[\text{P}_2\text{L}_2]} \quad (3)$$

The two additional equilibrium dissociation constants in the model, which characterize heterodimerization of free and ligand-bound monomers (K_{MDL}) and homodimerization of the ligand-bound monomer ($K_{\text{MDL}2}$), are related to the above independent parameters by the relationships:

$$K_{\text{MDL}} = \frac{[\text{P}][\text{PL}]}{[\text{P}_2\text{L}]} = \frac{K_{\text{MD}}K_{\text{DL}}}{K_{\text{ML}}} \quad (4)$$

and

$$K_{\text{MDL}2} = \frac{[\text{PL}]^2}{[\text{P}_2\text{L}_2]} = \frac{K_{\text{MD}}K_{\text{DL}}^2}{K_{\text{ML}}^2} \quad (5)$$

The influence of protein dimerization on ligand binding is represented by the cooperativity factor, c , defined as:

$$c = \frac{K_{DL}}{K_{ML}} = \frac{K_{MDL}}{K_{MD}} = \frac{K_{MDL2}}{K_{MDL}} \quad (6)$$

We aimed to determine each of the equilibrium constants and the cooperativity in the thermodynamic model from the three experimental observables described above and the total concentrations of protein (held constant) and ligand (varied) in a series of samples. The experimental observables are related to the concentrations of species in the thermodynamic model by the following relationships:

$$m = m_{\max} \frac{[PL]}{[P] + [PL]} \quad (7)$$

$$d = d_{\max} \frac{[P_2L] + 2[P_2L_2]}{2[P_2] + 2[P_2L] + 2[P_2L_2]} \quad (8)$$

$$r_{MD} = \frac{[P] + [PL]}{2[P_2] + 2[P_2L] + 2[P_2L_2]} \quad (9)$$

in which m_{\max} and d_{\max} represent the maximum changes in monomer and dimer chemical shifts, respectively, upon ligand binding. Similarly, the total concentrations of protein (P_i) and ligand (L_i) used in the experiment can be expressed as:

$$[P_i] = [P] + [PL] + 2[P_2] + 2[P_2L] + 2[P_2L_2] \quad (10)$$

and

$$[L_i] = [L] + [PL] + [P_2L] + 2[P_2L_2] \quad (11)$$

It is not possible to express the experimental observables explicitly in terms of the thermodynamic parameters. However, the relationships between these parameters can be determined using the iterative algorithm presented in the ESI (Fig. S2†). To illustrate these relationships, we have simulated the dependence of the experimental observables on ligand concentration for a constant protein concentration (50 μM) and various

combinations of equilibrium dissociation constants (Fig. 3). As expected intuitively, variation of the dimerization equilibrium constant (K_{MD} , Fig. 3a) influences the relative intensities of monomer and dimer peaks (r_{MD}) but has no effect on the positions of the two peaks (expressed as m/m_{\max} and d/d_{\max} , respectively). However, as anticipated for a coupled equilibrium system, variation of K_{ML} (Fig. 3b) influences not only the position of the monomer peak (m/m_{\max}) but also the position of the dimer peak (d/d_{\max}) and the relative peak intensities (r_{MD}). Similarly, variation of K_{DL} (Fig. 3c) influences all three observable parameters. Consequently, in order to determine the values of K_{MD} , K_{ML} and K_{DL} (and therefore the cooperativity factor c) it is necessary to globally fit all three experimental parameters to the thermodynamic model.

Determination of thermodynamic parameters from NMR data

We have used the above thermodynamic model (Fig. 2) to determine the influence of MCP-1 dimerization on binding to CCR2 sulfopeptides. ^{15}N -HSQC spectra were recorded for samples of 50 μM ^{15}N -labeled MCP-1 alone and in the presence of each of the two receptor peptides 1 and 2 at concentrations of 10, 20, 35, 50, 80 and 150 μM . Spectra were analyzed to yield average values and estimated standard errors of m , d and r_{MD} for the five residues for which both monomer and dimer resonances were resolved across the full range of peptide concentrations used (K19, L25, I42, F43 and C52). Finally, for each peptide the experimental observables were fit to the coupled thermodynamic model, using computational optimization and Monte Carlo simulations, to yield optimal values and standard errors for the independent equilibrium constants and the cooperativity factor.

The globally fitted data are presented in Fig. 4 and the resulting equilibrium constants and cooperativity values are listed in Table 1. Overall there is excellent agreement between the fitted curves and experimental data points. For comparison, we have also fit the binding data for the monomer and dimer peaks independently to a simple 1:1 equilibrium model (conventional fits, Table 1 and Fig. S3†). Although the simple model is not strictly valid for a coupled system, this conventional approach yields K_D values in reasonable agreement with those obtained from the global fitting approach. However, because the conventional K_D determinations are independent for monomer and dimer species, the calculated cooperativity is relatively poorly defined (14–21% error). In contrast, for the global fitting approach, there is a strong correlation between the K_{ML} and K_{DL} values determined for the many Monte-Carlo simulations (Fig. 5). Consequently, the cooperativity value (defined as the ratio of these two equilibrium constants; eqn (6)) is determined with substantially higher precision by the global fitting approach (error values <5%; Fig. 5 and Table 1). Importantly, the global fitting approach clearly shows that cooperativity is higher for sulfopeptide 2 than for sulfopeptide 1, suggesting that the interactions of the Tyr-28 sulfate group weaken MCP-1 dimerization.

It is noteworthy that the cooperativity values observed here are very low in comparison to classical cooperative binding

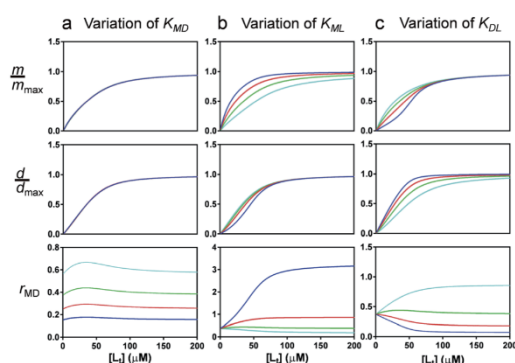


Fig. 3 Simulation of NMR parameters. Values of monomer and dimer peak positions (m/m_{\max} and d/d_{\max}) and the ratio of peak intensities (r_{MD}) were simulated for several different values of (a) K_{MD} , (b) K_{ML} and (c) K_{DL} (2 μM , blue; 5 μM , red; 10 μM , green; and 20 μM , cyan). In each case the other equilibrium constants were set to 10 μM .

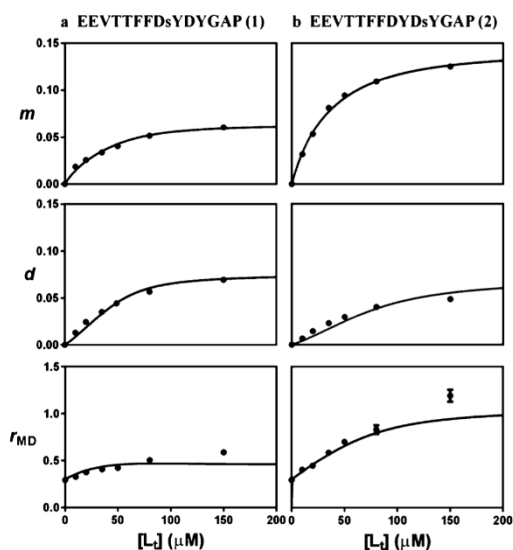


Fig. 4 Experimental NMR data fitted to the coupled thermodynamic model. Shown are values of monomer and dimer peak shifts (m and d) and the ratio of peak intensities (r_{MD}) determined for MCP-1 in the presence of increasing concentrations of CCR2-derived sulfopeptides (a) 1 and (b) 2. Experimental data are the averages for the 5 NH groups for which both monomer and dimer peaks were observable across the full range of peptide concentrations used. Error bars (representing standard errors) are plotted but are smaller than the data points in many cases. Solid lines show the best fits of the experimental data to the coupled thermodynamic model in Fig. 2.

Table 1 Fitted equilibrium binding constants and cooperativity values for binding of MCP-1 to CCR2-derived sulfopeptides 1 and 2

Peptide	K_{ML} (μM)	K_{DL} (μM)	c
Conventional fits^a			
1	27.8 ± 5.4	28.1 ± 2.1	1.01 ± 0.21
2	20.1 ± 1.2	46.1 ± 6.2	2.29 ± 0.33
Global fits to coupled thermodynamic model^b			
1	10.0 ± 1.7	14.4 ± 2.5	1.42 ± 0.04
2	15.5 ± 3.3	43.4 ± 10.5	2.80 ± 0.14

^a Conventional fits were performed independently for monomer and dimer data using a simple 1 : 1 binding model with the concentration of the monomer or dimer species assumed to be halfway between the two extreme concentrations deduced from the peak intensities in Fig. 4. ^b Global fits were performed using the coupled thermodynamic model in Fig. 2.

proteins or allosteric enzymes. Therefore, while binding of MCP-1 to the sulfated N-terminus of CCR2 does appear to weakly induce dimer dissociation, the biological consequences of this thermodynamic coupling are expected to be very subtle. It remains possible, albeit speculative, that subsequent interactions of MCP-1 with other regions of CCR2 further select for the monomeric, active form of the chemokine ligand.

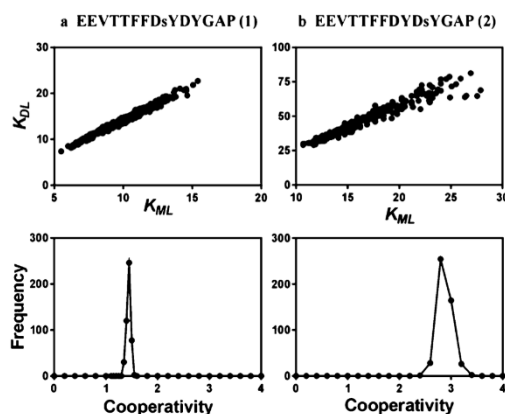


Fig. 5 Distributions of equilibrium binding constants and cooperativity values. Top panels show the fitted values of K_{ML} and K_{DL} obtained in each of the 475 best Monte-Carlo simulations for binding of MCP-1 to (a) 1 and (b) 2. Lower panels show the corresponding distributions of cooperativity (c) values. Methods for Monte-Carlo simulations are described in the ESI.†

A possible complicating factor in the method presented here is that the intensities of monomer and dimer resonances could be influenced not only by the populations of the two species but also by differences in their relaxation properties giving rise to differences in line shapes. This could be particularly significant if one species were undergoing a chemical exchange process not present in the other species or if one species were undergoing selective aggregation. Such relaxation effects would not influence r_{MD} values determined from peak integrals (rather than peak heights), but, as in the current application, accurate measurement of peak integrals is often impractical due to low signal-to-noise ratios or partial overlap of resonances. Line broadening effects could be further investigated by direct measurement of transverse relaxation rates for monomer and dimer resonances as a function of ligand concentration; in theory, it would then be possible to correct the r_{MD} values to compensate for line broadening.

In the current study, the dimer resonance for Leu-25 appears to be selectively broadened in the final titration point with sulfopeptide 2 (Fig. 1b), although for other residues both monomer and dimer resonances were broadened in the final titration point (Fig. S1†). These results suggest some sample aggregation may have occurred towards the end of the titration, possibly influencing the dimer more than the monomer and therefore contributing to the poorer fit of r_{MD} data for the later titration points of sulfopeptide 2 (Fig. 4). Nevertheless, such line broadening effects are not expected to influence the peak positions, which are the primary determinants of binding equilibrium constants (K_{ML} and K_{DL}) and therefore the cooperativity values. Thus, the observed line broadening does not change the overall conclusion that cooperativity is higher for sulfopeptide 2 than sulfopeptide 1.

Potential applicability to other systems

The method presented herein is theoretically applicable to any system involving two coupled equilibrium processes in which one process is fast and the other is slow on the NMR chemical shift time scale. This might include proteins whose dimerization is coupled to binding of oligosaccharides, small molecules, or metal ions, as reported previously.^{25–27} Alternatively the slow process of proline isomerization within proteins may be coupled to binding of partner proteins.^{28,29} For example, Breheny *et al.* have studied the slow equilibrium between proline *cis* and *trans* isomers within the Src homology 2 (SH2) domain of interleukin-2 tyrosine kinase (Itk).²⁹ The two isomers have similar populations in the unbound domain but binding to a phosphotyrosine-containing peptide biases the equilibrium towards the *trans* isomer whereas binding to the Itk SH3 domain biases the equilibrium towards the *cis* isomer. More broadly, one can envisage other slow equilibria, such as binding to a slowly-dissociating ligand, alteration of interdomain contacts or protein folding, being thermodynamically coupled to fast equilibria, such as binding to fast-dissociating ligands or side chain protonation/deprotonation.

In addition to the requirement that the two exchange processes occur with substantially different kinetics, several other factors may limit the practical application of the approach described here. First, the total concentration of protein used must be close enough to the K_{MD} value to yield observable populations (at least ~10%) of each species (monomer and dimer). Second, as with most binding experiments, the total protein concentration must be less than or similar to both the K_{ML} and K_{DL} values, allowing observation of non-linear chemical shift changes upon addition of ligand. Finally, the signal-to-noise ratios of all peaks must be high enough, and the line widths must be narrow enough, to allow quantification of peak positions and intensities for all species across the full range of ligand concentrations used. With current NMR technology, this method is therefore limited to the K_{MD} , K_{ML} and K_{DL} values in the micromolar to millimolar range. However, future technological innovations may allow higher affinity equilibria to also be investigated using this approach.

Conclusions

In summary, we have presented a general framework for analysis of 2D NMR spectra to evaluate the cooperativity of ligand binding and protein dimerization in coupled systems. This method is applicable to any system in which dimerization is slow and ligand binding is fast on the NMR chemical shift time scale and in which both monomer and dimer resonances are resolvable in a practical range of protein and ligand concentrations. We have applied this approach to a system in which the thermodynamics are well described by the simple thermodynamic model presented in Fig. 2. However, the same strategy could potentially be used for more sophisticated models involving, for example, higher order oligomers or non-independent binding sites on oligomeric proteins. The approach

presented here extends the array of NMR-based methods for characterisation of chemical and binding equilibria.

Acknowledgements

This work was supported by Australian Research Council grants DP1094884 and DP130101984 (to R.J.P. and M.J.S.) and LE0989504 (to M.J.S.).

Notes and references

- 1 N. J. Marianayagam, M. Sunde and J. M. Matthews, *Trends Biochem. Sci.*, 2004, **29**, 618.
- 2 *Advances in Experimental Medicine and Biology, Protein Dimerization and Oligomerization in Biology*, ed. J. M. Matthews, Springer, Berlin, Germany, 2012, vol. 747.
- 3 A. Levitzki and J. Schlessinger, *Biochemistry*, 1974, **13**, 5214.
- 4 A. V. Hill, *J. Physiol.*, 1910, **40**, iv.
- 5 L. W. Nichols and D. J. Winzor, *Biochemistry*, 1976, **15**, 3015.
- 6 G. Scatchard and N. Y. Ann, *Acad. Sci.*, 1949, **51**, 93.
- 7 C. Freiden, *J. Biol. Chem.*, 1967, **242**, 4045.
- 8 G. K. Wolfer, J. L. Neil and W. Barton Rippon, *J. Protein Chem.*, 1987, **6**, 441.
- 9 K. Julenius, J. Robblee, E. Thulin, B. E. Finn, R. Fairman and S. Linse, *Proteins: Struct., Funct., Genet.*, 2002, **47**, 323.
- 10 B. Moser, M. Wolf and P. Loetscher, *Trends Biochem. Sci.*, 2004, **25**, 75.
- 11 D. J. Scholten, M. Canals, D. Maussang, L. Roumen, M. J. Smit, M. Wijtmans, C. de Graaf, H. F. Vischer and R. Leurs, *Br. J. Pharmacol.*, 2012, **165**, 1617.
- 12 J. P. Ludeman and M. J. Stone, *Br. J. Pharmacol.*, 2014, **171**, 1167.
- 13 J. H. Y. Tan, J. P. Ludeman, J. Wedderburn, M. Canals, P. Hall, S. J. Butler, D. Taleski, A. Christopolous, M. J. Hickey, R. J. Payne and M. J. Stone, *J. Biol. Chem.*, 2013, **288**, 10024.
- 14 C. D. Paavola, S. Hemmerich, D. Grunberger, I. Polsky, A. Blom, R. Freedman, M. Mulkins, S. Bhakta, D. McCarty, L. Wiesent, B. Wong, K. Jarnagin and T. M. Handel, *J. Biol. Chem.*, 1998, **273**, 33157.
- 15 T. M. Handel and P. J. Domaille, *Biochemistry*, 1996, **35**, 6569.
- 16 J. F. Paolini, D. Willard, T. Consler, M. Luther and M. S. Krangel, *J. Immunol.*, 1994, **153**, 2704.
- 17 E. J. Fernandez and E. Lolis, *Annu. Rev. Pharmacol. Toxicol.*, 2002, **42**, 469.
- 18 J. H. Y. Tan, M. Canals, J. P. Ludeman, J. Wedderburn, C. Boston, S. J. Butler, A. M. Carrick, T. R. Parody, D. Taleski, A. Christopolous, R. J. Payne and M. J. Stone, *J. Biol. Chem.*, 2012, **287**, 14692.
- 19 H. Jin, X. Shen, B. R. Bagget, X. Kong and P. J. LiWang, *J. Biol. Chem.*, 2007, **282**, 27976.
- 20 C. T. Veldkamp, C. Seibert, F. C. Peterson, N. B. De la Cruz, J. C. Haugner III, H. Basnet, T. Sakmar and B. F. Volkman, *Sci. Signaling*, 2008, **1**, ra4.
- 21 M. W. Nasser, S. K. Raghuvanshi, D. J. Grant, V. R. Jala, K. Rajarathnam and R. M. Richardson, *J. Immunol.*, 2009, **183**, 3425.

- 22 L. Drury, J. J. Ziarek, S. Gravel, C. T. Veldkamp, T. Takekoshi, S. T. Hwang, N. Heveker, B. F. Volkman and M. B. Dwinell, *Proc. Natl. Acad. Sci. U. S. A.*, 2011, **108**, 17655.
- 23 P. Gangavarapu, L. Rajagopalan, D. Kolli, A. Guerrero-Plata, R. P. Garofalo and K. Rajarathnam, *J. Leukocyte Biol.*, 2012, **91**, 259.
- 24 A. Ravindran, K. V. Sawant, J. Sarmiento, J. Navarro and K. Rajarathnam, *J. Biol. Chem.*, 2013, **288**, 12244.
- 25 J. Flint, D. Nurizzo, S. E. Harding, E. Longman, G. J. Davies, H. J. Gilbert and D. N. Bolam, *J. Mol. Biol.*, 2004, **337**, 417.
- 26 C. T. Rollins, V. M. Rivera, D. N. Woolfson, T. Keenan, M. Hatada, S. E. Adams, L. J. Andrade, D. Yaeger, M. R. van Schravendijk, D. A. Holt, M. Gilman and T. Clackson, *Proc. Natl. Acad. Sci. U. S. A.*, 2000, **97**, 7096.
- 27 K. Julenius, J. Robblee, E. Thulin, B. E. Finn, R. Fairman and S. Linse, *Proteins: Struct., Funct., Genet.*, 2002, **47**, 323.
- 28 C. M. Santiveri, J. M. Perez-Canadillas, M. K. Vadivelu, M. D. Allen, T. J. Rutherford, N. A. Watkins and M. Bycroft, *J. Biol. Chem.*, 2004, **279**, 34963.
- 29 P. J. Breheny, A. Laederach, D. B. Fulton and A. H. Andreotti, *J. Am. Chem. Soc.*, 2003, **125**, 15706.

***Chapter 4. Characterisation of
Critical Regions of MCP-1 and
MCP-3 that Direct Partial
Agonism***

4.1. Introduction

Most chemokines bind and activate several chemokine receptors. Likewise, most chemokine receptors respond and bind to multiple chemokine ligands. Multiple ligands activating the same receptor, in the same tissue, are expected to compete with each other. Therefore, saturation of a particular receptor by a particular chemokine ligand depends on the availability and concentrations of other chemokines, which bind with the same receptor and of other receptors to which the same chemokine binds. Previously, the presence of different ligands for the same receptor was considered to represent functional redundancy among the chemokine-receptor network [216-218]. However, it has now been established that different chemokines can have different cellular effects by activating the same receptor, suggesting a more refined strategy, which enables the fine tuning of leukocyte recruitment in response to different inflammatory stimuli.

There are two major pharmacological mechanisms by which GPCRs can differentially respond to their ligands – partial (versus full) agonism and biased agonism. Examples of both phenomena have been observed for chemokines and their receptors. Different chemokines can behave as full or partial agonists of corresponding shared receptor [154]. Full agonists show higher maximal response as compared to partial agonists. As an example, Berchiche et al. [154] have shown that MCP-1 induces maximal β -arrestin recruitment at its receptor CCR2, whereas other chemokines (MCP-2, -3, -4, CCL11 and CCL24) induce a lower level of β -arrestin recruitment in the HEK293 cells showing reduced potency and efficacy. Wan et al. [219] have identified CCL11, CCL24 and MCP-4 as full agonists of CCR3 and they induce [35 S] GTP γ S binding, while MCP-3, CCL5, CCL26, vMIP-I and vMIP-II activate CCR3 as partial agonists, as they induce eosinophil chemotaxis but show less than maximal response for [35 S] GTP γ S binding as compared to the full agonists. It has been suggested by Martinelli et al. [220] that CCL11 is a partial agonist of CCR2 as it induces chemotaxis at CCR2B at higher concentrations of around 1 μ M, while MCP-1 works as full agonist of CCR2B inducing chemotaxis at sub-nanomolar concentrations.

While partial agonism has been widely recognised for many years, recently the alternative phenomenon of biased agonism or functional selectivity has generated lots of interest in the GPCR field. It has been reported that different ligands activate a shared receptor differentially, thus creating different populations of various activated forms of the receptor; thus, leading to different signalling pathways to the relative exclusion of others [221, 222]. The receptor can adopt multiple active states [223]. These active sites have a high affinity to agonists compared to antagonists. A particular active state conformation would be stabilised depending on the agonist which binds to the receptor [157]. As the receptors change conformation, different activated states of the receptor get stabilised, thus

all the signalling proteins are not activated uniformly through these conformations, ultimately inducing bias [224].

Kohout et al. have reported that CCL19 and CCL21 have shown biased agonism with CCR7. Both ligands are equally potent for G protein activation and calcium mobilisation, however, CCL19 showing 4-fold higher ERK phosphorylation as compared to CCL21 [176]. Rajagopal et al. have demonstrated that CCL27 and CCL28 show a bias in their interaction at CCR10. Both ligands achieve a maximal response with G protein signalling, but only CCL27 leads to receptor internalisation through interaction with β -arrestins [159]. Therefore, it is fascinating how chemokines can differentially influence the signalling pathways through all these mechanisms, ultimately fine tuning the inflammatory response [178].

It has been reported that MCP chemokines are differentially expressed in response to Th1 versus Th2 inflammatory stimuli and can have distinct temporal patterns of expression, suggesting that they may also activate distinct cellular responses via their shared receptor [225, 226]. However, so far, the exact mechanism and specific roles of the interacting regions of these effects are poorly understood for chemokines and their receptors. This question can be addressed by comparing two chemokines that have similar sequence and structure but distinct effects on binding and activation of the same receptor. This chapter describes a study of MCP chemokines, where we have focused on determining the essential sequence differences between MCP-1 and MCP-3 which are responsible for differential interaction with their shared receptor CCR2.

MCP-1 and MCP-3 share 71% sequence identity and have similar structures. Therefore, it was very interesting that with this high sequence similarity one can act as a full, and the other as a partial agonist at the same receptor. Considering that MCP-1 and MCP-3 are involved in several inflammatory diseases, and in spite of having a high degree of similarity, they still behave differently at their shared receptor CCR2. This provided a strong motivation to analyse the differences between these two chemokines and to understand the structural aspects of these chemokines which are responsible for these differences.

Our goal was to identify the most important structural features of the chemokines which are responsible for the differences in their ability to bind and activate the same receptor. Here, we have used a variety of chemokine chimeras to identify key structural elements of the chemokines that mediate this differential activation.

4.2. Selection of Signalling Readouts

As GPCRs, chemokine receptors couple to heterotrimeric G proteins and so are involved in activating secondary signalling pathways.

When chemokines bind to their receptor it brings a conformational change in the transmembrane helical domain of the receptor leading to a variety of downstream signalling events either by activation of G proteins or arrestins. These GPCRs, when active, promote the exchange of guanosine diphosphate (GDP) with guanosine triphosphate (GTP) working as guanine nucleotide exchange factors (GEFs), ultimately leading to dissociation of the $G\alpha$ subunit from the $\beta\gamma$ subunits. There are four different types of $G\alpha$ subunits and each is responsible for the activation of specific intracellular pathways (detail already mentioned in Chapter 1, 1.3.1). Both $G\alpha$ and $\beta\gamma$ subunits are capable to interact with independent effectors, which can lead to further downstream signals. According to the classical model of GPCR activation, this $G\beta\gamma$ complex is responsible for the transfer of G protein-coupled receptor kinases [71, 72] to the cell surface. These GRKs phosphorylate the receptor. The arrestins have an increased affinity for the phosphorylated receptor.

There are 4 subtypes of arrestins, which are expressed in a variety of cell types. There are 2 visual arrestins, arrestin-1 and arrestin-4 and 2 non-visual arrestins, arrestin-2 (or β -arrestin 1) and arrestin-3 (or β -arrestin 2). According to the classical model of receptor activation, β -arrestins are capable of G protein-dependent-arrestin signalling, which includes receptor internalisation, 1/2 ERK phosphorylation and desensitisation of the receptor [76, 227]. However, it has also been reported that β -arrestins are capable of G protein-independent-arrestin signalling [227-229]. This has been observed by using GPCR mutants which were unable to interact with G proteins but were still capable of signalling through the ERK phosphorylation pathway [228]. Other than ERK, β -arrestins are also involved in a variety of other signalling pathways, including Akt [83], JNK [78] and p38 MAP kinase [80].

GPCRs are able to stimulate a wide range of signalling pathways, the principal ones are summarised in the following figure (Fig 4.1)

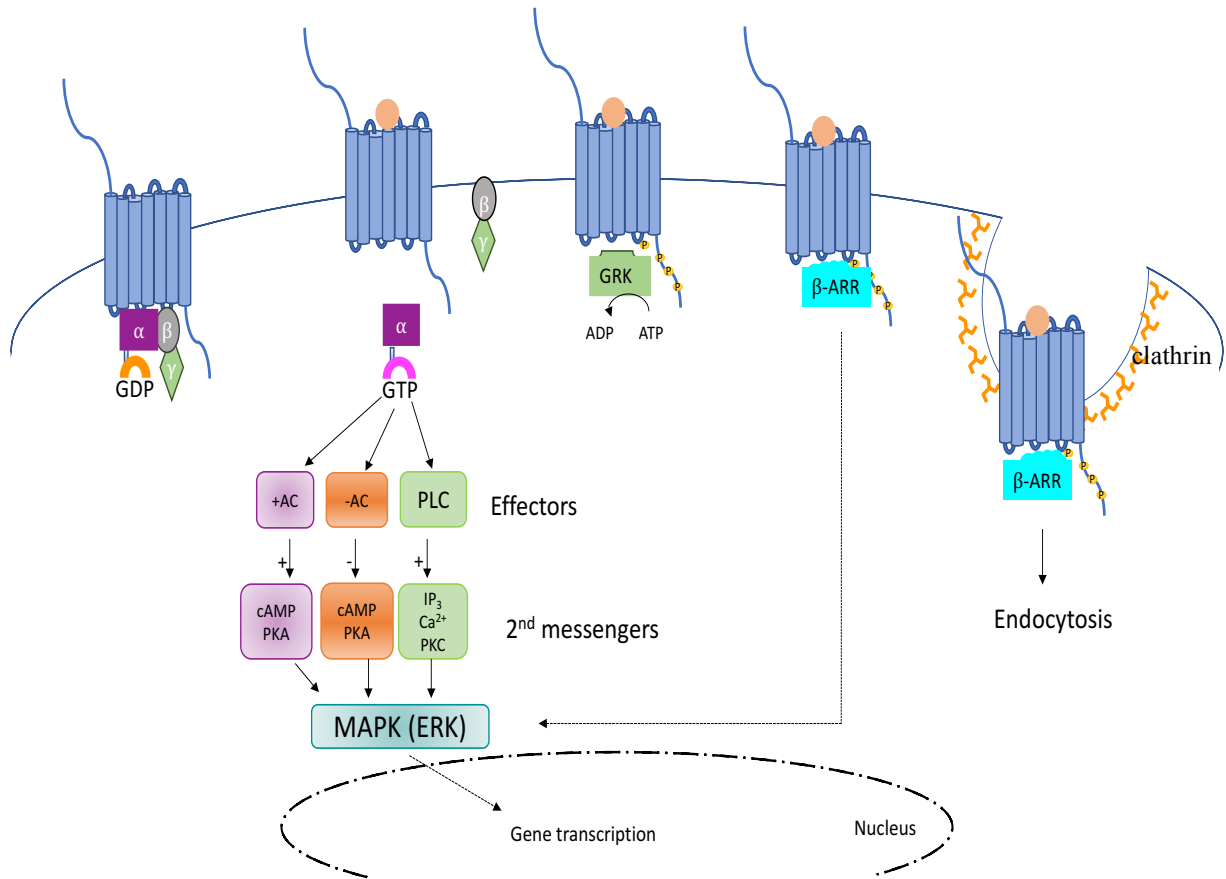


Figure 4.1. GPCR signalling pathways. GPCRs can couple to different G protein isoforms to activate or inhibit intracellular effectors. The major pathways that can be activated include cAMP production, ERK 1/2 phosphorylation, IP₃/calcium mobilisation and β-arrestin recruitment.

To detect partial agonism, we need to use a signal that is sensitive to the population of the activated state of the receptor. It can be detected by measuring the populations of signalling molecules coupled either directly to the receptor (proximal or non-amplified signals such as β -arrestin recruitment) or the downstream signals (amplified signals such as activation of kinases or the generation of second messengers). Because the downstream signals are considerably amplified, the maximal effect of full and partial agonists become identical when evaluated using these downstream signals; but differences in potency may allow one to differentiate between a full and partial agonist. We have used β -arrestin 2 recruitment here as an example of a proximal (non-amplified) signal and cAMP and ERK 1/2 phosphorylation as the amplified signalling read-outs.

The ability of chemokine receptors to identify and respond to the chemotactic environment directs the leukocytes' migration along a chemotactic gradient. The continuous sensitivity of these receptors to their ligands is achieved by the processes of receptor desensitisation, endocytosis and recycling of the resensitised receptor back to the cell membrane. Following the dissociation of G protein subunits after G protein activation, $G\beta\gamma$ subunits perform a critical role in recruiting G protein kinases (GRKs), which mediate receptor phosphorylation at serine and threonine residues in the intracellular loops and carboxyl-terminus of the receptor. This phosphorylation results in the uncoupling of G protein subunits and promotes the recruitment of β -arrestin molecules; which further initiate a cascade of downstream signalling events ultimately targeting the receptor for desensitisation [230]. β -arrestin binding also commences the formation of clathrin-coated pits. These pits endocytose the phosphorylated receptor, leading to formation of vesicles, which are then transported to endosomes. Following endosomal sorting, the receptor is either sent to lysosomes for degradation or are resensitised and recycled back to the plasma membrane [231].

Binding of chemokines to the chemokine receptor generates a cascade of events that ultimately results in activation of several downstream pathways. One of the important events is regulation of the activity of the enzyme adenylyl cyclase (AC). This enzyme is responsible for the production of the second messenger cyclic adenosine monophosphate (cAMP) from ATP. CCR2 binds to G proteins containing the $G\alpha_i$ subunit, which, after dissociation from the receptor and $G\beta\gamma$ subunits, directly inhibits the activity of AC [154].

Another important downstream event is phosphorylation and activation of the mitogen-activated protein kinases (MAPKs) or extra-cellular signal-regulated kinases 1 and 2 (ERK 1/2), which involves several distinct and overlapping signalling pathways. These kinases are involved in a vast array of fundamental cellular processes and they play central roles in cell proliferation, cell differentiation, motility, stress response, apoptosis and survival [232]. The coupling of chemokine

receptors to either $G\alpha_i$ or $G\beta\gamma$ subunit of G protein-coupled receptors lead to phosphorylation of ERK 1/2, which activates several cellular processes like leukocyte adhesion and chemotaxis [233, 234].

In these amplified assays (inhibition of cAMP and ERK1/2 phosphorylation), the maximal effects of full and partial agonists become indistinguishable (the signals are amplified to the full capacity of the pathway even when the activated state of the receptor is only partially populated). In such assays the relative potency of the chemokines is determined by both the affinities of the chemokines for CCR2 and their relative efficacies [235].

4.3. MCP Chemokines have Different Efficacies and Affinities at CCR2

For the preliminary data, we did experiments choosing MCP-1, -2 and -3 with their cognate receptor CCR2. Receptor recruitment of β -arrestin subtype 2 (also termed arrestin 3) was measured using a BRET based assay that was sensitive to changes in the proximity of CCR2-Rluc and β -arrestin 2-YFP (details in chapter 2, section 2.14.3).

Inhibition of forskolin induced cAMP production was carried out using a BRET based assay. The assay involved the use of a BRET biosensor CAMYEL which consisted of Rluc and YFP, linked to an exchange protein (Epac), which allows detection of relative cAMP levels (details in section 2.14.4).

ERK 1/2 phosphorylation was measured using the Alpha Screen Technology which employs antibodies against the phosphorylation epitopes and fluorescent donor and acceptor beads (details in section 2.14.5).

The three chemokines induced recruitment of β -arrestin 2 (β -arr2) with different potencies and significantly different maximal effects, E_{max} (Fig 4.2A, Table 4.1); relative to MCP-1, the E_{max} of MCP-2 and MCP-3 were $23 \pm 3\%$ and $56 \pm 4\%$, respectively. In the two amplified signalling assays, the three chemokines exhibited the same maximal effect as each other but significantly different potencies, and higher potencies than in the β -arr2 assay (Figs 4.2B, C, Table 4.1). The order of potencies between the three agonists in the amplified assays was the same as the order of their maximal effects in the proximal assay. Moreover, the same rank order of binding affinities was also observed in a radio-ligand binding assay (Fig 4.2D, Table 4.1). These results are in good agreement with the effects of MCP chemokines reported previously [154].

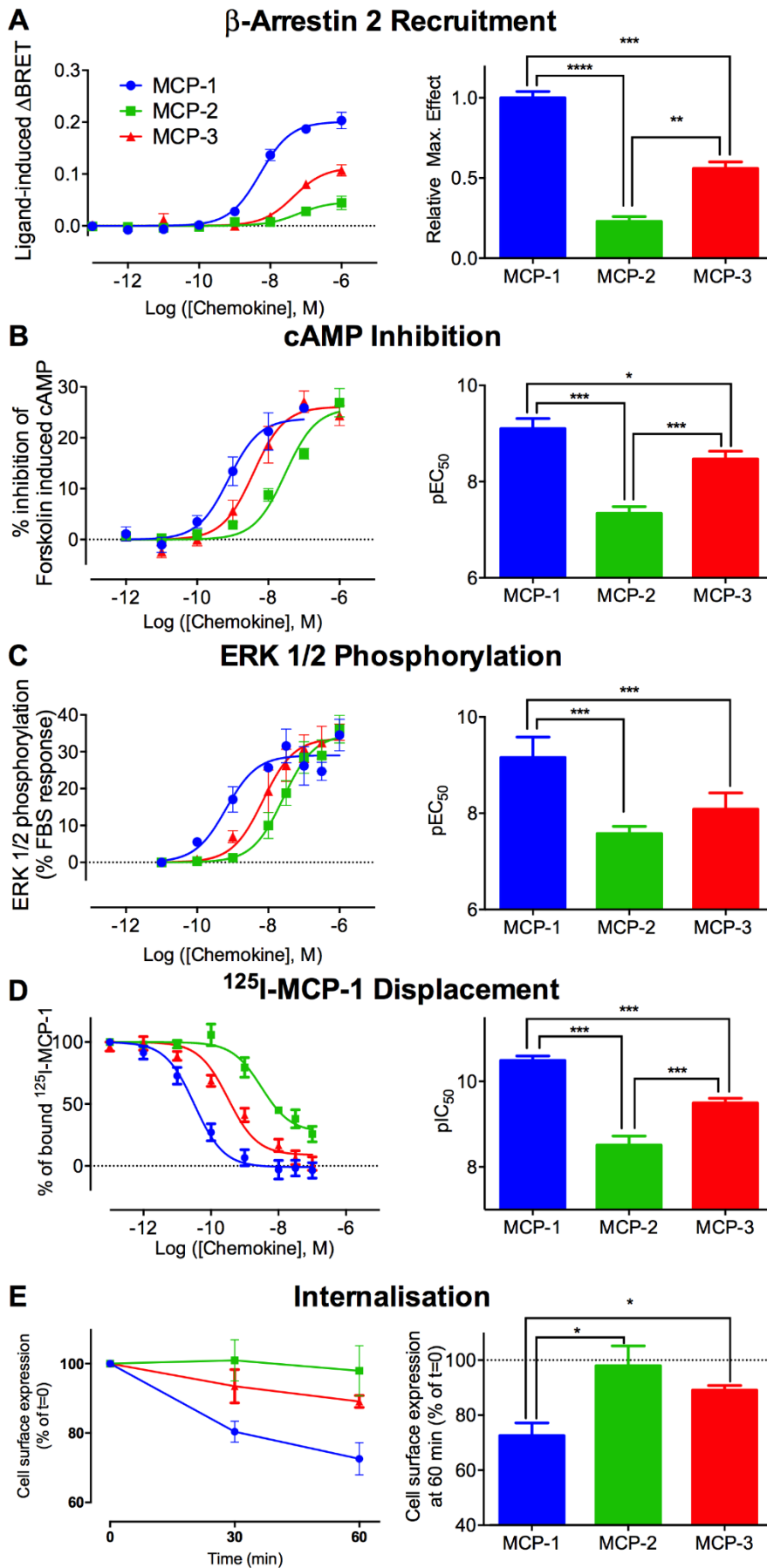


Figure 4.2. MCP chemokines display different efficacies and affinities at the CCR2. (A) β -arrestin 2 recruitment was assessed using BRET in FlpIn TRex 293 cells transiently transfected with CCR2-RLuc8 and β -arr2-YFP. (B) Inhibition of cAMP was measured using a BRET-based cAMP sensor transiently transfected in c-Myc-FLAG-CCR2 FlpIn TRex 293 cells. (C) ERK1/2 phosphorylation was measured 3 min after chemokine stimulation in c-Myc-FLAG-CCR2 FlpIn TRex 293 cells. (D) ^{125}I -MCP-1 competition binding was measured in membrane preparations of c-Myc-FLAG-CCR2 FlpIn TRex 293 cells. (E) Time-course of receptor internalisation in response to 100 nM of MCPs detected in c-Myc-FLAG-CCR2 FlpIn TRex 293 cells by whole cell anti c-Myc ELISA. Data are means \pm SEM from 3-5 experiments performed in triplicate. * $P < 0.05$, ** $P < 0.01$, *** $P < 0.001$, **** $P < 0.0001$ one-way ANOVA with Dunnett's multiple comparison test.

	β -arrestin recruitment		cAMP inhibition		ERK 1/2 phosphorylation		^{125}I -MCP1 binding
	pEC_{50}	E_{max}	pEC_{50}	E_{max}	pEC_{50}	E_{max}	pK_i
MCP-1	8.32 \pm 0.06	100 \pm 2	9.10 \pm 0.21	100 \pm 9	9.16 \pm 0.24	100 \pm 10	10.60 \pm 0.08
MCP-2	7.24 \pm 0.26 *	23 \pm 3 ***	7.34 \pm 0.14 ***	113 \pm 9	7.58 \pm 0.15 ***	119 \pm 9	8.88 \pm 0.14 ***
MCP-3	7.33 \pm 0.15 *	56 \pm 4 **	8.47 \pm 0.16 *	109 \pm 9	8.09 \pm 0.19 ***	116 \pm 10	9.50 \pm 0.12 ***

Table 4.1: Potency, efficacy and affinity of the different MCP chemokines at the CCR2 receptor in β -arrestin recruitment, Fsk-induced cAMP inhibition, pERK and radioligand binding assays. β -arrestin 2 recruitment was assessed using BRET in FlpIn TRex 293 cells transiently transfected with CCR2-RLuc8 and β -arr2-YFP. Inhibition of cAMP was measured using a BRET-based cAMP sensor transiently transfected in c-Myc-FLAG-CCR2 FlpIn TRex 293 cells. ERK1/2 phosphorylation was measured 3-5 min after chemokine stimulation in c-Myc-FLAG-CCR2 FlpIn TRex 293 cells. ^{125}I -MCP-1 competition binding was measured in membrane preparations of c-Myc-FLAG-CCR2 FlpIn TRex 293 cells. Data are mean \pm SEM from 3-4 experiments performed in triplicate. * $P < 0.05$, ** $P < 0.01$, *** $P < 0.001$, one-way ANOVA with Dunnett's multiple comparison test.

Several studies have shown that some chemokines act as biased agonists at their cognate receptors. To explore this possibility, we analysed our data using a derivation of the operational model of agonism developed by Black and Leff [212, 236]. This model can be fitted to concentration response data to derive a “transducer ratio” (τ/K_A) as an index of intrinsic activity of an agonist at a given pathway. The key parameters in the transducer ratio are the equilibrium dissociation constant of the agonist for the receptor (K_A) and an operational measure of signal efficacy (τ) [212]. We obtained transducer ratios for MCP-1, MCP-2 and MCP-3 at the CCR2 receptor at each signalling pathway and then normalised these values to that of MCP-1. Comparison of these normalised values across the different pathways revealed that neither MCP-2 nor MCP-3 displayed biased agonism relative to MCP-1 (Fig 4.3 and Table 4.2). Instead, our observations indicate that MCP-2 and MCP-3 are partial agonists of CCR2, relative to MCP-1.

The data in Fig 4.2 (A-D) highlight two underlying differences in the receptor interactions of the MCP chemokines. First, the three chemokines have different affinities for CCR2 (Fig 4.2D). Second, the three chemokines have different maximal effects in the proximal β -arr2 recruitment assay (Fig 4.2A). Although the rank order of these maximal effects is the same as the rank order of affinities for the three chemokines, the maximal effects occur at ligand concentrations at which the receptor is fully occupied so they do not result from differences in binding affinity. Instead, they indicate that the ligands have distinct efficacies, i.e. distinct intrinsic abilities to induce the receptor-mediated response.

However, the order of potency in the cAMP and pERK assays is consistent with both their relative affinities for the receptor and the populations they induce of the activated state of the receptor, indicated by their relative E_{max} values in the proximal assay (Fig 4.2A-D).

An important consequence of partial agonism in the context of the β -arrestin assay is that subsequent regulatory processes, such as receptor internalisation, will also be submaximally engaged by the action of partial agonists. In agreement with the work of Berchiche et al. [154], both MCP-2 and MCP-3, at saturating concentrations, caused very limited internalisation of CCR2, whereas MCP-1 induced significant internalisation (Fig 4.2E). These differences correlate with the relative efficacies of the three chemokines.

Considering the robust and consistent differences observed among the MCP chemokines for CCR2 binding and activation in the preliminary data (Fig 4.3), this system was ideally suited for investigation of the structural features influencing the relative affinities and efficacies of different chemokines at their shared receptor, as described later in this chapter.

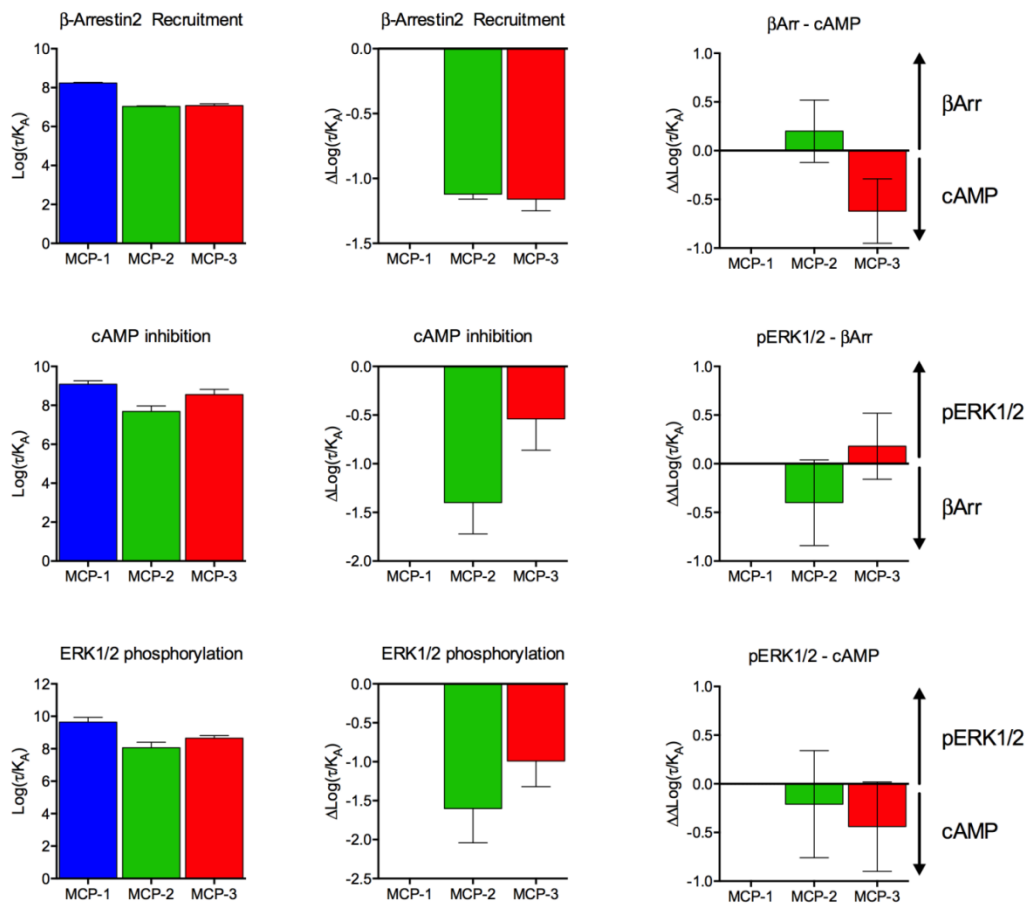


Figure 4.3. Neither MCP-2 nor MCP-3 is a biased agonist at CCR2 relative to MCP-1. Left: The concentration-response curves from the assays of β -arrestin 2 recruitment, inhibition of forskolin-induced cAMP generation, and ERK1/2 phosphorylation shown in Fig. 4.2 were fitted to the operational model of agonism to obtain transducer ratios [$\text{Log}(\tau/K_A)$]. Middle: Transducer ratios were normalized to MCP-1 [$\Delta\text{Log}(\tau/K_A)$]. Right: Bias factors between pathways [$\Delta\Delta\text{Log}(\tau/K_A)$] were calculated as described in Materials and Methods and indicate the absence of bias. MCP-1 (blue), MCP-2 (green), and MCP-3 (red).

	β -arrestin recruitment		cAMP inhibition		ERK1/2 phosphorylation		pERK - cAMP $\Delta\Delta\log(\tau/K_A)$	pERK - β Arr $\Delta\Delta\log(\tau/K_A)$	β Arr - cAMP $\Delta\Delta\log(\tau/K_A)$
	$\log(\tau/K_A)$	$\Delta\log(\tau/K_A)$	$\log(\tau/K_A)$	$\Delta\log(\tau/K_A)$	$\log(\tau/K_A)$	$\Delta\log(\tau/K_A)$			
MCP-1	8.24 \pm 0.03	0	9.09 \pm 0.17	0	9.65 \pm 0.29	0	0	0	0
MCP-2	7.04 \pm 0.02	-1.12 \pm 0.04	7.69 \pm 0.28	-1.40 \pm 0.32	8.05 \pm 0.34	-1.60 \pm 0.44	-0.21 \pm 0.55	-0.40 \pm 0.44	0.20 \pm 0.32
MCP-3	7.08 \pm 0.09	-1.16 \pm 0.09	8.55 \pm 0.27	-0.54 \pm 0.32	8.66 \pm 0.16	-0.99 \pm 0.33	-0.44 \pm 0.46	0.18 \pm 0.34	-0.62 \pm 0.33

Table 4.2: Biased agonism at CCR2. Fitted ($\log(\tau/K_A)$) and normalised ($\Delta\log(\tau/K_A)$) transducer ratios for MCP-1, MCP-2 and MCP-3 in β -arrestin 2 recruitment BRET, inhibition of forskolin-induced cAMP and ERK1/2 phosphorylation pathways. Calculation of the bias factor ($\Delta\Delta\log(\tau/K_A)$) between pathways shows the absence of biased agonism.

4.4. Design of Chimeric Chemokines

Mutational and structural studies have previously identified three regions of chemokines that interact with receptors [99, 197, 237, 238]. The so-called “N-loop” (a ~12 residue sequence between the conserved CC/CXC motif and the first β -strand) and the β 3 region (third β -strand and preceding turn) form the two sides of a shallow groove that binds to the flexible N-terminal tail of the receptor. The N-terminal region of the chemokine (preceding the CC/CXC motif) penetrates into the transmembrane helical bundle of the receptor. Previous work from the host lab has also shown that MCP-1 and MCP-3 show differential signalling via their common receptor CCR2. To further investigate the structural elements of MCP chemokines that contribute to partial versus full agonism and to relative CCR2 affinity, we designed a series of chimeric proteins in which these three regions of MCP-1 and MCP-3 were swapped between the two chemokines.

We chose to use MCP-3 rather than MCP-2 for these chimeras for the following reasons: (1) The sequence of MCP-1 is more closely related to MCP-3 (71% identity) than to MCP-2 (61% identity), allowing us to more easily draw conclusions about the roles of specific residues; (2) Both MCP-3 and the MCP-1(P8A) mutants used here are monomeric, whereas MCP-2 exists in equilibrium between monomeric and dimeric forms, potentially complicating the interpretation of chimera experiments if MCP-2 were used (especially determining whether the chimeras were correctly folded); (3) MCP-2 gives a very weak signal in the β -arrestin 2 recruitment assay so there may not have been a large enough window to reliably measure any decreases in efficacy when assessing the effects of chimeras, whereas MCP-3 gives a slightly higher signal (larger window) that allows for “confident” detection of both increases and decreases in efficacy; and (4) in our expression system, MCP-3 gives a higher yield than MCP-2 so preparation of chimeras was expected to be more straightforward.

Human MCP-1 and MCP-3 protein sequences were aligned and the three receptor-binding regions were identified (Fig 4.4A). The sequences were compared and 13 possible mutations (of each chemokine) were identified. Each of these was individually analysed, considering the chemical properties of each amino acid, the relative position of that amino acid in the chemokine and the structural changes, which could arise after replacing that residue with the one at the same position from the other chemokine. Two potential mutations (V22K and I46K) were anticipated to disturb the core structure of the chemokine and therefore were not introduced. All other potential mutations, which are present on the surface and not predicted to destabilize the structure, were accepted.

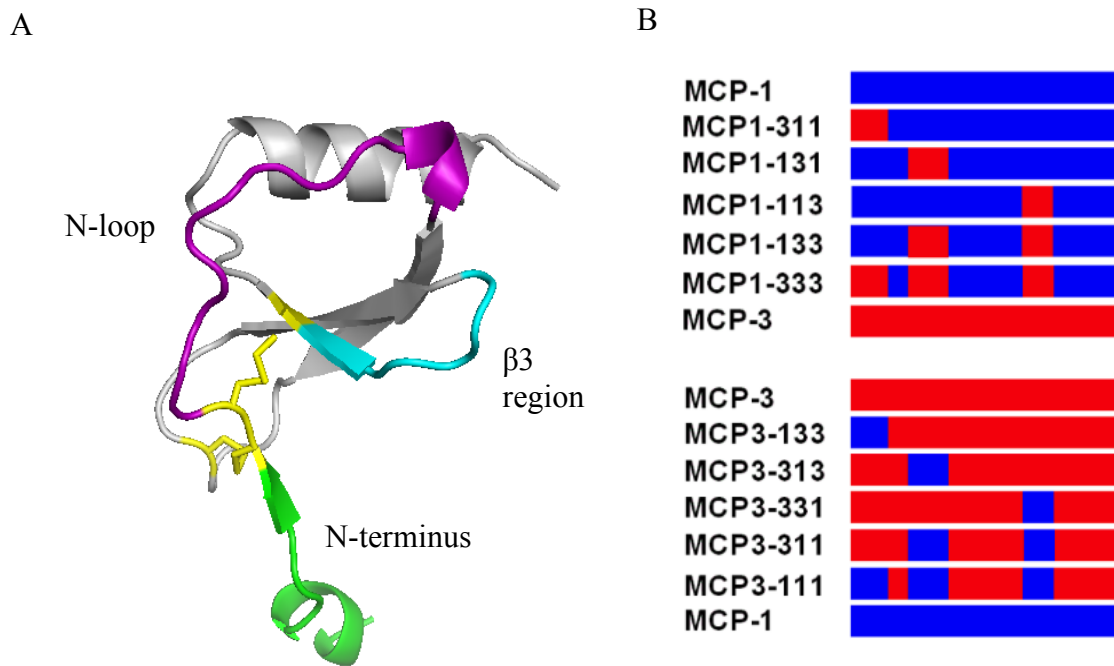


Figure 4.4. Design and schematics of MCP-1/MCP-3 chimeras. (A) Structure of MCP-1 showing the three important regions (PDB ID: 1DOK) highlighting the regions swapped in the chimeras (B) Schematic diagrams of the chimeras with regions from MCP-1 and MCP-3 in blue and red, respectively.

We prepared ten chimeras (Fig 4.4B). Five chimeras are on the MCP-1 background with three regions (N-terminus, N-loop and β 3-turn) replaced, individually or in combination, with the corresponding regions of MCP-3 (except the two excluded residues). The other five chimeras are on the MCP-3 background with the three important regions of MCP-1 introduced. All MCP-1 chimeras were of P8A sequence (monomeric mutants).

Each chimera was named according to the parental chemokine from which it is derived, followed by a sequence of three numbers representing the origin of the N-terminal, N-loop and β 3 elements, respectively; for example, MCP1-311 is a chimera derived from MCP-1 and containing the N-terminal region of MCP-3, the N-loop of MCP-1 and the β 3 region of MCP-1. Amino acid sequences of the chemokines and chimeras are listed in Fig 4.5.

We haven't chosen all the possible combinations, for instance MCP1-313 and MCP3-131 were not cloned, as the N-terminus and β 3-turn regions are far from each other so it seemed non-functional to mutate regions which were apart from each other.

4.5.2. Protein Production and Purification

Correctly sequenced expression plasmids were used for protein production. The methods which have already been established in our lab for the wild type chemokines were used for the production of all chimeras (see section 2.6). Briefly, the N-terminal His₆-tagged protein was expressed from BL21 (DE3) *E.coli* in LB media by induction with IPTG. Inclusion bodies containing the fusion proteins were isolated and dissolved in denaturing buffer and then purified by Ni²⁺-affinity chromatography. The fusion protein was refolded by drop-wise dilution. The His₆-tag was removed using human thrombin and the untagged protein (containing the native N-terminus) was further purified by size exclusion chromatography (Fig 4.6A, B). The fractions pooled for further experiments are marked. Their purity was evaluated by SDS-PAGE (Fig 4.6C, D) and protein identity was confirmed by MALDI-TOF mass spectrometry (Table 4.3).

The SEC fractions were run under both reducing (R) and non-reducing (NR) conditions. Presence of clear single bands in both conditions indicates pure and monomeric protein. (The SDS-PAGE of all chimeras are shown in appendix V)

	N-terminus	N-loop				β 3 region	
	1	10	13	24		46	52
MCP-1:	QPDAINAAVT	CC	YNFTNRKISVQR	LASYRRITSSKCPKEAVIFKT		IVAKEIC	ADPKQKVVQDSMDHLDKQTQTPKT
1-311:	QPVGINTSTT	CC	YNFTNRKISVQR	LASYRRITSSKCPKEAVIFKT		IVAKEIC	CADPKQKVVQDSMDHLDKQTQTPKT
1-131:	QPDAINAAVT	CC	YRFINKKIPVQR	LASYRRITSSKCPKEAVIFKT		IVAKEIC	CADPKQKVVQDSMDHLDKQTQTPKT
1-113:	QPDAINAAVT	CC	YNFTNRKISVQR	LASYRRITSSKCPKEAVIFKT		ILDKEIC	ADPKQKVVQDSMDHLDKQTQTPKT
1-133:	QPDAINAAVT	CC	YRFINKKIPVQR	LASYRRITSSKCPKEAVIFKT		ILDKEIC	ADPKQKVVQDSMDHLDKQTQTPKT
1-333:	QPVGINTSTT	CC	YRFINKKIPVQR	LASYRRITSSKCPKEAVIFKT		ILDKEIC	ADPKQKVVQDSMDHLDKQTQTPKT
MCP-3:	QPVGINTSTT	CC	YRFINKKIPKQR	LESYRRITSSHC	PREAVIFKT	KLDKEIC	ADPTQKVVQDFMKHLDKKTQTPKL
3-133:	QPDAINAAVT	CC	YRFINKKIPKQR	LESYRRITSSHC	PREAVIFKT	KLDKEIC	CADPTQKVVQDFMKHLDKKTQTPKL
3-313:	QPVGINTSTT	CC	YNFTNRKISKQR	LESYRRITSSHC	PREAVIFKT	KLDKEIC	CADPTQKVVQDFMKHLDKKTQTPKL
3-331:	QPVGINTSTT	CC	YRFINKKIPKQR	LESYRRITSSHC	PREAVIFKT	KVAKEIC	ADPTQKVVQDFMKHLDKKTQTPKL
3-311:	QPVGINTSTT	CC	YNFTNRKISKQR	LESYRRITSSHC	PREAVIFKT	KVAKEIC	CADPTQKVVQDFMKHLDKKTQTPKL
3-111:	QPDAINAAVT	CC	YNFTNRKISKQR	LESYRRITSSHC	PREAVIFKT	KVAKEIC	ADPTQKVVQDFMKHLDKKTQTPKL

Figure 4.5. The protein sequences of the MCP-1(P8A) and wild type MCP-3 chemokines and the chimeras. The green highlighted regions correspond to the N terminus (1-10), N loop (12-24) and β 3 strand (46-52) in MCP-1 and MCP-3. The yellow highlighted regions correspond to the regions that are mutated (from MCP-1 to MCP-3 in the five chimeras on MCP-1 background and from MCP-3 to MCP-1 in the five chimeras on MCP-3 background) and the red, underlined residues are the specific mutations made.

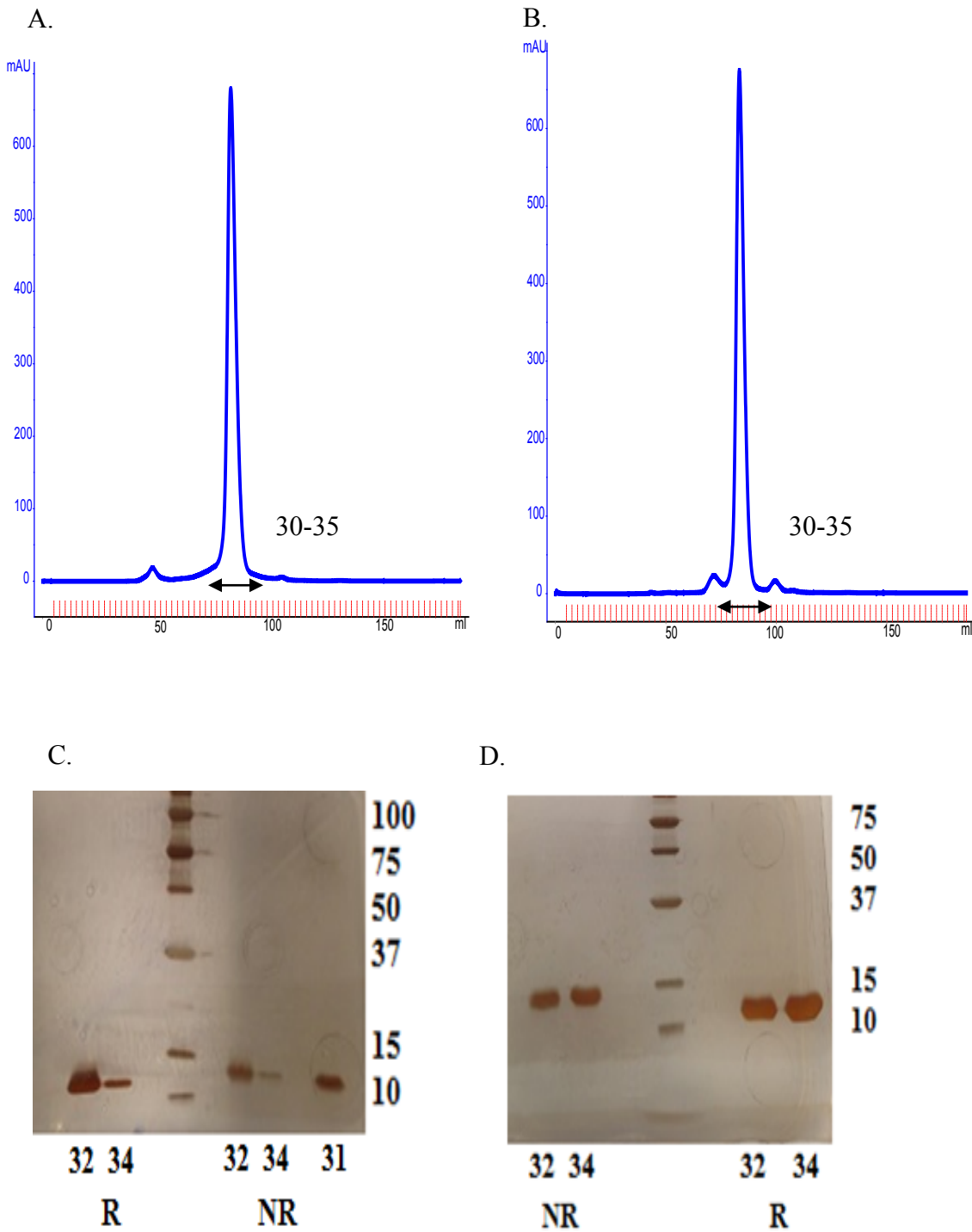


Figure 4.6. A and B. Size exclusion chromatograms of MCP-1(P8A) and MCP1-133 showing the elution of pure protein. **C and D.** SDS-PAGE showing MCP-1 (P8A) and MCP1-133 in reducing (R) and non-reducing (NR) conditions.

Wild type/Chimera	Mass Spectrometry	
	Predicted Mass	Observed Mass
MCP-1	8659.0	8658.4
1-311	8677.0	8675.3
1-131	8695.2	8695.1
1-113	8717.0	8716.8
1-133	8753.2	8750.1
1-333	8771.2	8768.7
MCP-3	8956.4	8951.7
3-133	8938.4	8935.1
3-313	8920.3	8919.3
3-331	8898.4	8892.5
3-311	8862.2	8859.1
3-111	8844.2	8843.2

Table 4.3. Comparison of predicted masses (calculated from ProtParam) and observed masses (MALDI-TOF) for the MCP-1/MCP-3 chimeras.

4.5.3. 1D NMR Comparison of Chimeric chemokines to Parent chemokines

¹H NMR spectra were collected for all the chimeras along with the wild type chemokines to confirm that they were correctly folded. Protein samples were exchanged into 20 mM sodium acetate-d₄, pH 7.0 containing 5% D₂O. ¹H NMR spectra were recorded at 25 °C, referenced to external DSS, on a Bruker Avance 600 MHz NMR spectrometer equipped with a triple-resonance cryoprobe and analysed using Bruker TopSpin software. Methyl groups in unstructured peptides resonate close to 1 ppm, while in these figures the resonance in -0.5 ppm upfield region indicate a folded tertiary structure (Fig 4.7A, B). The downfield regions also show well resolved peaks between 6.5 to 10 ppm. The NMR data indicate that all the chimeras are well folded and adopt the expected native 3D structures.

4.6. Assessment of Receptor Binding and Activation

To characterise the binding and signalling profiles of chemokine chimeras at CCR2, we used FlpIn TRex HEK 293 cell line stably expressing human CCR2B, N-terminally tagged with c-Myc and FLAG epitope tags (c-Myc-FLAG-CCR2).

4.6.1. Radioligand Binding

To assess the contributions of the three chemokine structural regions to CCR2 binding affinity, we measured the abilities of the MCP chimeras to compete with ¹²⁵I-MCP-1 binding to CCR2. MCP-1 has 10-fold higher affinity than MCP-3 at CCR2 (as shown in Fig 4.8A, E and Table 4.4). Replacement of the N-terminus of MCP-1 with that of MCP-3 caused a decrease in affinity such that this chimeric chemokine displayed an affinity comparable to that of MCP-3. Similarly, replacement of the N-terminus of MCP-3 with that of MCP-1 generated a chimeric chemokine with comparable affinity to that of MCP-1. These results clearly indicate that the N-terminus of MCP-1 has a significant role in determining its higher affinity as compared to MCP-3.

In contrast to the clear contribution of the N-terminal region to binding selectivity, replacement of the N-loop and/or β3 region of MCP-1 with that of MCP-3 did not affect the CCR2 binding affinity. Similarly, substitution of the β3 region of MCP-3 with that of MCP-1 had no significant effect on affinity. However, replacement of the N-loop of MCP-3 by that of MCP-1, alone or in combination with the β3 region (chimeras MCP3-313 and MCP3-311) reduced the affinity for CCR2. This is consistent with the previous findings that the N-loop is a major contributor to CCR2 binding but also suggests that the ability of the N-loop to interact favorably with the receptor is dependent on the background scaffold in which it is located.

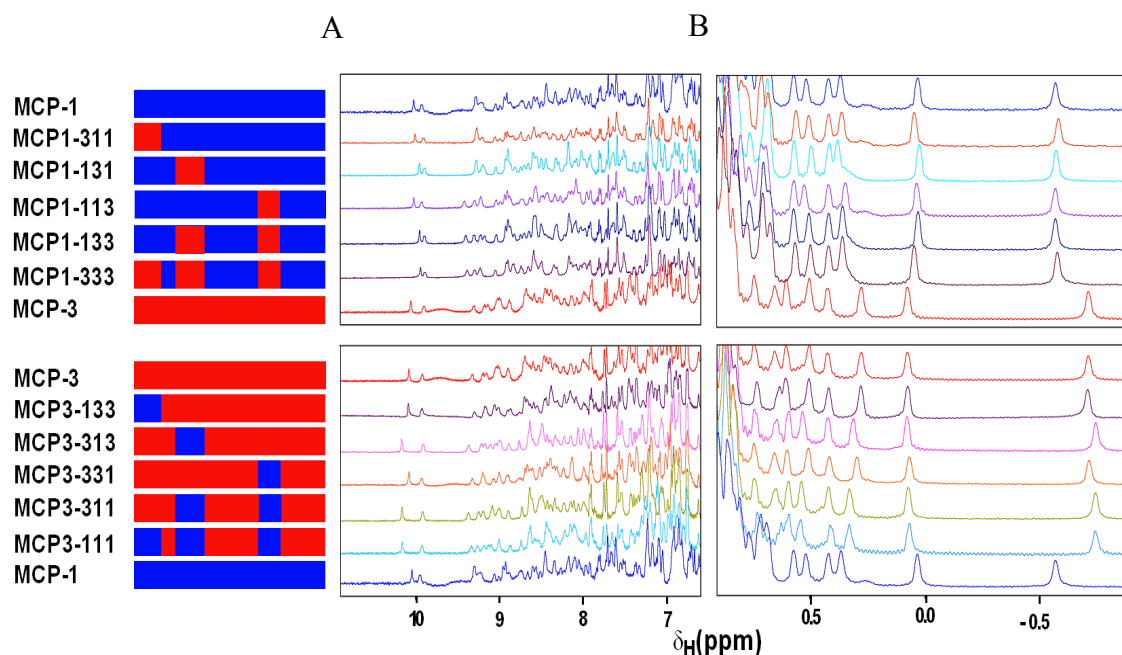


Figure 4.7. Structure validation of MCP-1/MCP-3 chimeras: 1D ^1H NMR spectra of all the ten chimeras show well-dispersed peaks indicative of correct folding of protein. (A) The downfield (amide and aromatic) region and (B) the upfield methyl regions of spectra. For chimeras, there are several peaks at the same position but still there are peaks for all of them which differ from one another, confirming that they have similar structures but are different proteins. Names and schematic diagrams of the chemokines and chimeras are shown on the left. All protein samples were in 20 mM sodium acetate- d_4 , pH 7.0 containing 5% D_2O . ^1H NMR spectra were recorded at 25 $^\circ\text{C}$, referenced to external DSS.

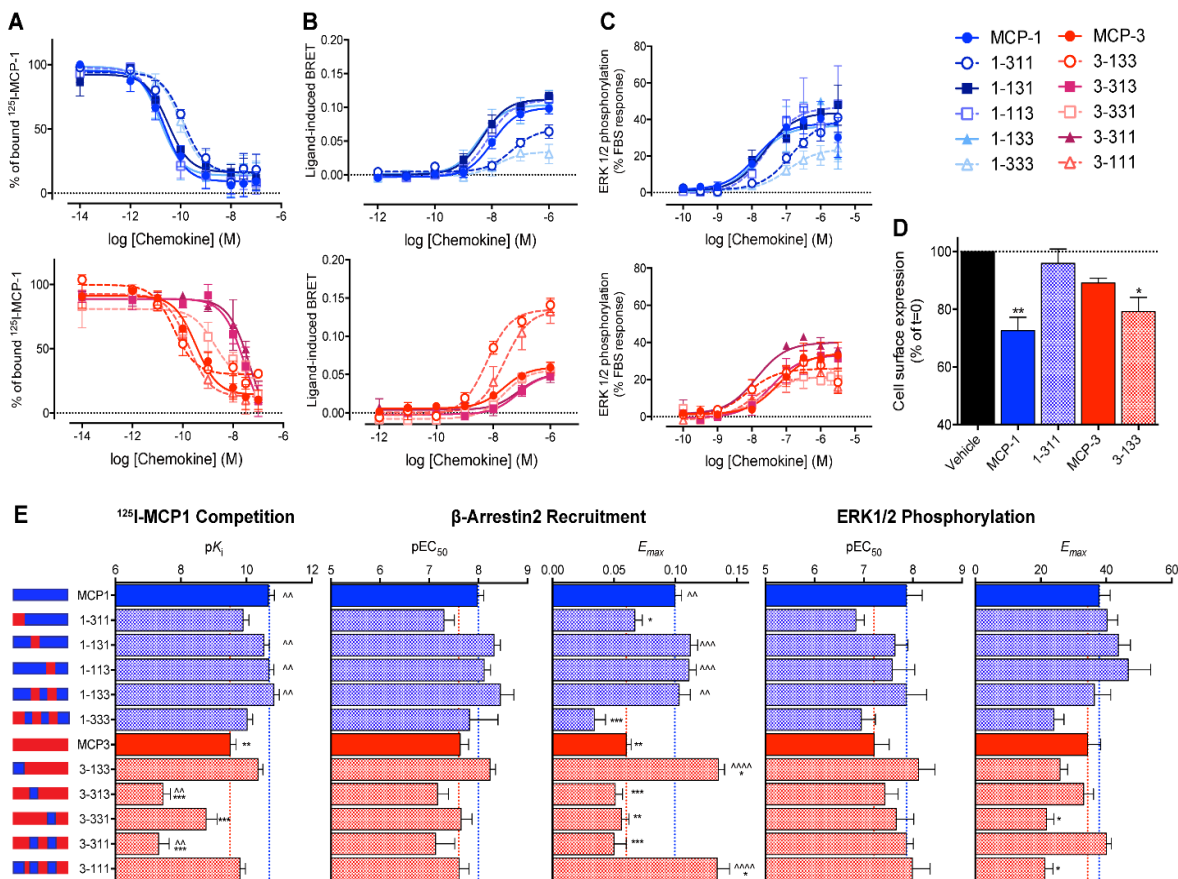


Figure 4.8. The N-terminal tail of MCP-1 and MCP-3 is a major determinant of affinity and efficacy. 125 I-MCP-1 competition binding, β -arrestin 2 recruitment BRET and ERK1/2 phosphorylation were assessed for MCP-1 and MCP-3 chimeric chemokines (top/blue and bottom/red, respectively). **(A)** 125 I-MCP-1 competition binding was measured in membrane preparations of c-Myc-FLAG-CCR2 FlpIn TRex 293 cells. **(B)** β -arrestin 2 recruitment was assessed using BRET in FlpIn TRex 293 cells transiently transfected with CCR2-RLuc8 and β -arr2-YFP. **(C)** ERK1/2 phosphorylation was measured 3 min after chemokine stimulation in c-Myc-FLAG-CCR2 FlpIn TRex 293 cells. **(D)** CCR2 internalisation upon stimulation with Vehicle, 100 nM MCP-1, MCP1-311, MCP-3 or MCP3-133 for 60 minutes was measured in c-Myc-FLAG-CCR2 FlpIn TRex 293 cells by whole cell anti c-Myc ELISA. Data are mean \pm SEM from 3-5 experiments performed in triplicate. * $P < 0.05$, ** $P < 0.01$, one-way ANOVA with Dunnett's multiple comparison test. **(E)** Affinity (pK_i), potency (pEC_{50}) and efficacy (E_{max}) for wild type and chimeric chemokines in 125 I-MCP-1 competition binding, β -arrestin 2 recruitment BRET and ERK1/2 phosphorylation. Data are mean \pm SEM from 3-5 experiments performed in triplicate. * $P < 0.05$, ** $P < 0.01$, ^ $P < 0.01$, *** $P < 0.001$, **** $P < 0.0001$ compared to MCP-1 or MCP-3 respectively; one-way ANOVA with Dunnett's multiple comparison test.

	β -arrestin recruitment		ERK 1/2 phosphorylation		¹²⁵ I-MCP1 binding
	pEC_{50}	E_{max}	pEC_{50}	E_{max}	pK_i
MCP-1	8.00 ± 0.13	0.100 ± 0.006 ^{^^^}	7.87 ± 0.32	37.8 ± 3.4	10.67 ± 0.18 ^{^^}
MCP1-311	7.30 ± 0.21	0.067 ± 0.006 [*]	6.84 ± 0.17	40.3 ± 3.2	9.90 ± 0.18
MCP1-131	8.32 ± 0.13	0.112 ± 0.006 ^{^^^}	7.64 ± 0.26	43.7 ± 3.7	10.53 ± 0.17 ^{^^}
MCP1-113	8.12 ± 0.13	0.111 ± 0.006 ^{^^^}	7.58 ± 0.46	46.7 ± 6.8	10.68 ± 0.16 ^{^^}
MCP1-133	8.45 ± 0.27	0.103 ± 0.009 ^{^^}	7.86 ± 0.42	36.4 ± 5.0	10.84 ± 0.16 ^{^^}
MCP1-333	7.82 ± 0.58	0.034 ± 0.009 ^{***}	6.95 ± 0.29	24.0 ± 3.1	10.02 ± 0.17
MCP-3	7.63 ± 0.17	0.060 ± 0.004 ^{**}	7.21 ± 0.31	34.3 ± 4.0	9.50 ± 0.19 ^{**}
MCP3-133	8.24 ± 0.11	0.0135 ± 0.005 ^{^^^}	8.12 ± 0.33	25.9 ± 2.3	10.36 ± 0.14
MCP3-313	7.17 ± 0.22	0.051 ± 0.006 ^{***}	7.43 ± 0.27	33.1 ± 3.0	7.45 ± 0.23 ^{***, ^^}
MCP3-331	7.65 ± 0.22	0.056 ± 0.006 ^{**}	7.66 ± 0.36	21.7 ± 2.3 [*]	8.77 ± 0.33 ^{***}
MCP3-311	7.13 ± 0.39	0.050 ± 0.010 ^{***}	7.87 ± 0.14	40.0 ± 1.6	7.32 ± 0.32 ^{***, ^^}
MCP3-111	7.61 ± 0.20	0.134 ± 0.010 ^{^^^}	7.99 ± 0.36	21.3 ± 2.4 [*]	9.80 ± 0.17

Table 4.4: Potency, efficacy and affinity of the MCP chemokine chimeras at the CCR2 receptor in β -arrestin recruitment, pERK and radioligand binding assays. ¹²⁵I-MCP-1 competition binding was measured in membrane preparations of c-Myc-FLAG-CCR2 FlpIn TRex 293 cells. β -arrestin 2 recruitment was assessed using BRET in FlpIn TRex 293 cells transiently transfected with CCR2-RLuc8 and β -arr2-YFP. ERK1/2 phosphorylation was measured 3-5 minutes after chemokine stimulation in c-Myc-FLAG-CCR2 FlpIn TRex 293 cells. Data are mean ± SEM from 3-4 experiments performed in triplicate. * $P < 0.05$, **, ^^ $P < 0.01$, ***, ^^[^] $P < 0.001$, compared to MCP-1 or MCP-3 respectively; one-way ANOVA with Dunnett's multiple comparison test.

Notably, subsequent introduction of the MCP-1 N-terminal region, to give the MCP3-111 chimera, increased CCR2 affinity 100-fold (relative to MCP3-311), again highlighting the importance of the N-terminus as a determinant of chemokine affinity at CCR2.

4.6.2. β -arrestin 2 Recruitment by Chemokine Chimeras

To assess the contributions of the three chemokine structural regions to the efficacy of CCR2 activation, the abilities of the chemokine chimeras to stimulate β -arr2 recruitment were measured (Fig 4.8B). As described above, MCP-3 displayed a significantly lower maximal effect than MCP-1 (Fig 4.1A and Figs 4.8B, E). Replacement of the N-loop and/or the β 3 region of MCP-1 with those of MCP-3 (or *vice versa*) caused no significant changes in E_{max} . In contrast, replacement of the N-terminus of MCP-1 with that of MCP-3, alone or in combination with replacement of both the N-loop and β 3 region, caused a significant decrease in maximal effect compared to MCP-1, to a level comparable to the maximal effect of MCP-3. This vital role of the N-terminus in determining chemokine efficacy at CCR2 was further highlighted in the reciprocal chimeras whereby integration of the N-terminus of MCP-1 into an MCP-3 background (MCP3-133 and MCP3-111) resulted in a significant increase in the maximal effect. Interestingly, the E_{max} values of these two chimeras were greater than that of wild type MCP-1, again emphasizing that the background chemokine “context” plays an additional role in determining efficacy at CCR2.

In addition to the above E_{max} values, we also compared the potencies of the chemokine chimeras in the β -arr2 recruitment. Although, no significant differences in the potencies was observed (Fig 4.8E, Table 4.4), the order of potencies is consistent with the order of binding affinities and of E_{max} values described above.

4.6.3. Induction of ERK 1/2 Phosphorylation by Chemokine Chimeras

A time course assay done in the beginning has identified that peak levels of ERK 1/2 phosphorylation were achieved 3 minutes post-stimulation with chemokine or the foetal bovine serum (FBS), which was used as a positive control. Therefore, in the following concentration response experiments the level of ERK 1/2 phosphorylation was measured at 3 minutes post-stimulation.

The wild type chemokines and the chimeras were used for the concentration response experiments. MCP-3 had a lower potency for signalling compared to MCP-1 (Fig 4.8C, E); replacing the N-terminus of MCP-1 by that of MCP-3 caused a decrease in potency whereas replacing the N-terminus of MCP-3 by that of MCP-1 caused an increase in potency, although these effects did not reach significance (Fig 4.8E, Table 4.4).

In the ERK1/2 phosphorylation assay, the two wild type chemokines and most chimeras displayed similar maximal effects (Fig 4.8E, Table 4.4). However, chimera MCP3-111 displayed a significantly lower E_{max} than wild type MCP-3 in the ERK1/2 phosphorylation assay despite exhibiting a significantly higher E_{max} than MCP-3 in the β -arr2 assay. Further analysis (Fig 4.9, Table 4.5) indicated that this chimera displayed significant biased agonism relative to WT MCP-3, suggesting that the three substituted regions of the chemokines may act cooperatively to influence signalling efficacy in a pathway specific manner.

From these data, it was clear that the N-termini of MCP-1 and MCP-3 have important roles in determining the relative affinities of the different chemokines at CCR2 as well as their relative efficacies.

4.6.4. Receptor Internalisation

Based on the above results, we predicted that the chimeric chemokines in which the N-terminal regions were swapped would have altered abilities to induce CCR2 internalisation. We used an anti-c-Myc ELISA assay to measure the levels of chemokine-induced CCR2 internalisation. Receptor cell surface and total expression were measured after incubation with 100 nM chemokine for 30 and 60 minutes. MCP-1 significantly internalised CCR2 whereas MCP-3 did not, as explained earlier (Fig 4.1E). As expected, MCP1-311 lost its ability to internalise the CCR2, while the reciprocal N-terminal swap chimera (MCP3-133) was now able to induce receptor internalisation (Fig 4.8D); confirming the importance of N-terminus region of chemokines in the functional outcomes that follow arrestin recruitment.

4.7. Discussion

Humans and other mammals express a complex array of chemokines and receptors that collectively orchestrate the trafficking of leukocytes, a central feature of the innate immune response. Around 50 different chemokines and 25 different chemokine receptors have been discovered so far, which control the migration of over 18 different leukocyte subtypes responsible for both homeostatic and inflammatory processes [239]. Different chemokine receptors are present on the same leukocytes; therefore, leukocytes will be subjected to a wide variety of chemokine:receptor interactions. For example, monocytes express the chemokine receptors CCR2, CCR5, CCR1, CCR8 and CX₃CR1, which are activated by around 13 chemokines [240].

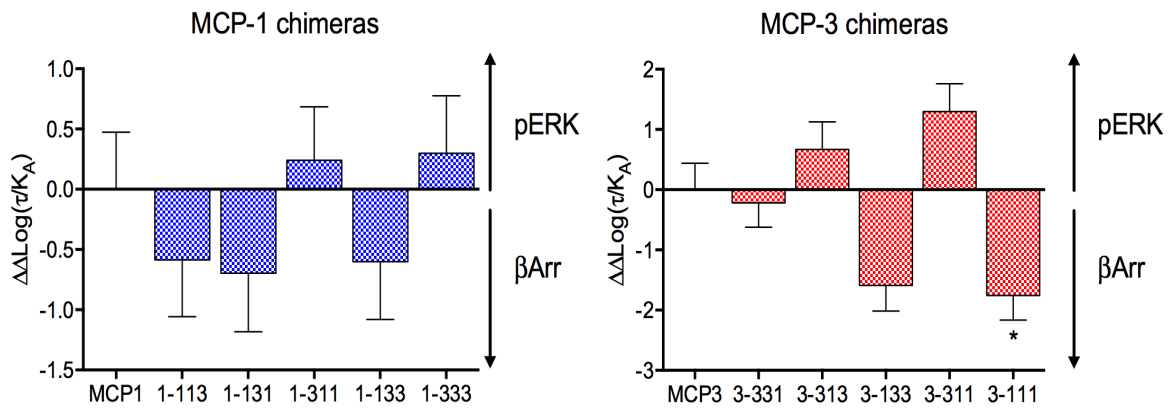


Figure 4.9. MCP3-111 displays biased agonism relative to MCP-3. Bias factors ($\Delta\Delta\text{Log}(\tau/K_A)$) between β -arrestin 2 recruitment and ERK1/2 phosphorylation, calculated from the data shown in Figure 4.8, show that the chimeric chemokine MCP3-111 is significantly ($P < 0.05$) biased towards β -arrestin 2 recruitment compared to MCP-3. Left: Bias factors for MCP-1 chimeras. Right: Bias factors for MCP-3 chimeras.

	β -arrestin recruitment		ERK1/2 phosphorylation		pERK - β Arr $\Delta\Delta\log(\tau/K_A)$
	$\log(\tau/K_A)$	$\Delta\log(\tau/K_A)$	$\log(\tau/K_A)$	$\Delta\log(\tau/K_A)$	
MCP-1	7.41 ± 0.16	0 ± 0.23	7.74 ± 0.29	0 ± 0.41	0 ± 0.47
MCP1-311	6.23 ± 0.17	-1.17 ± 0.24	6.80 ± 0.24	-0.93 ± 0.38	0.24 ± 0.44
MCP1-131	8.02 ± 0.17	0.61 ± 0.23	7.65 ± 0.31	-0.09 ± 0.42	-0.70 ± 0.48
MCP1-113	7.76 ± 0.17	0.35 ± 0.23	7.50 ± 0.29	-0.24 ± 0.41	-0.59 ± 0.47
MCP1-133	7.69 ± 0.29	0.56 ± 0.24	7.97 ± 0.18	-0.04 ± 0.41	-0.60 ± 0.48
MCP1-333	5.39 ± 0.25	-2.02 ± 0.30	6.01 ± 0.23	-1.72 ± 0.37	0.30 ± 0.48
MCP-3	6.22 ± 0.17	0 ± 0.17	7.33 ± 0.26	0 ± 0.37	0 ± 0.44
MCP3-133	8.23 ± 0.17	2.01 ± 0.17	7.75 ± 0.24	0.42 ± 0.35	-1.60 ± 0.42
MCP3-313	5.69 ± 0.20	-0.53 ± 0.19	7.47 ± 0.27	0.14 ± 0.38	0.67 ± 0.46
MCP3-331	6.01 ± 0.18	-0.21 ± 0.18	6.90 ± 0.19	-0.43 ± 0.32	-0.22 ± 0.40
MCP3-311	5.74 ± 0.21	-0.48 ± 0.21	8.14 ± 0.27	0.82 ± 0.37	1.30 ± 0.46
MCP3-111	7.65 ± 0.18	1.43 ± 0.18	6.99 ± 0.20	-0.33 ± 0.33	-1.76 ± 0.41 *

Table 4.5. MCP3-111 displays biased agonism at CCR2 compared to MCP-3. Fitted ($\log(\tau/K_A)$) and normalised ($\Delta\log(\tau/K_A)$) transducer ratios for MCP-1 and MCP-3 chimeras in β -arrestin 2 recruitment BRET and ERK1/2 phosphorylation pathways. Calculation of the bias factor ($\Delta\Delta\log(\tau/K_A)$) between pathways shows that only MCP3-111 displays significant bias towards β -arrestin 2 recruitment compared to its parental chemokine. * $P < 0.05$ one-way ANOVA with Dunnett's multiple comparison test.

The existence of multiple chemokines that activate the same receptor was previously thought to represent functional redundancy. However, recent results, including observations of partial agonism [154, 207, 219, 220, 241] and biased agonism [177, 221], increasingly suggest that these multiple interactions may coordinate to produce a range of specific leukocyte responses which are important for maintaining homeostatic and inflammatory functions. In this study, we have begun to elucidate the structural features underlying the partial agonism of MCP chemokines at their shared receptor CCR2.

4.7.1. Interpretation of Data within the 2-Site Model

Numerous previous structure-function studies of chemokines have identified residues within the N-loop and $\beta 3$ region as being critical for binding interactions and residues within the N-terminal region as being critical for receptor activation [99, 197, 237, 238]. These conclusions are encapsulated by the two-site model, which postulates that chemokines first use their N-loop/ $\beta 3$ residues (chemokine site 1; CS1) to bind to the receptor N-terminus (receptor site 1; RS1) and subsequently the chemokine N-terminus (chemokine site 2; CS2) activates the receptor by binding to its transmembrane helices (receptor site 2; RS2), inducing conformational changes and cellular signalling [238]. Recent structures of two chemokine-receptor complexes, vMIP1I: CXCR4 and CX₃CL1:US28 [105, 106] have helped to validate key features of the two-site model, but also suggested that the two sites may not be completely independent. As discussed in a recent, comprehensive review [107], a number of additional observations have also suggested that elaborations of the two-site model may be necessary. In summary, although the two-site model is broadly supported by structural and mutational data and has served as a useful guide for mechanistic studies, it is too simplistic to account for such subtle observations as partial or biased agonism.

The structure-function relationships of MCP-1 have been thoroughly examined in a seminal study by Handel and co-workers [197, 237]. Extensive mutagenesis studies by Hemmerich et al. [197] and Jarnigan et al. [237] have identified the residues of MCP-1 which are responsible for binding to CCR2 and downstream signalling. MCP-1 residues T10 (N-terminal region, immediately preceding the CC motif), Y13 and R24 (N-loop), K35 (“30s” loop) and K49 ($\beta 3$ region) make substantial contributions to CCR2 binding affinity and N-terminal residues I5 and V9 of MCP-1 contribute to signalling via CCR2. Almost all of the MCP-1 residues shown to play key roles in CCR2 binding or activation are identical in MCP-3. Thus, the interactions of these residues do not account for the differences in the CCR2 binding affinity or efficacy of MCP chemokines.

4.7.2. The Chemokine N-terminal Tail is a Major Determinant of Affinity and Efficacy

In good agreement with the previous observations of MCP-1 mutants and the two-site model, our β -arr2 recruitment data for MCP1-311 and MCP3-133 indicate that the chemokine N-terminal region is the major selectivity determinant of receptor activation manifested by changes in the intrinsic efficacy of these different chemokines.

However, surprisingly, our analysis of MCP-1/MCP-3 chimeras also identified the N-terminal region as being the primary determinant of the binding selectivity of these two chemokines to CCR2. The N-terminus of MCP-1 plays a significant role in determining higher affinity compared to MCP-3. Replacement of the N-terminus of MCP-3 with that of MCP-1, generated a chimeric chemokine with comparable affinity to that of MCP-1 and the reciprocal chimera exhibited a decrease in affinity similar to MCP-3 (Fig 4.8A). Residues within this region were not previously found to contribute to binding affinity, with the sole exception of T10 [197], which is identical in MCP-1 and MCP-3. Moreover, this region corresponds to CS2, which is considered in the two-site model to be the key determinant of receptor activation, but not to play a role in the initial binding step. However, from these data, it is clear that the N-termini of MCP-1 and MCP-3 have important roles in determining the relative affinities of the different chemokines at CCR2 as well as their relative efficacies.

4.7.3. Background Dependence of Chimeras

In contrast to the results with the N-terminal swap chimeras, substituting the N-loop or β 3 region of MCP-1 with those of MCP-3, or substitution of both regions simultaneously (chimeras MCP1-131, -113 and -133), has no effect on the CCR2 binding affinity (Fig 4.8A), efficacy of β -arr2 recruitment (Fig 4.8B), or the potency of ERK-1/2 phosphorylation (Fig 4.8C). Similarly, the converse chimeras (MCP3-313, -331 and -311) displayed properties more closely resembling those of the parental chemokine wild type MCP-3 than of wild type MCP-1. Interestingly, however, substitution of the N-loop yielded chimeras (MCP3-313 and -311) with lower CCR2 binding affinity than either wild type chemokine without affecting signalling efficacy or potency, suggesting that the ability of the N-loop to support receptor binding is not completely independent of the background scaffold. Nevertheless, these results indicate that the interactions of the N-loop and β 3 strand have minimal influence on the relative strengths of CCR2 agonism by MCP-1 and MCP-3.

Finally, two other chimeras (MCP1-333 and MCP3-111) were also analysed, in which all three receptor-interacting regions of one chemokine are substituted onto the other chemokine. We had predicted that the three regions, which we were mutating, would be enough to make the chimera

similar to the wild type chemokine whose regions were inserted onto the other chemokine. However, we found that MCP1-333 does not behave identically to MCP-3 and MCP3-111 does not behave identically to MCP-1. This could be due to several reasons. First, we did not mutate all the residues in the swapped regions. The residues which were not mutated were potentially important for the core structure of chemokine; but their interactions with the surrounding residues, which we mutated, might have an effect on the affinity and efficacy of chimeras. Second, these three regions might act cooperatively with each other and the strength of this cooperativity could be dependent on the background structural context. Finally, there are a number of residues outside these regions which are different between MCP-1 and MCP-3, potentially influencing the receptor interactions either directly or indirectly.

In summary, our results show that the distinct affinities and efficacies of CCR2 activation by MCP chemokines can be primarily attributed to the interactions of the chemokine N-terminal region. The N-terminus of the chemokine is the key feature that contributes to partial vs full agonism in MCP-3 and MCP-1 at their shared receptor CCR2. However, other regions of the chemokines, particularly the N-loop, may also contribute to chemokine efficacy, with their contributions being dependent on the background scaffold in which they are located.

The observation that the chemokine N-terminus is the major determinant of efficacy at CCR2 raised the question of which CCR2 residues can differentiate between MCP-1 and MCP-3. This question is addressed in the next chapter.

***Chapter 5. Identification of Key
CCR2 Elements that Interact
with the N-terminal Region of
Cognate Chemokines***

5.1. Introduction

As mentioned earlier, the chemokine-receptor network is quite complex. Most chemokine receptors bind multiple chemokines, and many chemokines can bind multiple chemokine receptors. Initially, the existence of multiple ligands for the same receptor was thought to create redundancy in their action towards the target cells. However, these multiple chemokine-receptor interactions fine tune leukocyte recruitment for different inflammatory stimuli.

CCR2 is a major chemokine receptor on monocytes and macrophages, cells that play central roles in the pathology of atherosclerosis, obesity and type 2 diabetes. The main ligands of CCR2 are the MCP chemokines. Berchiche et al. (2011) [154] have shown that MCP-1 and MCP-3 differentially activate CCR2. Our results from chapter 4 have also demonstrated the differential activation of CCR2 by MCP-1 and -3. MCP-1 acts as a full agonist of the receptor, while MCP-3 functions as a partial agonist.

In chapter 4, we have found that the N-terminus of the chemokines is the key region that contributes to this differential activation at the same receptor. The chimeras with N-terminal swaps showed affinity and efficacy differences from the parent chemokine and instead resembled the chemokine from which the N-terminal region was derived (Chapter 4, Figure 4.8)

It has been mentioned before, that chemokines interact with their chemokine receptors via a two-step process, the 2-site model [210, 238]. In the first step, the core structure of the chemokine (N-loop and the β 3 region-CS1) binds to the N-terminus of their receptor (RS1) [185]. In the second step, the chemokine N-terminus (CS2) then interacts with the transmembrane helices and/or extracellular loops (ECLs) of the receptor (RS2), which causes a conformational change thereby activating the receptor which starts a series of downstream signalling processes.

Mutational studies of different chemokine receptors have been helpful to explain the role played by each part of the receptor in binding or activation. Monteclaro et al. have shown through a chimeric approach that N-terminus of CCR2 is very important for high affinity binding to MCP-1 [98]. Samson et al. have also reported that the N-terminus of CCR2B determines the binding affinity of its cognate chemokines [109]. Pease et al. have made mutants of CCR1 and CCR3 by swapping the extracellular N-terminal segments to bind their respective ligands. They report that N-terminus is not the only site responsible for chemokine recognition, as the mutants still retain the ability to bind to their original chemokine ligands to a reduced level. Their findings support a multi-site model, where not only the N-terminus of the receptor is responsible for chemokine recognition, but more sites are involved in determining the specific chemokines which interact with a particular receptor [242]. Skelton et al. have presented an NMR structure of a complex between CXCL8 and a receptor-

based peptide of CXCR1. This peptide is reported to bind in a groove between N loop and β 3 strand of CXCL8. As compared to the wild type receptor, the affinity of this peptide is much lower, ultimately leading to the concept that other extracellular regions of the receptor are also required for high affinity binding to IL-8 [243].

Brelot and coworkers (2000) have performed mutagenesis studies on CXCR4. Mutation in the NT of CXCR4, of E14, E15 and Y21 affects CXCL12 binding, confirming the site 1 interactions from the two-site model [108]. Blanpain et al. have characterised the role of and N-terminus of CCR5 in the chemokine binding and they concluded that CCL3 and CCL5 interact with specific residues in the CCR5 [244].

Mutants of TM and ECL residues of the chemokine receptors have shown, that these residues contribute to chemokine binding and activation. Samson et al. [109] have also investigated the regions of CCR5 and CCR2B which are involved in activation by their specific ligands. They have determined that residues from ECL2 and TM regions in CCR5 are responsible for binding and activation by CCL3, CCL4 and CCL5. The ECL residues also play an important role in the transmembrane signalling by CCR2B [109].

Mirzadegan et al. have identified D284 and E291 as important residues in CCR2, which contribute to the binding interactions between MCP-1 and CCR2 [245]. Brelot and co-workers (2000) have also pointed out the importance of some residues in ECL2 and TMs for chemokine interaction. Certain residues in ECLs and TM region like D187 in ECL2, D97 in TM2, and E288 in TM7 were found to be very important for both binding and signalling of CXCL12, confirming that the residues of ECLs/TM are involved in RS2 interactions [108]. Govaerts et al. have described about the presence of a proline and threonine in TM2 of all chemokine receptors. They have explained through mutagenesis studies that this sequence TXP motif in TM2 of the CCR5 is important for normal functioning of the receptor. This motif is mainly involved in activation of the receptor but also plays a minor role in ligand binding [246].

Blanpain et al. have also reported about the role of ECL2 and transmembrane helices. They have specified that the residues, which are responsible for selective binding of chemokines, are in ECL2, while, the transmembrane helices play a part in activation of the receptor. They have characterised several mutations in the extracellular domains of the CCR5 (E172A, R168A, K191A and D276A) which have affected the binding of CCL3, but not CCL5. Several receptor mutants were designed by changing few residues in the TM2 and TM3 (L104F, L104F/F109H/F112Y, F85L/L104F). CCL3 has shown 10-100 fold less potency with these mutants compared to the wild type CCR5; while there was not much effect on the activation by CCL5 [108].

Kofuku et al. have highlighted the importance of two residues, D97^{2.63} and E288^{7.39} in TM2 and TM7 respectively, of CXCR4 in interactions with the N terminus of CXCL12 [247]. Rodriguez et al. [248] have reported that mutation of Y139 residue leads to formation of a non-functional receptor CCR2, which is unable to signal. Berkhout et al. [249] have reported about another residue E291, which plays a very important role in MCP-1 binding with CCR2 located in TM7 region.

In summary, the mutational data suggests that in most cases studied, the N-terminus makes a significant contribution to the chemokine binding. However, other regions are also required for high affinity interactions. These mutational studies also suggest that TM and ECL residues are critical for TM signalling. However, different receptors may utilise different regions for binding and activation, or, one receptor may use different residues for recognition of different chemokines. These results are broadly consistent with the two-site model, although binding and activation may not be as clearly separated as suggested by the two-site model.

In addition to these mutational studies, two recent structural studies have provided some support for the two-site model. Qin et al. [105] have reported the crystal structure of the chemokine receptor CXCR4 in complex with a viral chemokine antagonist vMIP-II, whereas Burg et al. [106] have reported the structure of a complex between human cytomegalovirus GPCR US28 and the CX₃CL1 chemokine. These structures provide the most detailed insight to date of the interactions between chemokines and their cognate receptors. These chemokine-receptor complexes have confirmed that the N-terminal regions of chemokines penetrate the transmembrane (TM) helical bundles of their receptors, where they presumably induce structural rearrangement and signalling. They have shown that the N-terminus of the chemokine binds to one part of the TM cavity of the receptor. This suggests that different residues in the CS2 (chemokine N-terminus) interact with specific residues in the receptor TM region, resulting in different conformations of the activated receptor. This might lead to a change in the intracellular signals.

Recently reported structures of CCR2 and CCR9 [250, 251] have given new insights about the mode of action of chemokine receptors and their ligands. Considering the recent advances in knowledge of chemokine receptor structure, we are now able to investigate the structural basis of differential activation by chemokine ligands. We have used a variety of CCR2 mutants to identify key structural elements of the receptor that mediate differential activation by MCP-1 and MCP-3. Data are interpreted considering the recent structures of chemokine-receptor complexes [105, 106], yielding insights towards the design of selective pharmacological agents.

Herein we describe an analysis of the structural features underlying differential activation of a chemokine receptor by its cognate chemokine ligands, which have helped us to identify specific residues of the receptor CCR2 that differentiate between MCP-1 and MCP-3.

5.2. Design of CCR2 Mutants

As explained in chapter 4, the chemokine N-terminal region contributes to both the affinity of CCR2 binding and the efficacy of CCR2 activation. We therefore sought to identify the residues within CCR2 with which the chemokine N-terminal region interacts. Based on the previous mutational and structural results described above, we decided to make a series of mutations of specific CCR2 residues within receptor site 2 (TM helices/ ECLs), which is implicated in interaction with the N-terminal region of the chemokines.

A CCR2:MCP-1 homology model was used to identify likely residues of the CCR2 to be involved in interactions with the chemokines. The model was based on the reported structure of CXCR4:vMIPII (PDB ID: 4RWS) [105]. The initial selection of the target residues was based on their orientation within receptor site 2. Most of the mutations were to alanine, except the two tyrosines, which were mutated to phenylalanine, as mutation to alanine was considered to be structurally disruptive. The final selection led us to design six point mutants and four double mutants at positions pointing towards the interior of the TM bundle. These selections were based on the close position of the residues in the protein sequence. (Fig 5.1; Table 5.1).

5.3. Determination of Receptor Expression Levels

Each mutant was stably expressed in FlpIn TRex HEK-293 cells with an N-terminal c-Myc epitope tag, enabling measurement of cell surface expression. The expression level of all mutants was checked by anti-c-Myc ELISA and found to be not significantly different from the wild type CCR2. (detail in chapter 2, 2.14.1.) (Table 5.1). Thus, we were able to interpret the effects of mutations on binding affinity and chemokine activation (determined below) as resulting from changes in receptor structure and/or function rather than changes in expression levels.

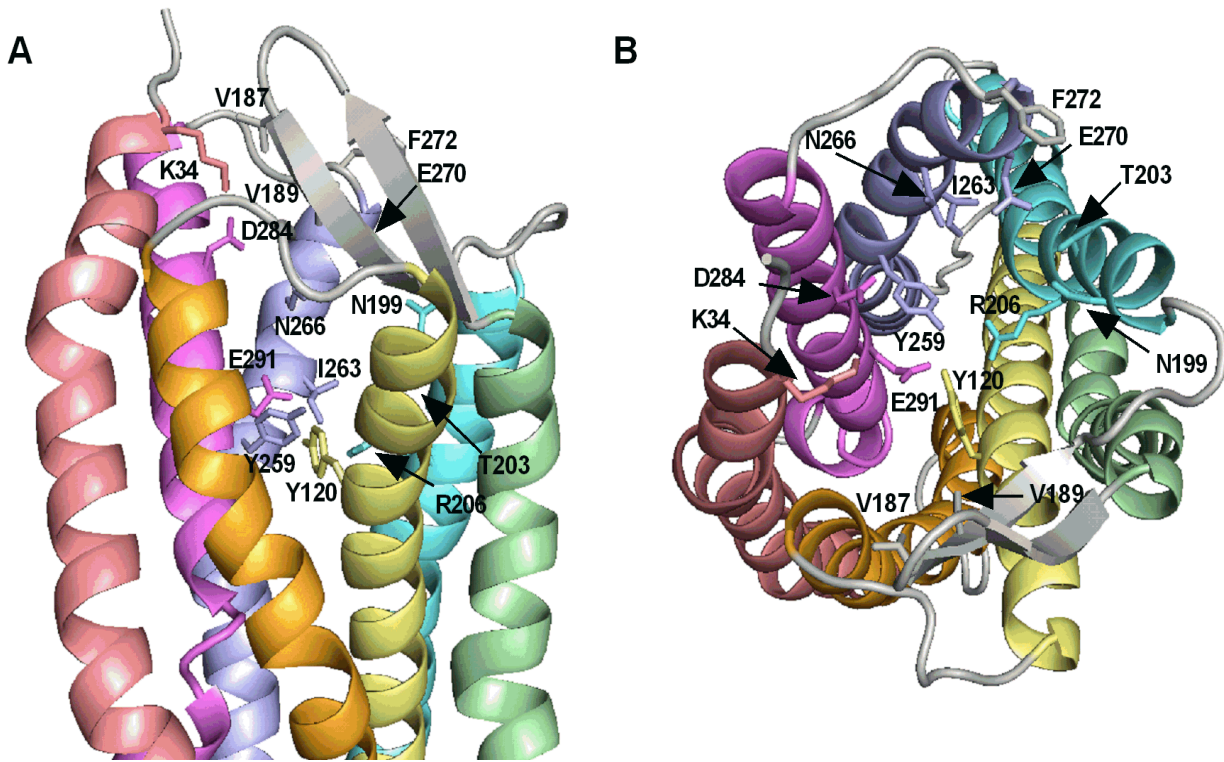


Figure 5.1. Homology model of CCR2 bound to MCP-1, showing the positions of the mutated residues. (A) Side view and (B) end-on view (from the extracellular perspective). CCR2 transmembrane helices are coloured salmon (TM1), orange (TM2), pale yellow (TM3), pale green (TM4), aquamarine (TM5), light blue (TM6) and violet (TM7); other receptor residues are in grey. Side chain sticks are shown for mutated residues in the same colours as the helices/loops in which they are located.

Mutation	Location [#]	Cell surface expression	pK _i		pERK1/2 pEC ₅₀		pERK1/2 E _{max} (% FBS)	
			MCP-1	MCP-3	MCP-1	MCP-3	MCP-1	MCP-3
WT		100 ± 3	10.82 ± 0.18	9.64 ± 0.19 [^]	8.01 ± 0.23	7.30 ± 0.23	38.9 ± 3	35.5 ± 4.5
K34A	TM1 (1.28)	119 ± 12	10.42 ± 0.27	9.70 ± 0.42	8.41 ± 0.24	7.70 ± 0.23	55.5 ± 2.5 ^{***}	45.0 ± 2.8
Y120F	TM3 (3.32)	118 ± 13	11.15 ± 0.18	9.65 ± 0.26 [^]	7.92 ± 0.32	7.58 ± 0.33	25.4 ± 2 ^{**}	16.6 ± 1.6 ^{***}
V187/V189A	ECL2	108 ± 6	11.36 ± 0.29	9.85 ± 0.32 [^]	7.99 ± 0.26	7.28 ± 0.23	30.5 ± 2	30.8 ± 2.3
N199A/T203A	TM5 (5.35/5.39)	116 ± 7	11.42 ± 0.29	10.17 ± 0.47	7.66 ± 0.23	7.35 ± 0.33	32.8 ± 2	20.2 ± 2.3 ^{**}
R206A	TM5 (5.42)	112 ± 7	10.29 ± 0.22	10.12 ± 0.33	8.25 ± 0.31	7.81 ± 0.34	11.0 ± 0.8 ^{***}	14.8 ± 2.5 ^{***}
Y259F	TM6 (6.51)	99 ± 6	10.44 ± 0.23	10.20 ± 0.14	8.78 ± 0.36 [*]	8.57 ± 0.26 ^{**}	31.9 ± 1.7	39.3 ± 1.7
I263A/N266A	TM6 (6.55/6.58)	107 ± 8	10.79 ± 0.24	8.99 ± 0.17 [^]	9.46 ± 0.39 ^{**}	8.22 ± 0.38	24.7 ± 2 ^{***}	36.9 ± 3.4
E270A/F272A	TM6/ECL3	99 ± 13	11.68 ± 0.39	10.06 ± 0.31 [^]	7.36 ± 0.20	7.36 ± 0.20	22.3 ± 1.3 ^{***}	22.1 ± 1.5 ^{**}
D284A	TM7 (7.32)	104 ± 5	10.91 ± 0.16	9.52 ± 0.25 [^]	8.83 ± 0.40 ^{**}	7.80 ± 0.18	34.9 ± 2	39.1 ± 1.9
E291A	TM7 (7.39)	107 ± 9	10.26 ± 0.24	9.03 ± 0.22 [^]	7.66 ± 0.40	7.09 ± 0.48	27.9 ± 3 [*]	12.1 ± 2.2 ^{***}

Table 5.1: Characterisation of CCR2 mutants. Cell surface expression was measured by anti c-Myc ELISA in c-Myc-FLAG-CCR2 FlpIn TRex 293 cells. Affinity (pK_i) of MCP-1 and MCP-3 for wild type or mutant CCR2 was measured by ¹²⁵I-MCP-1 competition binding with cell membrane preparations. Potency (pEC₅₀) and efficacy (E_{max}) of MCP-1 and MCP-3 for wild type or mutant CCR2 in ERK1/2 phosphorylation was measured 3 minutes after chemokine stimulation in c-Myc-FLAG-CCR2 FlpIn TRex 293 cells. Data are mean ± SEM from 3-4 experiments performed in triplicate. For radioligand binding, [^] P<0.05, compared to MCP-1 for each mutant, multiple t-test. For ERK1/2 phosphorylation, * P<0.05, ** P<0.01, *** P<0.001, compared to CCR2 WT, one-way ANOVA with Dunnett's multiple comparison test. [#] Ballesteros and Weinstein numbering of TM residues are shown in parentheses [252].

5.4. Effects of CCR2 Mutations on Binding and Activation by Wild type Chemokines

First, we evaluated the affinity of chemokine binding at each mutant receptor. Further, we extended this evaluation to measure the potency and efficacy of MCP-1 and MCP-3 at the mutant receptors using ERK 1/2 phosphorylation as a convenient measurement of receptor activation that does not require the use of modified receptor fusion constructs or overexpression of signalling effectors.

None of the mutations significantly changed the affinities for MCP-1 or MCP-3 compared to WT CCR2 (Table 5.1, Fig 5.2, Fig 5.3A). However, comparison of the relative affinities of MCP-1 and MCP-3 at the different mutants was more revealing. MCP-3 displays a 10-fold lower affinity than MCP-1 at the WT CCR2. While this difference in affinity was maintained at most of the CCR2 mutants, no such difference in affinity was observed at the R206A and Y259F mutations. Therefore, the difference in affinity between MCP-1 and MCP-3 appears to be governed, at least in part, by these two residues.

As shown previously at wild type CCR2, MCP-1 displays a significantly higher potency than MCP-3. This difference in potency was maintained across most mutants, in accordance with the relative affinities for the two ligands (Fig 5.2, 5.3B). Nevertheless, mutant Y259F displayed increased potency for both chemokines; double mutant I263A/N266A displayed significantly increased potency for MCP-1 ($p = 0.003$) and a smaller, but not significant, increase for MCP-3; and D284A showed a significant potency increase for MCP-1 but not MCP-3 (Fig 5.3B).

Although the potencies of ERK1/2 phosphorylation correlate well with CCR2 binding affinities for the wild type chemokines (Chapter 4, Fig 4.1), there is a poor correlation between affinity and potency comparing the same chemokine across the set of CCR2 mutants (Fig 5.4A and B).

This suggests that some of the mutations influence the mechanism of receptor signalling rather than ligand binding. To further explore this possibility, we examined the maximal effects induced by the two chemokines in the ERK1/2 phosphorylation assay (Fig 5.2, 5.3C, 5.4C). CCR2 mutants Y120F, R206A, E270A/F272A and E291A displayed significantly lower E_{max} values for both MCP-1 and MCP-3 as compared to WT CCR2. Interestingly, the maximal effect of MCP-1 but not MCP-3, was significantly reduced at the I263A/N266A mutant. Conversely, the double mutant N199A/T203A displayed a significantly reduced E_{max} for MCP-3, but not MCP-1. Finally, the mutation K34A caused an increase in E_{max} relative to WT for MCP-1 and a similar trend was observed for MCP-3.

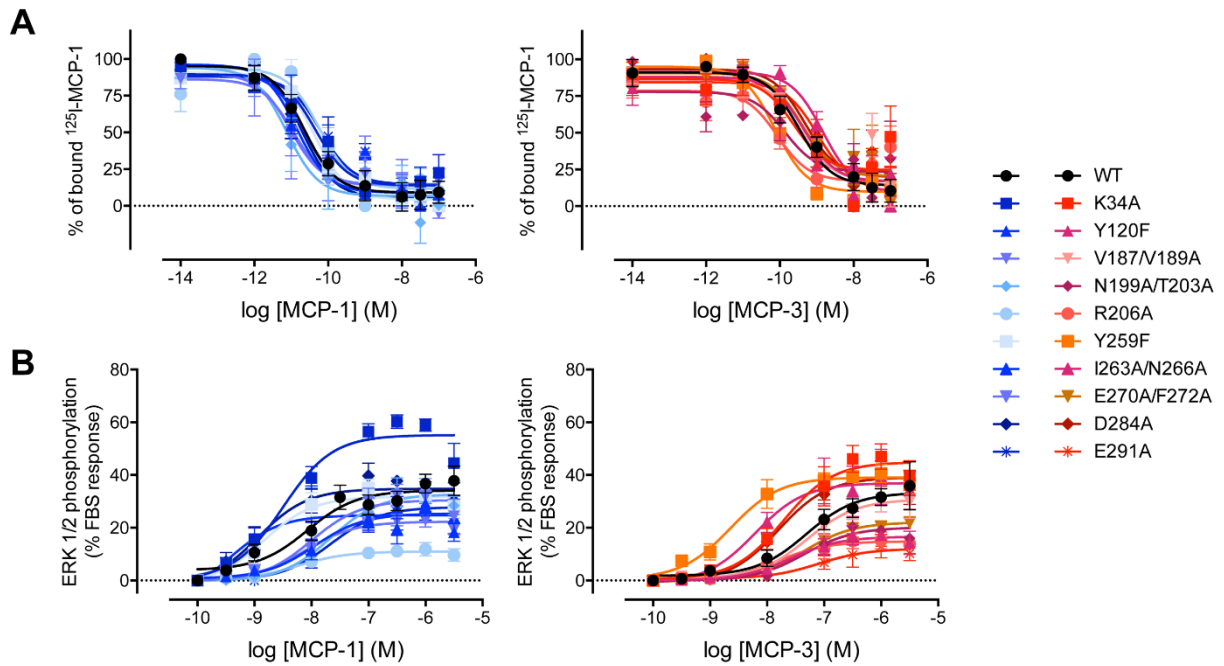


Figure 5.2. ^{125}I -MCP-1 competition binding and ERK1/2 phosphorylation concentration response curves for CCR2 mutants. ^{125}I -MCP-1 competition binding and ERK1/2 phosphorylation were assessed for MCP-1 and MCP-3 at the wild type (WT) and mutant CCR2 expressed in FlpIn TRex 293 cells. **(A)** Competition binding curves of MCP-1 (blue) and MCP-3 (red) for WT or mutant CCR2 measured in cell membrane preparations. **(B)** ERK1/2 phosphorylation concentration response curves of MCP-1 (blue) and MCP-3 (red) for WT or mutant CCR2. Data are the mean \pm SEM from 3-5 experiments performed in triplicate.

Chapter 5. Identification of Key CCR2 Elements

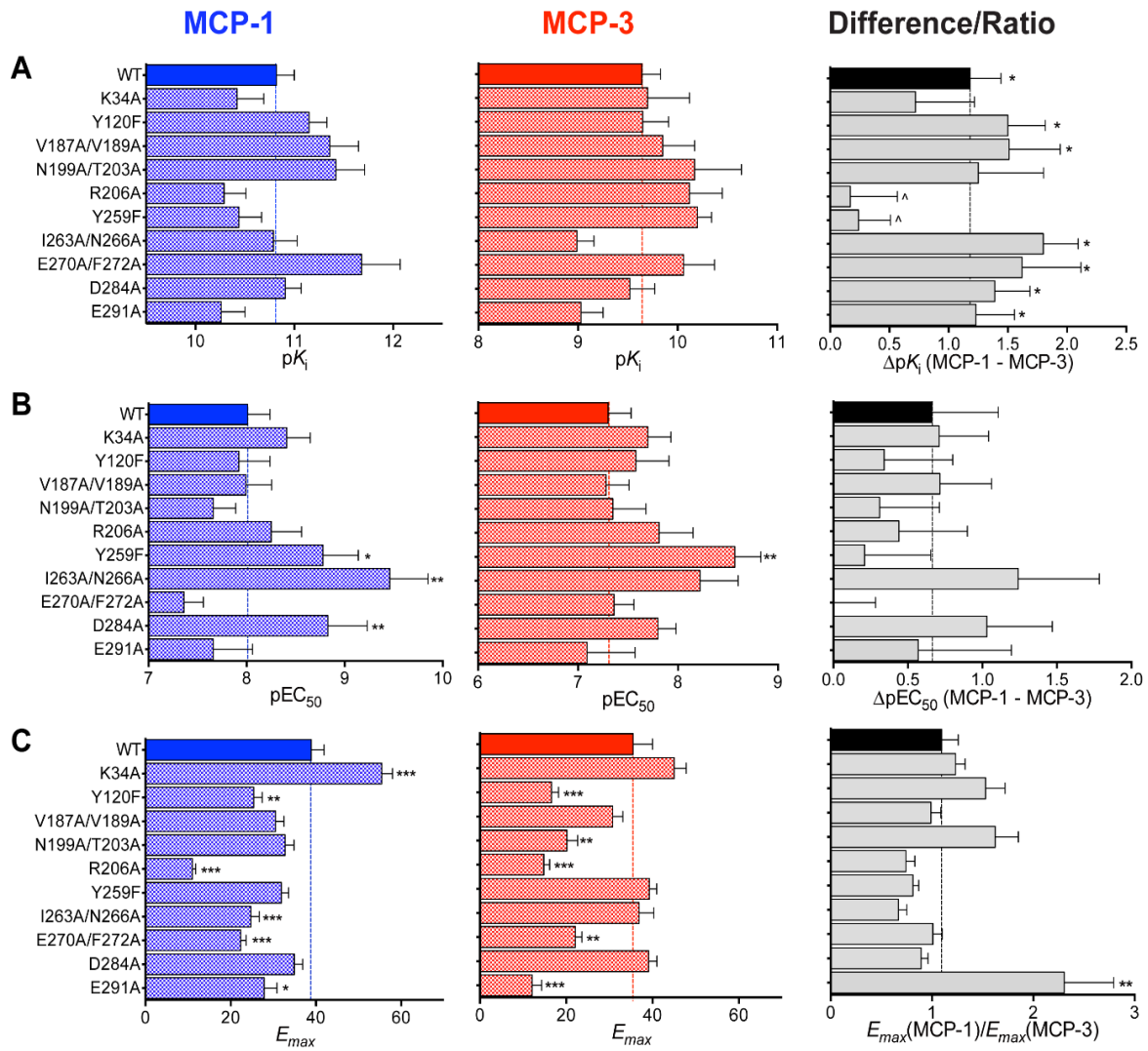


Figure 5.3. Identification of CCR2 residues contributing to MCP-1 and MCP-3 binding and agonism. ^{125}I -MCP-1 competition binding and ERK1/2 phosphorylation were assessed for MCP-1 and MCP-3 at the wild type (WT) and mutant CCR2 expressed in FlpIn TRex 293 cells. **(A)** Affinity ($\text{p}K_i$) of MCP-1 (blue) and MCP-3 (red) for WT or mutant CCR2 measured by ^{125}I -MCP-1 competition binding with cell membrane preparations. Right/grey panel: differences in affinity between MCP-1 and MCP-3 at each mutant. $^{\wedge} P < 0.05$, compared to the difference observed at the WT and $* P < 0.05$, compared to zero (i.e. indicating difference between chemokines), multiple t-test. **(B)** Potency (pEC_{50}) of MCP-1 (blue) and MCP-3 (red) for WT or mutant CCR2 in ERK1/2 phosphorylation. Right/grey panel: differences in potency between MCP-1 and MCP-3 at each mutant receptor. $* P < 0.05$, $** P < 0.01$ compared to the difference observed at the WT one-way ANOVA with Dunnett's multiple comparison test. **(C)** Efficacy (E_{max}) of MCP-1 (blue) and MCP-3 (red) for WT or mutant CCR2 in ERK1/2 phosphorylation. Right/grey panel; ratio of efficacies between MCP-1 and MCP-3 at each mutant. $* P < 0.05$, $** P < 0.01$, $*** P < 0.001$, $**** P < 0.0001$ compared to ratio observed at the WT, one-way ANOVA with Dunnett's multiple comparison test. Data are means \pm SEM from 3-5 experiments performed in triplicate.

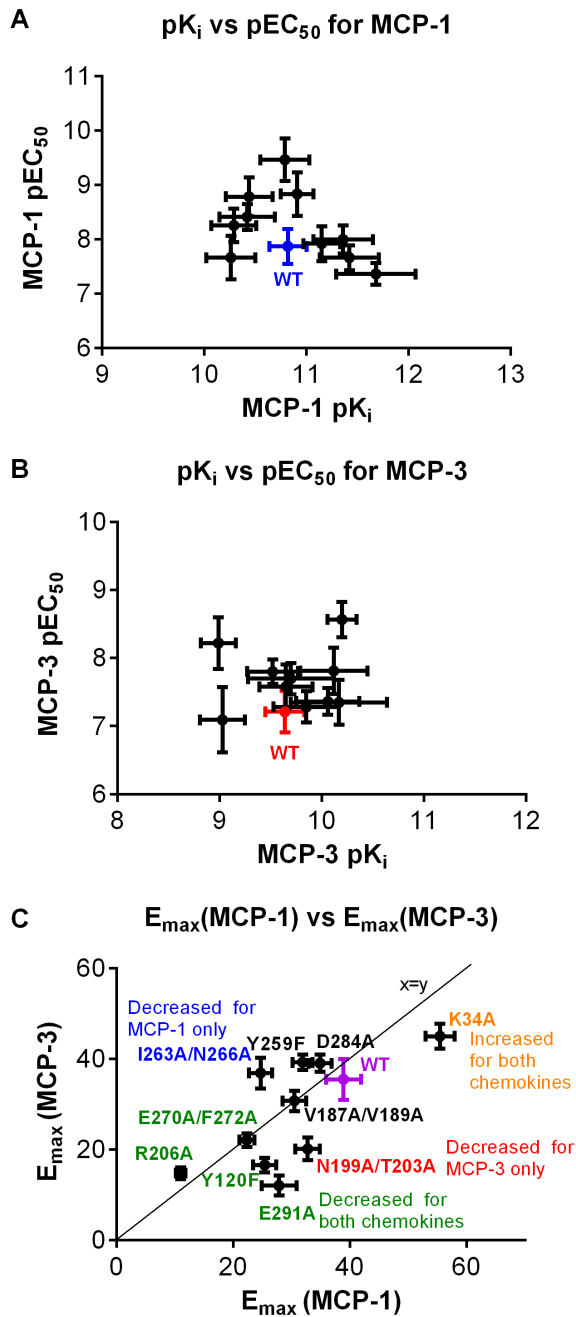


Figure 5.4. Graphical comparisons of chemokine binding and ERK1/2 phosphorylation parameters across the set of CCR2 mutants. (A, B) Binding affinity (pK_i) versus potency (pEC₅₀) for (A) MCP-1 and (B) MCP-3. (C) Efficacy (E_{max}) for activation by MCP-1 versus MCP-3.

It should be noted that the cell surface expression levels for all mutants was not significantly different. Thus, these changes in maximal signalling likely reflect the roles of these residues in conformational rearrangement of CCR2 coupled to ERK1/2 signalling pathways

5.5. Discussion

To identify receptor residues that interact with the N-terminal regions of MCP-1 and/or MCP-3, we mutated residues in CCR2 whose side chains are predicted to point towards the interior of the transmembrane helical bundle. Several of the mutants displayed altered chemokine binding. In particular, mutation of R206^{5.42} or Y259^{6.51} (superscripts indicate Ballesteros-Weinstein numbering [252]) completely abolished the ~10-fold binding selectivity of CCR2 for MCP-1 over MCP-3. These residues form a closely packed cluster with residues Y120^{3.32}, I263^{6.55} and E291^{7.39} in a region where TM helices 3, 5, 6 and 7 come together, previously defined as the “major subpocket” of the receptor (Fig 5.5A-C) [253].

Residue R206^{5.42} forms hydrogen bonds with histidine 121 (TM3) and 202^{5.38} (one turn above in TM5) [249]. Replacement of arginine by alanine may disrupt those hydrogen bonds, leading to loss of affinity and lower maximal effect for chemokines at the R206A mutant.

In support of the contribution of this structural region to binding, mutation of I263 (in the I263A^{6.55}/N266A^{6.58} double mutant) slightly reduced affinity for MCP-3 and mutation of E291^{7.39} slightly reduced affinity for both MCP-1 and MCP-3 (Table 5.1). Importantly, these residues are adjacent to the extreme N-terminus of the bound chemokine in our homology model (Fig 5A-C), suggesting that they interact directly with the chemokine ligands. This conclusion is supported by a recent exhaustive mutagenesis study of CXCR4 defining a similar cluster of signal “initiation residues” adjacent to the N-terminus of CXCL12 [254]. Notably, in the complex of vMIP-II with CXCR4 from which our homology model was derived, the N-terminus of vMIP-II points slightly away from these residues into the “minor subpocket” of CXCR4 (Fig 5.5D and E) [105].

Our data suggest that the interactions of the CCR2 major subpocket with the chemokine N-terminus play a critical role in stabilising the chemokine-receptor complex and in determining the relative affinities of MCP-1 and MCP-3 at their shared receptor.

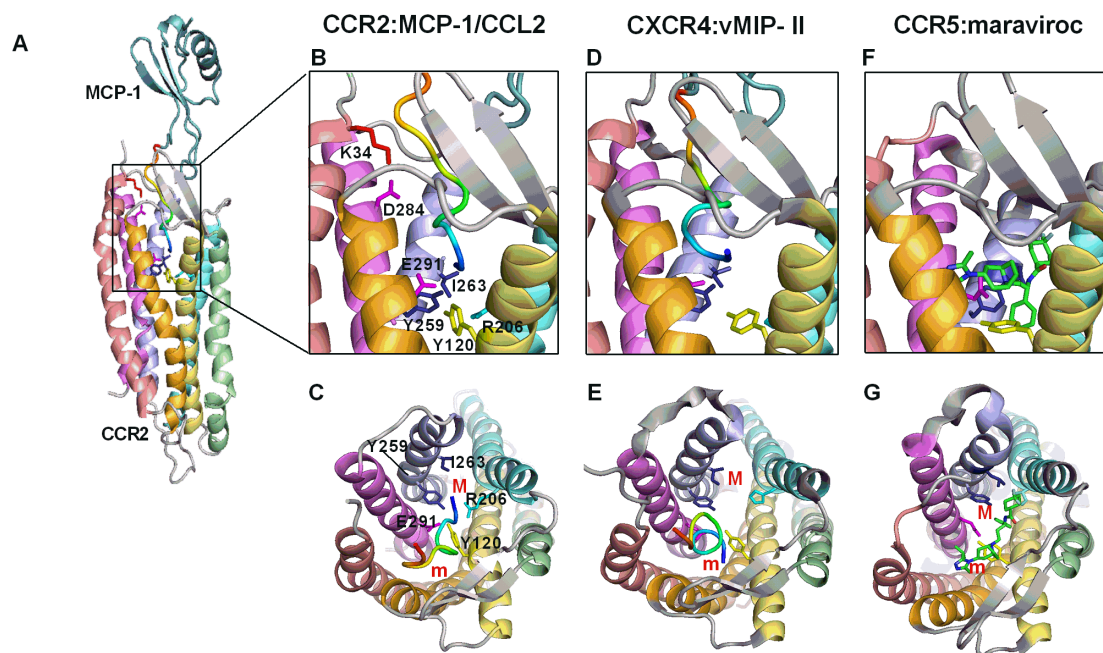


Figure 5.5. The major subpocket of CCR2 recognises the N-termini of MCP chemokines. (A) Full and (B) detailed side views and (C) end-on view (from the extracellular perspective) showing the homology model of CCR2 bound to MCP-1. CCR2 transmembrane helices are coloured salmon (TM1), orange (TM2), pale yellow (TM3), pale green (TM4), aquamarine (TM5), light blue (TM6) and violet (TM7); other receptor residues are in grey. Side chain sticks are shown for several residues discussed in the text in darker shades of the same colours as the helices in which they are located. MCP-1 is in teal with the N-terminus in rainbow colours from blue (residue 1) to red (residue 10). In (C) the major (M) and minor (m) subpockets are labelled in red. (D) and (E) The CXCR4:vMIP-II complex (pdb code: 4rws) displayed as in (B) and (C), respectively. (F) and (G) The CCR5:maraviroc complex (pdb code: 4mbs) displayed as in (B) and (C), respectively; maraviroc is shown as sticks coloured by element (C, green; N, blue; O, red).

Among the CCR2 mutations that reduced chemokine binding affinity, the Y259F and I263A/N266A mutations surprisingly caused increased potency of MCP-1 and/or MCP-3. This lack of correlation between potency and affinity can be rationalised by considering the possible interactions of these residues in the chemokine-receptor complex prior to undergoing the conformational change required for activation (the inactive state) and after this conformational change (the active state).

Our affinity measurements were performed in the presence of guanine nucleotides and therefore are likely to probe interactions in the inactive state (i.e. not bound to G protein), whereas the potency of ERK1/2 phosphorylation is likely to be more sensitive to interactions in the active state (G protein-coupled). We suggest that the Y259F and I263A/N266A mutations disrupt interactions in the inactive state but favor the transition to the active state, thereby enhancing potency. In contrast, the R206A and E291A mutants displayed decreased affinity and decreased efficacy of ERK1/2 phosphorylation without any significant change in potency. Disruption of these residues may alter the structure of the active state such that it is no longer well coupled to ERK signalling effectors.

Several CCR2 mutations influenced ERK1/2 phosphorylation without affecting chemokine binding affinity. The D284A^{7.32} mutation enhanced the potency of ERK phosphorylation in response to MCP-1 and the K34A^{1.28} mutation enhanced the efficacy of ERK phosphorylation in response to both chemokines. These two residues are located adjacent to each other and form a salt bridge in our homology model (Fig 5.5B). We propose that these residues do not contribute directly to ligand interactions but instead stabilise the inactive state of the receptor by interacting with each other and/or with other residues on adjacent TM helices. Disruption of these interactions may therefore facilitate the transition to the active state, albeit at the expense of destabilising the unbound receptor structure.

Our findings are consistent with two previous mutational studies of CCR2. It has been reported by Berkhout et al. [249] that residues in TM helices of the receptor are very important for activation of the receptor as they are involved in binding to the ligand, especially highlighting the importance of a glutamate on TM2 and then E291^{7.39} and D284^{7.32} present on TM7. They predicted that out of these three E291^{7.39} is thought to form a salt bridge with an antagonist molecule. They have observed a small decrease in affinity of chemokine with E291^{7.39} and D284^{7.32} mutants. However, two of our receptor mutants E291A^{7.39} and D284A^{7.32} showed no significant change in affinity with MCP-1 and -3, although we found that these residues play a part in receptor activation.

Hall et al. [255] have identified certain residues that are important for chemokine binding in both CCR2 and CCR5. They have shown that Y49^{1.39}, W98^{2.60}, Y120^{3.32} and E291^{7.39} of CCR2 form

a tight network between transmembrane helices 1, 2, 3, and 7. They have mentioned that I263^{6.55} and T292^{7.40} also contribute to binding of some antagonists, but not others. In agreement with the importance of this region of the receptor, we have identified Y120^{3.32}, I263^{6.55} and E291^{7.39} as residues not only responsible for differential binding of MCP-1/-3, but also responsible for differential activation.

Wescott et al. [254] have used shotgun mutagenesis to identify a possible pathway which an extracellular signal follows from binding of chemokine to the N-terminus of its receptor till the signal reaches the G protein [254]. This signal transmission from the extracellular environment occurs through the transmembrane helices of the receptor to the intracellular environment. It was identified that most of the residues are connected to each other forming an intra-molecular chain, from extracellular environment to intracellular environment, that signals through transmembrane helices [254]. They have reported 41 amino acid residues of CXCR4 which are involved in transmission of signal, of which 33 are present in the TM region, specifically in the TM helices 3, 6 and 7. They identified three residues from CXCR4 proposed to be very close to the N-terminus of CXCL12 and responsible for binding and signal initiation. Two of these are Y116^{3.32} and E288^{7.39}, which correspond to Y120^{3.32} and E291^{7.39} in CCR2. These residues were considered by Wescott et al. [254] to play a critical role in receptor activation. The Wescott model is in excellent agreement with our results as we have identified Y120^{3.32} and E291^{7.39} in CCR2 as being important for binding and activation.

It is instructive to consider our findings in light of the recently reported structure of CCR2 bound to orthosteric and allosteric antagonists (BMS-681 and CCR2-RA-[R], respectively) [250]. Figure 5.6A shows a comparison between our model of CCR2 bound to MCP-1 and the reported inhibitor-bound structure. As with other chemokine receptors, the ligand-binding channel in the transmembrane region of CCR2 is bifurcated into two branches, previously defined as the major and minor subpockets. Residues Y120^{3.32} and E291^{7.39} are located at the interface between these two subpockets and the side chains of these residues are well overlaid between our model and the recent structure. However, BMS-681 binds in the minor subpocket of CCR2, whereas our data suggest that the N-termini of the chemokines bind to the major subpocket (Fig 5.6B). Zheng et al. have proposed that BMS-681 directly competes with chemokine ligands for binding to CCR2. Interestingly, in the overlaid structures there is no direct steric overlap between BMS-681 and the N-terminus of MCP-1. As suggested by Zheng et al., BMS-681 does interact with several residues that are important for MCP-1 binding.

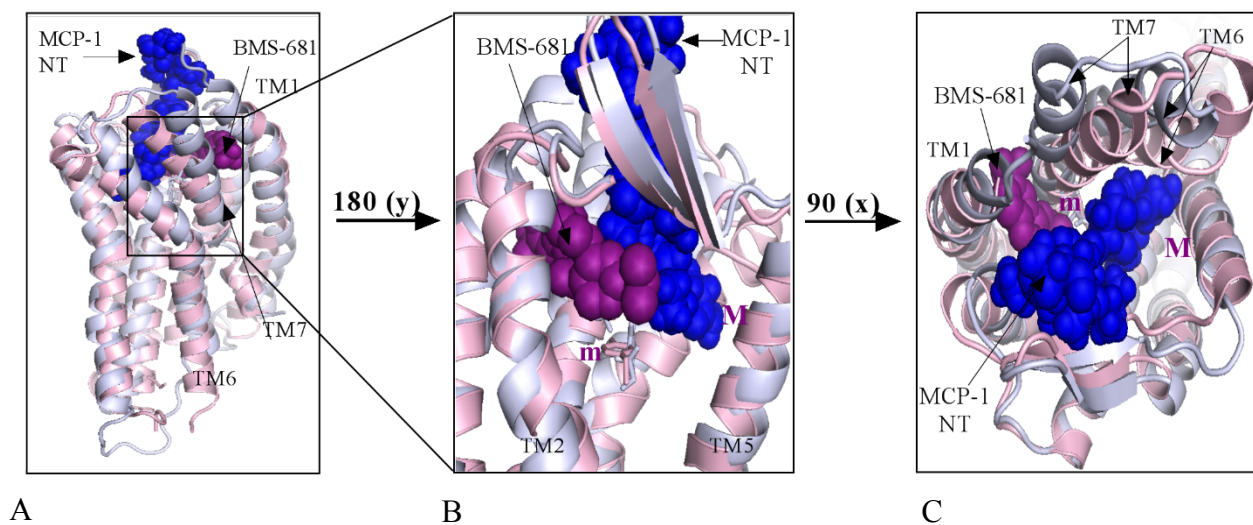


Figure 5.6. Comparison of the homology model-of CCR2 bound to MCP-1 with the structure of CCR2 bound to the antagonist BMS-681. (A) Overlaid structures of CCR2 (homology model in light blue ribbons with residues 1-10 of MCP-1 shown as blue spheres; antagonist-bound structure in pink ribbons with BMS-681 shown as violet spheres). BMS-681 protrudes between TM1 and TM7, causing displacement of TM 6 and TM7 on the front face of receptor as shown. **(B)** Close-up view of BMS-681 in the minor pocket (m) and the MCP-1 N-terminus in the major pocket (M) of CCR2 (helices TM3 and TM4 have been removed to enable this view of the binding pocket). **(C)** Top view showing the displacement of TM7 and TM6 due to presence of BMS-681 between TM1 and TM7.

In addition, we note that the extracellular halves of TM6 and TM7 are not well overlaid between our model and the inhibitor-bound structure (Fig 5.6A, C). We propose that this is a consequence of the quinazoline ring of BMS-681 being wedged between TM1 and TM7 of the receptor. We suggest that this binding causes the extracellular half of TM7 to bend away from the bound inhibitor, which, in turn, induces a similar distortion of TM6. Since both TM7 and TM6 form part of the major subpocket, this structural distortion appears to compress the major subpocket such that it can no longer accommodate the N-terminus of MCP-1.

In summary, by analysis of CCR2 mutants, we have identified a cluster of CCR2 residues nestled between transmembrane helices 3, 5, 6 and 7 (the major subpocket) that appears to be the key binding site for the chemokine N-terminus. Although the CCR2 inhibitor BMS-681 binds to the alternative (minor) subpocket, the major subpocket of chemokine receptor CCR5 comprises a substantial part of the binding site for the anti-HIV drug maraviroc (Fig 5.5F and G) [256]. Therefore, we propose that this site within CCR2 is likely to be an excellent target for future development of small molecule inhibitors with potential applications in atherosclerosis, obesity/diabetes and other macrophage-associated inflammatory diseases.

Chapter 6. General Discussion

6.1. Chemokine:Receptor Interactions

The chemokine receptor system was previously suggested to be highly redundant, as multiple chemokines bind and activate the same receptor and similarly different receptors interact with multiple chemokines [216-218]. However, during the past few years the perspective about the way chemokines interact with their receptors has changed. It has been established that different chemokines can act through the same receptor to give distinct signalling outcomes. This is thought to fine tune the responses of leukocytes, which is essential for normal immune surveillance.

6.2. Existing 2-Site, 2-Step Model

The currently prevailing two-site model for chemokine-receptor interactions describes these interactions as a simple 2-step process [238], which involves binding of the chemokine to its receptor followed by the activation of the receptor (Fig 6.1). The presumption that binding and activation occur in two discrete steps rather than concomitantly is not derived from kinetic measurements but instead deduced from indirect evidence such as the ability of N-terminally truncated chemokines to bind strongly without activating their receptors [100, 257].

6.3. Elaboration of the Existing Model

6.3.1. Fitting Dimerisation into the Two-Site Model

An important aspect of the two-site model is that initial binding to the chemokine is mediated by the N-terminal region of the receptor. Previous studies had indicated that a tyrosine residue in this region is often post-translationally sulfated [125, 191]. Studies by our laboratory and others have shown that tyrosine sulfation enhances the chemokine binding affinity of this region of the receptor [184]. Moreover, we had observed that both the active monomeric form and the inactive dimeric form of MCP-1 bound to sulfated peptides derived from the N-terminal region of CCR2 [126]. However, Tan et al. have reported that binding to the dimeric form causes some conformational changes in those parts of the N-terminal region of the chemokine, which is involved in dimer formation. This conformational change destabilises the dimer interface, resulting in its dissociation to the active monomeric state [126], which indicates that the sulfated receptor promotes dimer dissociation and chemokine activation.

The first results chapter (Chapter 3) include the outcome of studying the energetics of this important allosteric mechanism and is in the form of a published journal article. It explains the use of 2D NMR to characterise the dynamic properties of MCP-1 monomer and dimer in coupled equilibria.

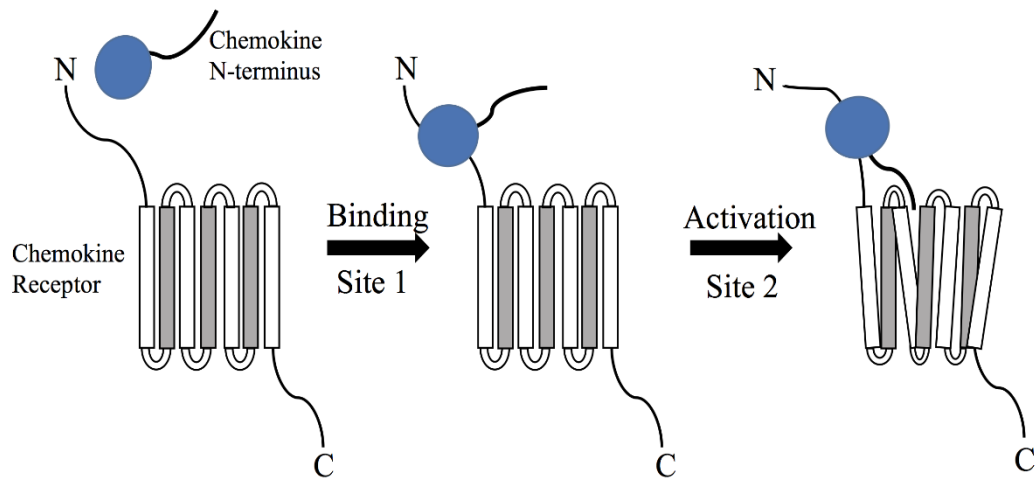


Figure 6.1. Existing two-site model of chemokine:receptor interaction. In the first step, the main core of the chemokine interacts with the N-terminus of the chemokine receptor and in the second step, the N-terminus of the chemokine binds to the receptor groove at the top of the helices, leading to activation of the receptor, depicted by the change in conformation of receptor helices.

To better understand the interplay between chemokine dimerisation and receptor binding, we developed a computational algorithm to model the positions and relative intensities of monomer and dimer peaks in ^1H - ^{15}N correlation NMR spectra of a ^{15}N -labelled protein (e.g. MCP-1) samples containing different concentrations of an unlabelled ligand (e.g. a receptor-derived sulfopeptide). Three experimental parameters (monomer chemical shift, dimer chemical shift and relative monomer:dimer peak intensity) were fitted globally, as a function of ligand concentration, to yield equilibrium constants for dimerisation, monomer:ligand binding and dimer:ligand binding as well as the cooperativity between ligand binding and dimerisation. We have applied this approach to characterise dimerisation of the chemokine MCP-1 coupled to binding of peptides derived from the chemokine receptor CCR2. The global fitting approach allowed evaluation of cooperativity with much higher precision than is possible by alternative methods. In summary, these results provided evidence for a novel mechanism by which chemokine activity can be regulated.

Our results from chapter 3 give an idea about the way a CC chemokine dimer is able to interact with the receptor, which is not explained by the existing 2-site model. The current two-site model fails to fit the chemokine dimerisation into the context of receptor interaction. We know that most chemokines form dimers or higher order oligomers. And each of these forms has its own roles to play. The dimeric form is essential for GAG-binding, which is essential for leukocyte recruitment *in vivo* [16]. Our results confirm that the receptor binding causes dissociation of the MCP-1 dimeric form (inactive) to the monomeric form (active). We therefore suggest an addition to the existing model (Fig 6.2A), which incorporates dissociation of the CC chemokine dimer as part of the model. In this extended model, we propose that activation requires three steps. First, the chemokine dimer binds to the N-terminus of the receptor. Second, binding of the receptor causes an allosteric change in the dimer interface, which leads to its dissociation and formation of the monomeric form, still bound to the receptor N-terminal region. Finally, as in the original two-step model, the N-terminus of the chemokine penetrates into the transmembrane part of the receptor, causing receptor activation.

This extended model is consistent with our knowledge of CC chemokine dimer structure. As mentioned in chapter 1, the CC chemokines dimerise by formation of an antiparallel β -sheet between the N-terminal regions of the two protomers (Chapter 1, Fig 1.3B). Due to the importance of the N-terminal regions in receptor activation, CC chemokine dimers are unable to activate their receptors [38, 258]. However, the N-loops and $\beta 3$ region remain exposed in the CC chemokine dimers so they are able to bind the (tyrosine-sulfated) N-terminal regions of their receptors.

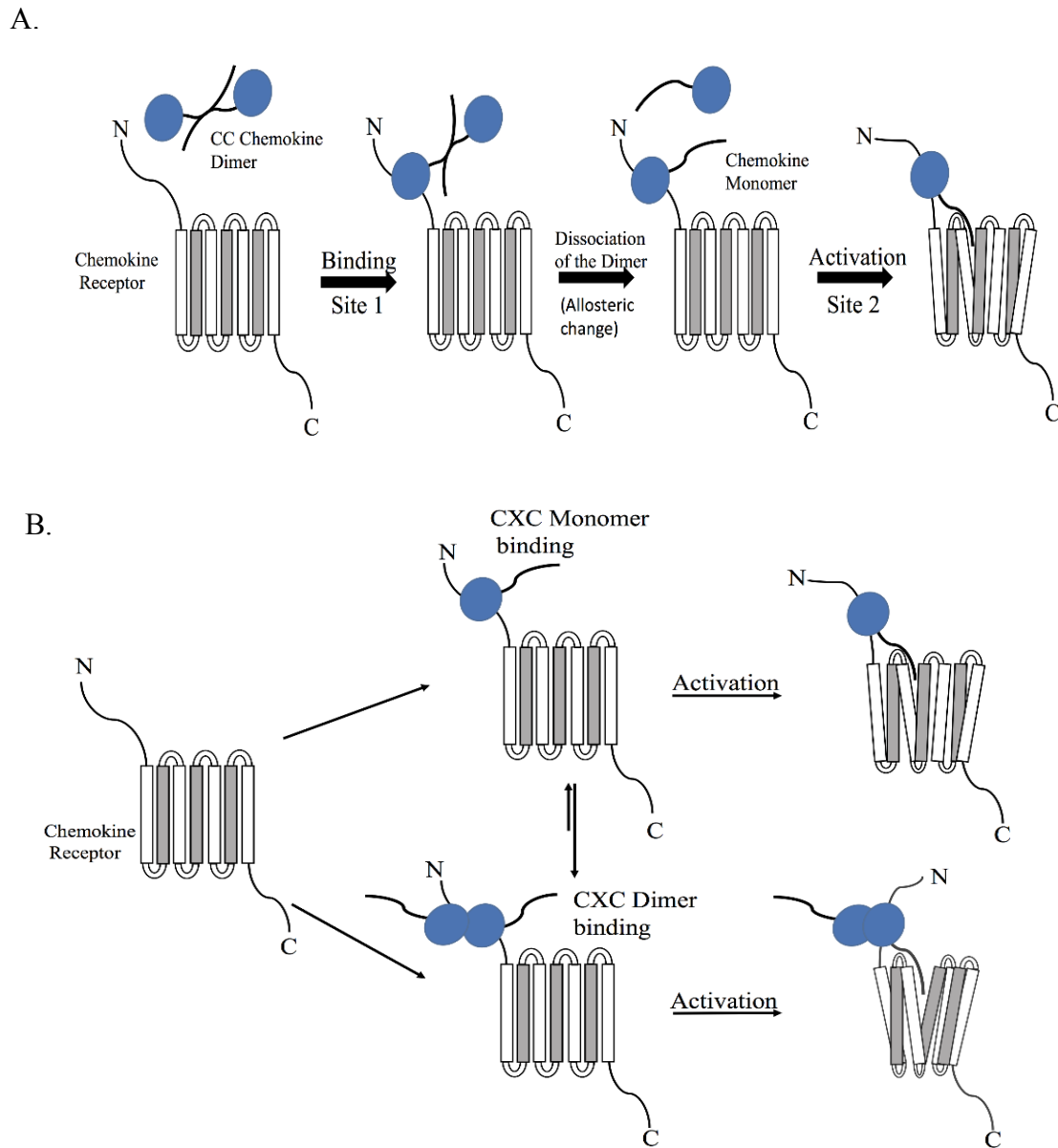


Figure 6.2. Extension of the existing model. (A) Proposed interaction of the CC chemokine dimer with the chemokine receptor. **(B)** Proposed interaction of the CXC dimer with the chemokine receptor.

Although dimer dissociation is required for CC chemokines, CXC chemokine dimers can activate their receptors [31, 259-261]. This can also be understood in terms of chemokine dimer structure. We know that CXC chemokines dimerise via their β 1-strands, thereby forming a continuous 6-strand antiparallel β -sheet with the α -helices of both protomers adjacent to each other on the same face of the β -sheet (Chapter 1, Fig1.3A) [42]. Importantly, this dimer structure leaves the N-terminus, N-loop and β 3-strand exposed on the surface of the dimer, explaining why CXC chemokine dimers can both bind and activate their receptors. Interestingly, some studies have reported that the trapped forms of the CXCL8 and CXCL12 dimers (those that cannot dissociate to the monomeric state), display distinct receptor activation properties relative to the corresponding monomeric chemokines [259, 260, 262]. Furthermore, based on receptor (CXCR4) sulfotyrosine peptide binding studies with the chemokine CXCL12, Ziarek and colleagues have proposed an allosteric model in which binding to the N-terminus of the receptor promotes dimer formation [263], in contrast to the dimer dissociation we observed for MCP-1. In light of these studies, we propose an alternative extension to the two-site, two-step model for CXC chemokines and their receptors (Fig 6.2B). In this model, either the monomeric or dimeric form of the chemokine can bind to the N-terminus of the receptor. However, these two bound forms can interconvert, with the equilibrium apparently favouring the dimer-bound form, at least for CXCL12 bound to CXCR4. Subsequently, either of these bound forms can stimulate receptor activation by penetration of the chemokine N-terminus into the transmembrane part of the receptor.

In summary, comparison of our cooperativity data for a CC chemokine with published data for a CXC chemokine have led us to propose that different classes of chemokines, due to their structural differences, have evolved different mechanisms of receptor activation. As mentioned above, similar peptide binding studies with other chemokines and receptor fragments can be carried out in the future to confirm our suggestions. Trapped dimers/monomers can be constructed to characterise the interactions of dimers and monomers with the chemokine receptors. Mutants with altered dimerisation pattern could also be used to study any allosteric interaction between chemokines and their receptors.

6.3.2. The Structural Interactions of the Chemokine:Receptor Pair

At the start of this study, there were few experimentally determined structures available for chemokine receptors. However, during the last four years there has been an amazing advancement in the field of GPCR and chemokine receptor structures. After late 2013, several structures of chemokine receptors have been reported which have provided insights to the mechanism of activation of these

receptors, thus broadening our understanding of chemokine receptor:ligand interactions.

The crystal structure of CCR5 in complex with an allosteric inhibitor maraviroc has been solved and has provided vital information about the class A GPCRs [264]. The CXCR4 structure was also reported at the same time with a small molecule antagonist, IT1t and with a cyclic peptide inhibitor, CVX15 providing further details about the structures of chemokine receptors [265]. The CXCR1 NMR structure reported in 2012 highlighted the importance of the features which are responsible for G protein activation and signalling [266]. Two bound chemokine receptor structures reported in 2015 by Qin et al. and Burg et al. have validated the key features of the two-site model but have also suggested that the two sites may not be completely independent. Qin et al. have resolved the crystal structure of CXCR4 in complex with a viral chemokine antagonist vMIP-II, while Burg et al. have analysed a complex between human cytomegalovirus GPCR US28 and the chemokine CX₃CL1. Both structures have identified the receptor residues that influence interactions with the chemokines [105, 106]. More recently, at end of 2016, the structures of CCR9 (bound to Vercirnon) and CCR2 (bound to BMS-681 and CCR2-RA-[R]) have also been reported [250, 251], providing an insight about the way different antagonists interact with the chemokine receptors.

In addition to these structural studies, Wescott et al. [254] have identified, through a comprehensive mutagenesis study, 41 important residues of CXCR4 required for CXCL12 signal transmission, of which 33 are positioned on the TM helices. Most of these residues are in contact with each other, forming a chain through the TM helices connecting the residues from the extracellular surface involved in chemokine recognition to the intracellular residues coupled to G proteins [254].

Arimont et al., after a comparative study of all reported chemokine receptor structures, suggest that there are certain residues in the TM regions of the chemokine receptors which play a major role in affecting the affinity of different chemokine:receptor complexes. However, different residues are suggested to be important for different chemokine:receptor pairs [267]. The recent structural and mutational studies now enable us to investigate the mechanisms of chemokine receptor signalling in much more detail than was previously possible.

As mentioned earlier, different chemokines can act through the same receptor to give distinct signalling outcomes. In the fourth chapter, we aimed to identify the structural interactions of the MCP chemokines that are responsible for their differences in the activation of the receptor CCR2. A series of chimeras were prepared in which three functionally important regions (N-terminal region, N-loop and β 3 region) were swapped between MCP-1 and MCP-3 to identify the effects of different regions of chemokines on chemokine agonism and affinity. Radioligand binding assays were carried out to determine the affinity of these chimeras for CCR2 and both β -arrestin recruitment and ERK

phosphorylation assays were carried out as measures of their ability to activate CCR2. We observed that swapping of N-loop/ β 3 region did not bring any significant change in either of the chimeras. However, the N-terminus was found to play an important role both in binding and activation of the chimeras. We have been able to deduce that chemokine N-terminus is a vital element in controlling the partial versus full agonism.

As the MCP chemokines differentially activate CCR2, we predicted that certain residues within CCR2 may be interacting preferentially with MCP-1 than other MCP chemokines. We aimed to identify the key features of CCR2 that enable it to respond differently to the different chemokines. To identify these residues, we made several receptor mutants, with different mutations lining the TM cavity. A homology model of CCR2 bound to MCP chemokines (based on the CXCR4:vMIP-II structure) was used to choose the mutations in the TM bundle. Our results (Chapter 5) confirmed that some CCR2 mutations do affect the affinity and/or efficacy of the MCP chemokines, thus being responsible for differential activation of these chemokines. These mutations form a “hot spot”, being clustered together in the major orthosteric subpocket of the receptor. Our homology model identifies this as the point of interaction of the MCP-1 N-terminus. Hence, we have identified some of the TM residues which contribute to the binding affinity and activation.

Our results are in good agreement with the activation model of the chemokine receptor proposed by Wescott et al. Most of the critical residues responsible for ligand recognition and activation of the receptor are in the TM helices 3, 6 and 7 [254]. These residues have been assigned to specific groups depending on the mechanistic role they play towards receptor activation. Some of the receptor residues which we have identified as responsible for affecting the binding and activation have been reported by Wescott et al. as responsible for initiation of signal transmission.

As our results from chapter 4 suggest that chemokine N-terminus is involved in controlling the affinity at the chemokine receptor, we propose that interactions between the chemokine N-terminus and receptor transmembrane helices either contribute to the formation of a stable complex before the receptor activation or to stabilising the activated structure. Once the chemokine core binds to the N-terminus of the chemokine receptor, it is followed by interaction of the chemokine N-terminus with the transmembrane helices of the receptor. These critical residues present on the transmembrane helices (at the base of ligand binding pocket), which are described by Wescott for signal transmission, form a continuous network as they are further linked to other residues, which are responsible for signal propagation, which transmits conformational change through the transmembrane helices to the microswitch residues. This is a highly conserved region that controls the G protein interface and is further linked to the residues, which are coupled directly to G proteins.

However, there is a need for several structures of the activated states of the chemokine receptors, i.e. bound to different chemokine agonists and in conformations which determine a specific signalling response.

6.3.3. Extensions of the 2-Step Model for Partial Agonists

As discussed above, the thermodynamic study reported in Chapter 3 suggested an elaboration of the two-step model to account for the receptor interactions of chemokine dimers. However, even without considering dimerisation, the two-step model may need to be extended to account for the observations of the partial agonists and chemokine chimeras reported in Chapters 4 and 5. One important finding from these experiments was that the interaction between the TM residues of the chemokine receptor and chemokine N-terminus contribute to the binding affinity. This interaction is not yet formed in the binding step (step 1) of the two-step model, but our data suggest that there is a bound (not yet activated) state in which this interaction exists. Previous binding studies have demonstrated that many chemokines bind to the N-terminal regions of their receptors; indeed, the structural basis of this binding has been described for CCL11, CXCL8 and CXCL12 [102, 207, 243]. However, it is important to note that these latter interactions are generally fairly weak, typically with K_d values in the low micromolar range, whereas binding of chemokines to intact receptors occurs with apparent K_d values in the low nanomolar range. These observations prompt us to suggest an extension of the two-site model (Fig 6.3A) in which there are two different bound states. First, the main core of the chemokine interacts with the receptor N-terminus (depicted as state 1, Fig 6.3A), forming a relatively low affinity interaction. Subsequently, the N-terminus of the chemokine interacts with the transmembrane helices of the receptor, increasing the binding affinity, and stabilising state 2 (Fig 6.3A). Finally, a conformational change of the receptor gives rise to the activated state, leading to initiation of downstream signalling (depicted as state 3, Fig 6.3A). The existence of the high affinity bound state (state 2) is supported by our results from Chapters 4 and 5 and also by some previous mutational studies. For example, Mayer et al. have reported that mutation of residues in the N-terminal region of CCL11 contribute to binding affinity for the receptor CCR3 [268]. It has also been reported for CXCL8 that the N-terminal region plays a critical role in determining the binding affinity. Different N-terminal mutants show reduced binding affinity as compared to the wild type CXCL8 [269-271]. The N-terminal residues of CXCL12 have also been identified to play an important role in determining the binding affinity at the CXCR4 [238].

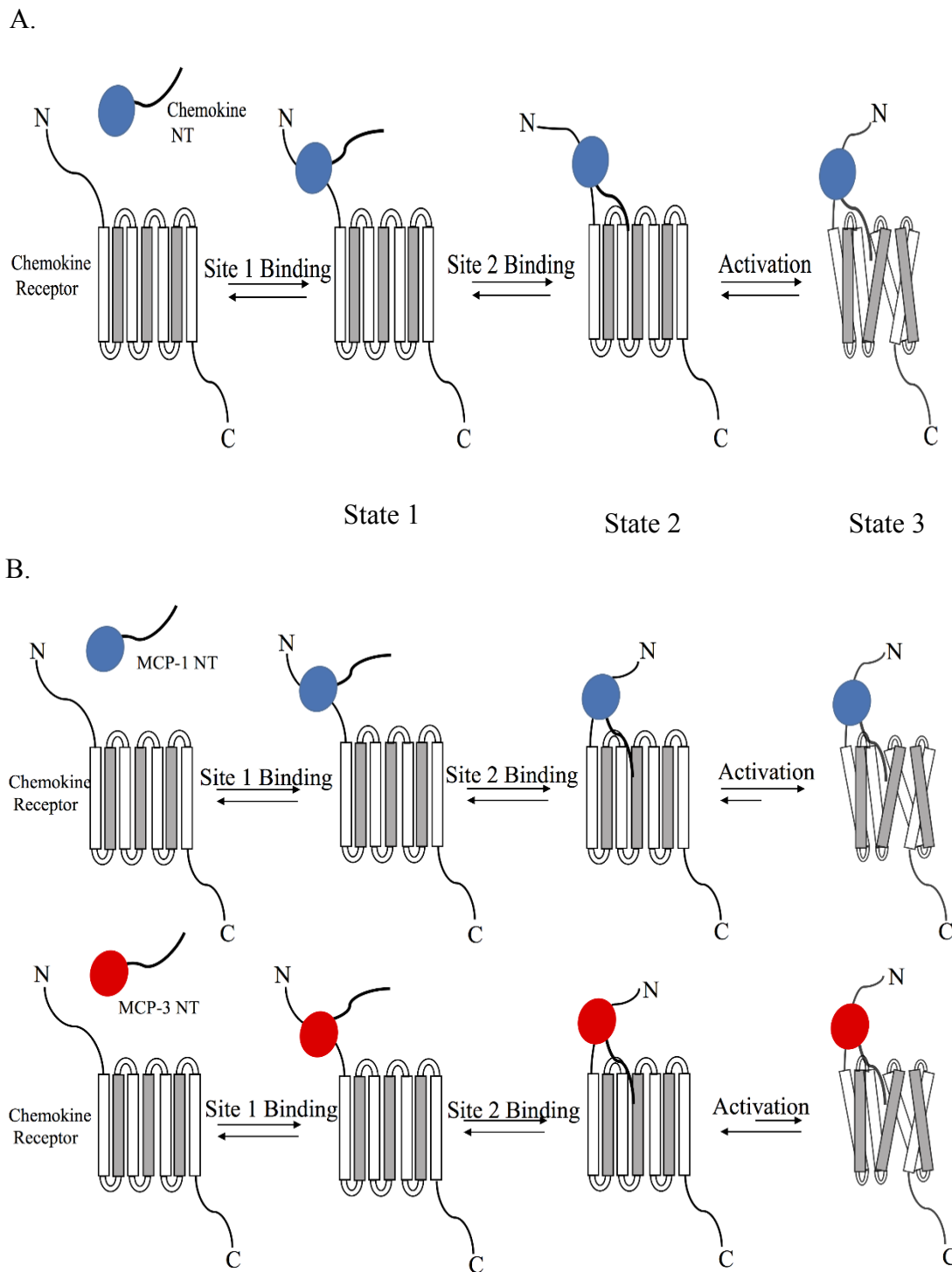


Figure 6.3. Elaboration of the two-site model (A) Binding interactions followed by activation, showing site 1 and 2 binding separate from activation **(B)** Possible explanation of full vs partial agonism.

An advantage of the three-step model presented in Fig 6.3A is that it can account for both partial and full agonists. These would differ in their ability to shift the equilibrium between the high affinity, inactive state (state 2) and the activated state (state 3); a full agonist shift would strongly favour state 3 as compared to a partial agonist, which would allow a higher proportion of state 2. In terms of structural interactions, this difference could occur because full agonist forms tighter interaction in state 3 or because a partial agonist forms tighter interactions in state 2. For the MCP chemokines interacting with CCR2, the full agonist (MCP-1) binds to the receptor with higher affinity than the partial agonists do. Therefore, it seems unlikely that partial agonism would be due to tighter interactions by the partial agonists in state 2 and more likely that the full agonist forms tighter interactions in state 3 (Fig 6.3B). This situation could potentially differ for other receptors and their chemokine ligands.

It is important to note that the two-step model and the alternative models presented here are all based on the assumption of chemokine:receptor interactions being at equilibrium. However, the system is probably never at true equilibrium so kinetics could also play a role in influencing such phenomena as partial versus full agonism. In addition, the models also assume that the interactions at site 1 and site 2 are independent of each other, whereas there is the potential for them to be coupled or cooperative. There is little experimental data available to evaluate these possibilities but they should be investigated in future studies.

6.4. Future Studies of Differential Agonism

Over the past two years, a number of chemokine receptor structures have been reported [105, 106, 250, 251] and there was an extensive shotgun mutagenesis study of CXCR4 receptor [254] reported in late 2016. Together, these new data have provided the first detailed structural model for chemokine receptor activation. These models provide an opportunity to design structure-guided chemokine and receptor mutants which can yield insights into partial or biased agonism. Wescott et al. have identified residues in the transmembrane bundle which are important for signal transduction from extracellular to the intracellular G proteins. They have divided these residues into five functional groups, which are responsible for: (i) chemokine engagement, (ii) signal initiation, (iii) signal propagation, (iv) microswitch activation, and (v) G protein coupling. Activation of the chemokine receptor with chemokine causes a rearrangement of the G protein subunits, which can be detected as a change in BRET approach (as mentioned in the Materials and Methods).

As described by Manglik et al. [272], agonists shift the conformational equilibrium of receptors, favouring a conformation, which can engage G proteins. However, depending on the

agonists, there always exists a multi-state equilibrium with different activated states of the receptor (section 6.5). We have speculated above that a full agonist favours state 3 over state 2 while a partial agonist favours state 2 over state 3 of the receptor (Fig 6.3B). To verify this proposed model, the relative populations of the activated versus inactive states of the receptor should be measured experimentally. This has been achieved by Manglik et al. [272] for β 2-adrenergic receptor using NMR and double electron-electron resonance spectroscopy techniques. Similar experiments could be performed using chemokine receptors, alone and in the presence of different chemokine ligands, to test the model proposed above.

We have identified the N-terminus of the chemokine as the determinant of partial vs full agonism through a series of chimeras which had multiple mutations in one defined region of the chemokine. Therefore, further work can be carried out to identify the contributions of individual N-terminal residues to CCR2 activation by designing single-site chemokine mutants and measuring CCR2 affinity, potency and efficacy across the different signalling readouts. Modification of these N-terminal residues will alter the interactions with the chemokine receptor, ultimately affecting the chemokine agonism at the receptor. Further these single-site chemokine mutants can be tested with the receptor mutants described in Chapter 5. This “double-mutant” analysis could reveal which pairs of chemokine and receptor residues interact directly with each other, thus guiding us further about the detailed mechanism of activation of the receptor.

We have identified amino acids residues within CCR2 that are critical for activation of particular chemokines. Further work can be carried out by making alanine mutations of adjacent residues and non-alanine mutations of the same receptor residues and test their binding and activation by both MCP-1 and -3. Our findings can guide further development of small molecule inhibitors which can achieve similar results and can be used to target the transmembrane regions of CCR2 as partial antagonists. Thus, signalling from certain ligands could be blocked and CCR2 activity could be tuned rather than complete blockage of the receptor.

6.5. Biophysical Studies of Receptor Activation and Dynamics

The studies of partial agonism described in this thesis use cell-based signalling and binding assays to draw inferences about the molecular mechanism of chemokine receptor activation. In the future, these should be complemented by using biophysical approaches. We have already noted the importance of solving structures of chemokine receptors bound to chemokine agonists. In addition, it will be informative to probe the dynamics of chemokine receptors in both free and bound states. GPCRs exist in a variety of different conformations, even when they are not bound to their ligands.

So, activation of GPCRs is not a simple process where they can switch from the inactive to the active state. The unbound receptor exists in multiple conformations of low energy level [273, 274]. Depending on the ligand which binds, the receptor attains a range of conformations, ultimately changing the energy level of the receptor. Manglik et al. have used biophysical methods (¹⁹F NMR and double electron-electron resonance spectroscopy (DEER)) to study structural dynamics of the cytoplasmic domain of the β 2-adrenergic receptor [272]. Further protein dynamics of the CCR2 could be studied in a similar way which could give further insight about the relative population distribution of the activated states when bound to each chemokine [272]. It will be of great interest to find the interactions, which are critical for stabilising active versus inactive states. These methods can help to characterise the transition between different conformations. NMR can be used to study the kinetics of these conformational changes. Similar methods can be used to analyse different activated states of the other mutant chemokine receptors. The chemokine chimeras and receptor mutants described in Chapters 4 and 5 will be valuable resources in these studies.

6.6. Cellular and Physiological Outcomes of Differential Agonism

This study has demonstrated that different MCP chemokines have different effects on the CCR2 signal transduction and at least one downstream cellular outcome, receptor internalisation. However, additional cellular and physiological consequences of partial versus full agonism by these chemokines remain to be explored. Our experiments were performed using a model cell line FlpIn HEK293, which were expressing c-Myc-FLAG-CCR2. It will be important to confirm the relevance of the observations in this model system by performing similar experiments in cell lines, such as human basophilic cell line KU-82 and human monocytic cell line THP-1, which both endogenously express CCR2 [275-277]. Additional downstream signalling pathways could be identified, in both model cell lines and cell lines endogenously expressing CCR2, using phosphoproteomics methods, which can simultaneously detect changes in the phosphorylation status of numerous intracellular signalling proteins, allowing researchers to observe activation or suppression of complex signalling pathways and networks. Such studies would generate a variety of hypotheses regarding the cellular consequences of differential CCR2 activation, which could be subsequently tested using cell-based functional assays. Ultimately, distinct physiological consequences of these differential interactions could be studied in knockout mice or disease models.

6.7. Conclusion

In summary, the research described in this thesis has provided new insights into two different mechanisms by which chemokine:receptor interactions can be regulated. Our results from chapter 3

describe a novel approach to interpret 2D NMR data for measuring ligand binding and dimerisation simultaneously. Results from chapter 4 and 5 establish that interactions of different chemokine N-termini with the transmembrane bundle of a shared receptor induce distinct signalling responses. This study has begun to elucidate the molecular mechanisms by which cognate chemokines induce differential activation of CCR2, which will have important outcomes for our understanding of GPCR signalling. This project presents the first evidence that, in addition to being critical for receptor activation, the N-terminus of the chemokine is the major determinant of the differential affinity of chemokines for a shared receptor. We have also highlighted the parts of the chemokine receptor which are responsible for differential activation by chemokines. In light of recent structural data on chemokine receptors, our findings contribute to ongoing efforts to elucidate the molecular mechanisms of receptor activation and provide insights towards understanding the functional selectivity of different chemokines.

References

- [1] Ben-Baruch A, Michiel DF, Oppenheim JJ. Signals and receptors involved in recruitment of inflammatory cells. *J. Biol. Chem.* 1995; 270: 11703-6.
- [2] Ali S, Palmer AC, Banerjee B, Fritchley SJ, Kirby JA. Examination of the function of RANTES, MIP-1 α , and MIP-1 β following interaction with heparin-like glycosaminoglycans. *J. Biol. Chem.* 2000; 275: 11721-7.
- [3] Lau EK, Allen S, Hsu AR, Handel TM. Chemokine-receptor interactions: GPCRs, glycosaminoglycans and viral chemokine binding proteins. *Adv. Protein Chem.* 2004; 68: 351-91.
- [4] Dwir O, Grabovsky V, Alon R. Selectin avidity modulation by chemokines at subsecond endothelial contacts: a novel regulatory level of leukocyte trafficking. *Ernst Schering Res Found Workshop.* 2004: 109-35.
- [5] Springer TA. Traffic signals on endothelium for lymphocyte recirculation and leukocyte emigration. *Annu. Rev. Physiol.* 1995; 57: 827-72.
- [6] Campbell JJ, Butcher EC. Chemokines in tissue-specific and microenvironment-specific lymphocyte homing. *Curr. Opin. Immunol.* 2000; 12: 336-41.
- [7] Kunkel EJ, Butcher EC. Plasma-cell homing. *Nat. Rev. Immunol.* 2003; 3: 822-9.
- [8] Baggiolini M. Chemokines and leukocyte traffic. *Nature.* 1998; 392: 565-8.
- [9] Rossi D, Zlotnik A. The biology of chemokines and their receptors. *Annu. Rev. Immunol.* 2000; 18: 217-42.
- [10] Ren M, Guo Q, Guo L, Lenz M, Qian F, Koenen RR, et al. Polymerization of MIP-1 chemokine (CCL3 and CCL4) and clearance of MIP-1 by insulin-degrading enzyme. *EMBO J.* 2010; 29: 3952-66.
- [11] Mackay CR. Chemokines: immunology's high impact factors. *Nat Immunol.* 2001; 2: 95-101.
- [12] Peatman E, Liu Z. Evolution of CC chemokines in teleost fish: a case study in gene duplication and implications for immune diversity. *Immunogenetics.* 2007; 59: 613-23.
- [13] Thelen M. Dancing to the tune of chemokines. *Nat. Immunol.* 2001; 2: 129-34.
- [14] Baggiolini M. Chemokines in pathology and medicine. *J. Intern. Med.* 2001; 250: 91-104.
- [15] Middleton J, Neil S, Wintle J, Clark-Lewis I, Moore H, Lam C, et al. Transcytosis and surface presentation of IL-8 by venular endothelial cells. *Cell.* 1997; 91: 385-95.
- [16] Proudfoot AE, Handel TM, Johnson Z, Lau EK, LiWang P, Clark-Lewis I, et al. Glycosaminoglycan binding and oligomerization are essential for the in vivo activity of certain chemokines. *Proc. Natl. Acad. Sci. U S A.* 2003; 100: 1885-90.

References

- [17] Sasisekharan R, Shriver Z, Venkataraman G, Narayanasami U. Roles of heparan-sulphate glycosaminoglycans in cancer. *Nat Rev Cancer*. 2002; 2: 521-8.
- [18] Liu D, Shriver Z, Qi Y, Venkataraman G, Sasisekharan R. Dynamic regulation of tumor growth and metastasis by heparan sulfate glycosaminoglycans. *Semin Thromb Hemost*. 2002; 28: 67-78.
- [19] Fernandez EJ, Lolis E. Structure, function, and inhibition of chemokines. *Annu. Rev. Pharmacol. Toxicol*. 2002; 42: 469-99.
- [20] Lubkowski J, Bujacz G, Boque L, Domaille PJ, Handel TM, Wlodawer A. The structure of MCP-1 in two crystal forms provides a rare example of variable quaternary interactions. *Nat. Struct. Biol*. 1997; 4: 64-9.
- [21] D'Ambrosio D, Panina-Bordignon P, Sinigaglia F. Chemokine receptors in inflammation: an overview. *J. Immunol. Methods*. 2003; 273: 3-13.
- [22] Murphy PM. Chemokines and the molecular basis of cancer metastasis. *N. Engl. J. Med*. 2001; 345: 833-5.
- [23] Ben-Baruch A. Host microenvironment in breast cancer development: inflammatory cells, cytokines and chemokines in breast cancer progression: reciprocal tumor-microenvironment interactions. *Breast Cancer Res*. 2003; 5: 31-6.
- [24] Sica A, Saccani A, Mantovani A. Tumor-associated macrophages: a molecular perspective. *Int. Immunopharmacol*. 2002; 2: 1045-54.
- [25] Handel TM, Domaille PJ. Heteronuclear (¹H, ¹³C, ¹⁵N) NMR assignments and solution structure of the monocyte chemoattractant protein-1 (MCP-1) dimer. *Biochemistry*. 1996; 35: 6569-84.
- [26] Moser B, Loetscher P. Lymphocyte traffic control by chemokines. *Nat. Immunol*. 2001; 2: 123-8.
- [27] Moser B, Wolf M, Walz A, Loetscher P. Chemokines: multiple levels of leukocyte migration control. *Trends Immunol*. 2004; 25: 75-84.
- [28] Ye J, Kohli LL, Stone MJ. Characterization of binding between the chemokine eotaxin and peptides derived from the chemokine receptor CCR3. *J. Biol. Chem*. 2000; 275: 27250-7.
- [29] Crump MP, Spyropoulos L, Lavigne P, Kim KS, Clark-lewis I, Sykes BD. Backbone dynamics of the human CC chemokine eotaxin: fast motions, slow motions, and implications for receptor binding. *Protein Sci*. 1999; 8: 2041-54.
- [30] Wang X, Sharp JS, Handel TM, Prestegard JH. Chemokine oligomerization in cell signaling and migration. *Prog. Mol. Biol. Transl. Sci*. 2013; 117: 531-78.

- [31] Rajarathnam K, Prado GN, Fernando H, Clark-Lewis I, Navarro J. Probing receptor binding activity of interleukin-8 dimer using a disulfide trap. *Biochemistry*. 2006; 45: 7882-8.
- [32] Chung CW, Cooke RM, Proudfoot AE, Wells TN. The three-dimensional solution structure of RANTES. *Biochemistry*. 1995; 34: 9307-14.
- [33] Clore GM, Appella E, Yamada M, Matsushima K, Gronenborn AM. Three-dimensional structure of interleukin 8 in solution. *Biochemistry*. 1990; 29: 1689-96.
- [34] Paolini JF, Willard D, Consler T, Luther M, Krangel MS. The chemokines IL-8, monocyte chemoattractant protein-1, and I-309 are monomers at physiologically relevant concentrations. *J Immunol*. 1994; 153: 2704-17.
- [35] Rajarathnam K, Sykes BD, Kay CM, Dewald B, Geiser T, Baggiolini M, et al. Neutrophil activation by monomeric interleukin-8. *Science*. 1994; 264: 90-2.
- [36] Paavola CD, Hemmerich S, Grunberger D, Polsky I, Bloom A, Freedman R, et al. Monomeric monocyte chemoattractant protein-1 (MCP-1) binds and activates the MCP-1 receptor CCR2B. *J Biol Chem*. 1998; 273: 33157-65.
- [37] Laurence JS, Blanpain C, Burgner JW, Parmentier M, LiWang PJ. CC chemokine MIP-1 β can function as a monomer and depends on Phe13 for receptor binding. *Biochemistry*. 2000; 39: 3401-9.
- [38] Tan JHY, Canals M, Ludeman JP, Wedderburn J, Boston C, Butler SJ, et al. Design and Receptor Interactions of Obligatory Dimeric Mutant of Chemokine Monocyte Chemoattractant Protein-1 (MCP-1). *J Biol Chem*. 2012; 287: 14692-702.
- [39] Mortier A, Van Damme J, Proost P. Overview of the mechanisms regulating chemokine activity and availability. *Immunol Lett*. 2012; 145: 2-9.
- [40] Salanga CL, Handel TM. Chemokine oligomerization and interactions with receptors and glycosaminoglycans: the role of structural dynamics in function. *Exp Cell Res*. 2011; 317: 590-601.
- [41] Duma L, Haussinger D, Rogowski M, Lusso P, Grzesiek S. Recognition of RANTES by extracellular parts of the CCR5 receptor. *J Mol Biol*. 2007; 365: 1063-75.
- [42] Stone MJ, Hayward JA, Huang C, Z EH, Sanchez J. Mechanisms of Regulation of the Chemokine-Receptor Network. *Int J Mol Sci*. 2017; 18.
- [43] Scholten DJ, Canals M, Maussang D, Roumen L, Smit MJ, Wijtmans M, et al. Pharmacological modulation of chemokine receptor function. *Br J Pharmacol*. 2012; 165: 1617-43.
- [44] Gether U. Uncovering molecular mechanisms involved in activation of G protein-coupled receptors. *Endocr Rev*. 2000; 21: 90-113.
- [45] Sakmar TP. Structure of rhodopsin and the superfamily of seven-helical receptors: the same and not the same. *Curr Opin Cell Biol*. 2002; 14: 189-95.

References

- [46] Miller AF, Falke JJ. Chemotaxis receptors and signaling. *Adv. Protein Chem.* 2004; 68: 393-444.
- [47] Ulvmar MH, Hub E, Rot A. Atypical chemokine receptors. *Exp. Cell Res.* 2011; 317: 556-68.
- [48] Galliera E, Jala VR, Trent JO, Bonecchi R, Signorelli P, Lefkowitz RJ, et al. β -Arrestin-dependent constitutive internalization of the human chemokine decoy receptor D6. *J. Biol. Chem.* 2004; 279: 25590-7.
- [49] Mantovani A, Bonecchi R, Locati M. Tuning inflammation and immunity by chemokine sequestration: decoys and more. *Nat. Rev. Immunol.* 2006; 6: 907-18.
- [50] Pierce KL, Premont RT, Lefkowitz RJ. Seven-transmembrane receptors. *Nat. Rev. Mol. Cell. Biol.* 2002; 3: 639-50.
- [51] Katritch V, Cherezov V, Stevens RC. Structure-function of the G protein-coupled receptor superfamily. *Annu. Rev. Pharmacol. Toxicol.* 2013; 53: 531-56.
- [52] Fredriksson R, Lagerstrom MC, Lundin LG, Schiöth HB. The G-protein-coupled receptors in the human genome form five main families. Phylogenetic analysis, paralogon groups, and fingerprints. *Mol. Pharmacol.* 2003; 63: 1256-72.
- [53] Kobilka BK. G protein coupled receptor structure and activation. *Biochim. Biophys. Acta.* 2007; 1768: 794-807.
- [54] Davenport AP, Alexander SP, Sharman JL, Pawson AJ, Benson HE, Monaghan AE, et al. International Union of Basic and Clinical Pharmacology. LXXXVIII. G protein-coupled receptor list: recommendations for new pairings with cognate ligands. *Pharmacol. Rev.* 2013; 65: 967-86.
- [55] Deupi X, Kobilka B. Activation of G Protein Coupled Receptors. *Adv Protein Chem.* 2007; 74: 137-66.
- [56] Venkatakrishnan AJ, Deupi X, Lebon G, Tate CG, Schertler GF, Babu MM. Molecular signatures of G-protein-coupled receptors. *Nature.* 2013; 494: 185-94.
- [57] Palczewski K, Kumasaka T, Hori T, Behnke CA, Motoshima H, Fox BA, et al. Crystal structure of rhodopsin: A G protein-coupled receptor. *Science.* 2000; 289: 739-45.
- [58] Gilman AG. G proteins: transducers of receptor-generated signals. *Annu. Rev. Biochem.* 1987; 56: 615-49.
- [59] Brandt DR, Ross EM. GTPase activity of the stimulatory GTP-binding regulatory protein of adenylate cyclase, Gs. Accumulation and turnover of enzyme-nucleotide intermediates. *J. Biol. Chem.* 1985; 260: 266-72.
- [60] Milligan G, Kostenis E. Heterotrimeric G-proteins: a short history. *Br. J. Pharmacol.* 2006; 147 Suppl 1: S46-55.

- [61] Yokoyama S, Starmer WT. Phylogeny and evolutionary rates of G protein α subunit genes. *J. Mol. Evol.* 1992; 35: 230-8.
- [62] Sutherland EW, Rall TW, Menon T. Adenyl cyclase. I. Distribution, preparation, and properties. *J. Biol. Chem.* 1962; 237: 1220-7.
- [63] Codina J, Hildebrandt J, Iyengar R, Birnbaumer L, Sekura RD, Manclark CR. Pertussis toxin substrate, the putative Ni component of adenylyl cyclases, is an $\alpha\beta$ heterodimer regulated by guanine nucleotide and magnesium. *Proc. Natl. Acad. Sci. U S A.* 1983; 80: 4276-80.
- [64] Smith FD, Samelson BK, Scott JD. Discovery of cellular substrates for protein kinase A using a peptide array screening protocol. *Biochem. J.* 2011; 438: 103-10.
- [65] Berridge MJ. Inositol trisphosphate and calcium signalling. *Nature.* 1993; 361: 315-25.
- [66] Taylor SJ, Exton JH. Two α subunits of the Gq class of G proteins stimulate phosphoinositide phospholipase C- β 1 activity. *FEBS Lett.* 1991; 286: 214-6.
- [67] Abeyweera TP, Chen X, Rotenberg SA. Phosphorylation of $\alpha 6$ -tubulin by protein kinase C α activates motility of human breast cells. *J. Biol. Chem.* 2009; 284: 17648-56.
- [68] Kolch W, Heidecker G, Kochs G, Hummel R, Vahidi H, Mischak H, et al. Protein kinase C α activates RAF-1 by direct phosphorylation. *Nature.* 1993; 364: 249-52.
- [69] Hart MJ, Jiang X, Kozasa T, Roscoe W, Singer WD, Gilman AG, et al. Direct stimulation of the guanine nucleotide exchange activity of p115 RhoGEF by G α 13. *Science.* 1998; 280: 2112-4.
- [70] Logothetis DE, Kurachi Y, Galper J, Neer EJ, Clapham DE. The $\beta\gamma$ subunits of GTP-binding proteins activate the muscarinic K $^{+}$ channel in heart. *Nature.* 1987; 325: 321-6.
- [71] Violin JD, Lefkowitz RJ. β -arrestin-biased ligands at seven-transmembrane receptors. *Trends Pharmacol. Sci.* 2007; 28: 416-22.
- [72] DeWire SM, Ahn S, Lefkowitz RJ, Shenoy SK. β -arrestins and cell signaling. *Annu. Rev. Physiol.* 2007; 69: 483-510.
- [73] Homan KT, Tesmer JJ. Structural insights into G protein-coupled receptor kinase function. *Curr. Opin. Cell Biol.* 2014; 27: 25-31.
- [74] Shukla AK, Westfield GH, Xiao K, Reis RI, Huang LY, Tripathi-Shukla P, et al. Visualization of arrestin recruitment by a G-protein-coupled receptor. *Nature.* 2014; 512: 218-22.
- [75] Thomas WG, Thekkumkara TJ, Baker KM. Molecular mechanisms of angiotensin II (AT1a) receptor endocytosis. *Clin. Exp. Pharmacol. Physiol.* 1996; 23 Suppl 3: S74-80.
- [76] Lefkowitz RJ, Shenoy SK. Transduction of receptor signals by β -arrestins. *Science.* 2005; 308: 512-7.

References

- [77] Eichel K, Jullie D, von Zastrow M. β -Arrestin drives MAP kinase signalling from clathrin-coated structures after GPCR dissociation. *Nat. Cell. Biol.* 2016; 18: 303-10.
- [78] McDonald PH, Chow CW, Miller WE, Laporte SA, Field ME, Lin FT, et al. β -arrestin 2: a receptor-regulated MAPK scaffold for the activation of JNK3. *Science.* 2000; 290: 1574-7.
- [79] Miller WE, McDonald PH, Cai SF, Field ME, Davis RJ, Lefkowitz RJ. Identification of a motif in the carboxyl terminus of β -arrestin2 responsible for activation of JNK3. *J. Biol. Chem.* 2001; 276: 27770-7.
- [80] Miller WE, Houtz DA, Nelson CD, Kolattukudy PE, Lefkowitz RJ. G-protein-coupled receptor (GPCR) kinase phosphorylation and β -arrestin recruitment regulate the constitutive signaling activity of the human cytomegalovirus US28 GPCR. *J. Biol. Chem.* 2003; 278: 21663-71.
- [81] Witherow DS, Garrison TR, Miller WE, Lefkowitz RJ. β -Arrestin inhibits NF- κ B activity by means of its interaction with the NF- κ B inhibitor I κ B α . *Proc. Natl. Acad. Sci. U S A.* 2004; 101: 8603-7.
- [82] Barnes WG, Reiter E, Violin JD, Ren XR, Milligan G, Lefkowitz RJ. β -Arrestin 1 and G α q/11 coordinately activate RhoA and stress fiber formation following receptor stimulation. *J. Biol. Chem.* 2005; 280: 8041-50.
- [83] Beaulieu JM, Sotnikova TD, Marion S, Lefkowitz RJ, Gainetdinov RR, Caron MG. An Akt/ β -arrestin 2/PP2A signaling complex mediates dopaminergic neurotransmission and behavior. *Cell.* 2005; 122: 261-73.
- [84] Jin H, Kagiampakis I, Li P, Liwang PJ. Structural and functional studies of the potent anti-HIV chemokine variant P2-RANTES. *Proteins.* 2010; 78: 295-308.
- [85] Cashin K, Roche M, Sterjovski J, Ellett A, Gray LR, Cunningham AL, et al. Alternative coreceptor requirements for efficient CCR5- and CXCR4-mediated HIV-1 entry into macrophages. *J. Virol.* 2011; 85: 10699-709.
- [86] Liu R, Paxton WA, Choe S, Ceradini D, Martin SR, Horuk R, et al. Homozygous defect in HIV-1 coreceptor accounts for resistance of some multiply-exposed individuals to HIV-1 infection. *Cell.* 1996; 86: 367-77.
- [87] Deng H, Liu R, Ellmeier W, Choe S, Unutmaz D. Identification of a major coreceptor for primary isolates of HIV-1. *Nature.* 1996; 381: 661-6.
- [88] Pease J, Horuk R. Chemokine receptor antagonists. *J. Med. Chem.* 2012; 55: 9363-92.
- [89] Wang T, Duan Y. HIV co-receptor CCR5: structure and interactions with inhibitors. *Infect. Disord. Drug Targets.* 2009; 9: 279-88.

-
- [90] Lieberman-Blum SS, Fung HB, Bandres JC. Maraviroc: a CCR5-receptor antagonist for the treatment of HIV-1 infection. *Clin. Ther.* 2008; 30: 1228-50.
- [91] De Clercq E. The AMD 3100 story : the path to the discovery of a stem cell mobilizer (Mozobil). *Biochem. Pharmacol.* 2009; 77: 1655-64.
- [92] Proudfoot AE, Power CA, Schwarz MK. Anti-chemokine small molecule drugs: a promising future? *Expert. Opin. Investig. Drugs.* 2010; 19: 345-55.
- [93] Salanga CL, O'Hayre M, Handel T. Modulation of chemokine receptor activity through dimerization and crosstalk. *Cell. Mol. Life Sci.* 2009; 66: 1370-86.
- [94] Mellado M, Rodriguez-Frade JM, Vila-Coro AJ, Fernandez S, Martin de Ana A, Jones DR, et al. Chemokine receptor homo- or heterodimerization activates distinct signaling pathways. *EMBO J.* 2001; 20: 2497-507.
- [95] Wuyts A, Van Osselaer N, Haelens A, Samson I, Herdewijn P, Ben-Baruch A, et al. Characterization of synthetic human granulocyte chemotactic protein 2: usage of chemokine receptors CXCR1 and CXCR2 and in vivo inflammatory properties. *Biochemistry.* 1997; 36: 2716-23.
- [96] Allen SJ, Crown SE, Handel TM. Chemokine: receptor structure, interactions, and antagonism. *Annu. Rev. Immunol.* 2007; 25: 787-820.
- [97] Rajagopalan L, Rajarathnam K. Ligand selectivity and affinity of chemokine receptor CXCR1. Role of N-terminal domain. *J. Biol. Chem.* 2004; 279: 30000-8.
- [98] Monteclaro FS, Charo IF. The amino-terminal domain of CCR2 is both necessary and sufficient for high affinity binding of monocyte chemoattractant protein 1. Receptor activation by a pseudo-tethered ligand. *J. Biol. Chem.* 1997; 272: 23186-90.
- [99] Clark-Lewis I, Dewald B, Loetscher M, Moser B, Baggiolini M. Structural requirements for interleukin-8 function identified by design of analogs and CXC chemokine hybrids. *J. Biol. Chem.* 1994; 269: 16075-81.
- [100] Clark-Lewis I, Mattioli I, Gong JH, Loetscher P. Structure-function relationship between the human chemokine receptor CXCR3 and its ligands. *J. Biol. Chem.* 2003; 278: 289-95.
- [101] Proudfoot AE, Power CA, Hoogewerf AJ, Montjovent MO, Borlat F, Offord RE, et al. Extension of recombinant human RANTES by the retention of the initiating methionine produces a potent antagonist. *J. Biol. Chem.* 1996; 271: 2599-603.
- [102] Millard CJ, Ludeman JP, Canals M, Bridgford JL, Hinds MG, Clayton DJ, et al. Structural Basis of Receptor Sulfotyrosine Recognition by a CC Chemokine: The N-Terminal Region of CCR3 Bound to CCL11/Eotaxin-1. *Structure.* 2014; 22: 1571-81.

References

- [103] Tuinstra RL, Peterson FC, Elgin ES, Pelzek AJ, Volkman BF. An engineered second disulfide bond restricts lymphotactin/XCL1 to a chemokine-like conformation with XCR1 agonist activity. *Biochemistry*. 2007; 46: 2564-73.
- [104] Wells TN, Power CA, Lusti-Narasimhan M, Hoogewerf AJ, Cooke RM, Chung CW, et al. Selectivity and antagonism of chemokine receptors. *J. Leukoc. Biol.* 1996; 59: 53-60.
- [105] Qin L, Kufareva I, Holden LG, Wang C, Zheng Y, Zhao C, et al. Structural biology. Crystal structure of the chemokine receptor CXCR4 in complex with a viral chemokine. *Science*. 2015; 347: 1117-22.
- [106] Burg JS, Ingram JR, Venkatakrishnan AJ, Jude KM, Dukkipati A, Feinberg EN, et al. Structural biology. Structural basis for chemokine recognition and activation of a viral G protein-coupled receptor. *Science*. 2015; 347: 1113-7.
- [107] Kleist AB, Getschman AE, Ziarek JJ, Nevins AM, Gauthier PA, Chevigne A, et al. New paradigms in chemokine receptor signal transduction: Moving beyond the two-site model. *Biochem. Pharmacol.* 2016; 114: 53-68.
- [108] BreLOT A, Heveker N, Montes M, Alizon M. Identification of residues of CXCR4 critical for human immunodeficiency virus coreceptor and chemokine receptor activities. *J. Biol. Chem.* 2000; 275: 23736-44.
- [109] Samson M, LaRosa G, Libert F, Paindavoine P, Detheux M, Vassart G, et al. The second extracellular loop of CCR5 is the major determinant of ligand specificity. *J. Biol. Chem.* 1997; 272: 24934-41.
- [110] Stephens B, Handel TM. Chemokine receptor oligomerization and allostery. *Prog. Mol. Biol. Transl. Sci.* 2013; 115: 375-420.
- [111] Springael JY, Urizar E, Parmentier M. Dimerization of chemokine receptors and its functional consequences. *Cyto. Growth factor Rev.* 2005; 16: 611-23.
- [112] Rajagopalan L, Rajarathnam K. Structural basis of chemokine receptor function--a model for binding affinity and ligand selectivity. *Biosci. Rep.* 2006; 26: 325-39.
- [113] Xanthou G, Williams TJ, Pease JE. Molecular characterization of the chemokine receptor CXCR3: evidence for the involvement of distinct extracellular domains in a multi-step model of ligand binding and receptor activation. *Eur. J. Pharmacol.* 2003; 33: 2927-36.
- [114] Chu HX, Arumugam TV, Gelderblom M, Magnus T, Drummond GR, Sobey CG. Role of CCR2 in inflammatory conditions of the central nervous system. *J. Cereb. Blood Flow Metab.* 2014; 34: 1425-9.

- [115] Connor SJ, Paraskevopoulos N, Newman R, Cuan N, Hampartzoumian T, Lloyd AR, et al. CCR2 expressing CD4⁺ T lymphocytes are preferentially recruited to the ileum in Crohn's disease. *Gut*. 2004; 53: 1287-94.
- [116] Zweemer AJ, Bunnik J, Veenhuizen M, Miraglia F, Lenselink EB, Vilums M, et al. Discovery and mapping of an intracellular antagonist binding site at the chemokine receptor CCR2. *Mol. Pharmacol.* 2014; 86: 358-68.
- [117] Zimmermann HW, Sterzer V, Sahin H. CCR1 and CCR2 antagonists. *Curr. Top. Med. Chem.* 2014; 14: 1539-52.
- [118] Doranz BJ, Rucker J, Yi Y, Smyth RJ, Samson M, Peiper SC, et al. A dual-tropic primary HIV-1 isolate that uses fusin and the beta-chemokine receptors CKR-5, CKR-3, and CKR-2b as fusion cofactors. *Cell*. 1996; 85: 1149-58.
- [119] Xue CB, Wang A, Meloni D, Zhang K, Kong L, Feng H, et al. Discovery of INCB3344, a potent, selective and orally bioavailable antagonist of human and murine CCR2. *Bioorg. Med. Chem. Lett.* 2010; 20: 7473-8.
- [120] Brodmerkel CM, Huber R, Covington M, Diamond S, Hall L, Collins R, et al. Discovery and pharmacological characterization of a novel rodent-active CCR2 antagonist, INCB3344. *J. Immunol.* 2005; 175: 5370-8.
- [121] Aiello RJ, Perry BD, Bourassa PA, Robertson A, Weng W, Knight DR, et al. CCR2 receptor blockade alters blood monocyte subpopulations but does not affect atherosclerotic lesions in apoE(-/-) mice. *Atherosclerosis*. 2010; 208: 370-5.
- [122] Okamoto M, Fuchigami M, Suzuki T, Watanabe N. A novel C-C chemokine receptor 2 antagonist prevents progression of albuminuria and atherosclerosis in mouse models. *Biol. Pharm. Bull.* 2012; 35: 2069-74.
- [123] Horuk R. Chemokine receptor antagonists: overcoming developmental hurdles. *Nat. Rev. Drug Discov.* 2009; 8: 23-33.
- [124] Liu J, Merritt JR. CC chemokine receptor small molecule antagonists in the treatment of rheumatoid arthritis and other diseases: a current view. *Curr. Top. Med. Chem.* 2010; 10: 1250-67.
- [125] Preobrazhensky AA, Dragan S, Kawano T, Gavrilin MA, Gulina IV, Chakravarty L, et al. Monocyte chemoattractant protein-1 receptor CCR2B is a glycoprotein that has tyrosine sulfation in a conserved extracellular N-terminal region. *J Immunol.* 2000; 165: 5295-303.
- [126] Tan JHY, Ludeman JP, Wedderburn J, Canals M, Hall P, Butler SJ, et al. Tyrosine Sulfation of Chemokine Receptor CCR2 Enhances Interactions with Both Monomeric and Dimeric Forms of the Chemokine Monocyte Chemoattractant Protein-1 (MCP-1). *J. Biol. Chem.* 2013; 288: 10024-34.

References

- [127] Charo IF, Myers SJ, Herman A, Franci C, Connolly AJ, Coughlin SR. Molecular cloning and functional expression of two monocyte chemoattractant protein 1 receptors reveals alternative splicing of the carboxyl-terminal tails. *Proc. Natl. Acad. Sci. U S A.* 1994; 91: 2752-6.
- [128] Tanaka S, Green SR, Quehenberger O. Differential expression of the isoforms for the monocyte chemoattractant protein-1 receptor, CCR2, in monocytes. *Biochem. Biophys. Res. Commun.* 2002; 290: 73-80.
- [129] Navratilova Z. Polymorphisms in CCL2&CCL5 chemokines/chemokine receptors genes and their association with diseases. *Biomed. Pap. Med. Fac. Univ. Palacky. Olomouc. Czech. Repub.* 2006; 150: 191-204.
- [130] Daly C, Rollins BJ. Monocyte chemoattractant protein-1 (CCL2) in inflammatory disease and adaptive immunity: therapeutic opportunities and controversies. *Microcirculation.* 2003; 10: 247-57.
- [131] Van Coillie E, Van Damme J, Opdenakker G. The MCP/eotaxin subfamily of CC chemokines. *Cytokine Growth Factor Rev.* 1999; 10: 61-86.
- [132] Melgarejo E, Medina MA, Sanchez-Jimenez F, Urdiales JL. Monocyte chemoattractant protein-1: a key mediator in inflammatory processes. *Int. J. Biochem. Cell Biol.* 2009; 41: 998-1001.
- [133] Proost P, Wuyts A, Van Damme J. Human monocyte chemotactic proteins-2 and -3: structural and functional comparison with MCP-1. *J. Leukoc. Biol.* 1996; 59: 67-74.
- [134] O'Hayre M, Salanga CL, Handel TM, Allen SJ. Chemokines and cancer: migration, intracellular signalling and intercellular communication in the microenvironment. *Biochem. J.* 2008; 409: 635-49.
- [135] Van Damme J, Proost P, Put W, Arens S, Lenaerts JP, Conings R, et al. Induction of monocyte chemotactic proteins MCP-1 and MCP-2 in human fibroblasts and leukocytes by cytokines and cytokine inducers. Chemical synthesis of MCP-2 and development of a specific RIA. *J. Immunol.* 1994; 152: 5495-502.
- [136] Van Coillie E, Proost P, Van Aelst I, Struyf S, Polfliet M, De Meester I, et al. Functional comparison of two human monocyte chemotactic protein-2 isoforms, role of the amino-terminal pyroglutamic acid and processing by CD26/dipeptidyl peptidase IV. *Biochemistry.* 1998; 37: 12672-80.
- [137] Van Damme J, Proost P, Lenaerts JP, Opdenakker G. Structural and functional identification of two human, tumor-derived monocyte chemotactic proteins (MCP-2 and MCP-3) belonging to the chemokine family. *J. Exp. Med.* 1992; 176: 59-65.
- [138] Minty A, Chalon P, Guillemot JC, Kaghad M, Liauzun P, Magazin M, et al. Molecular cloning of the MCP-3 chemokine gene and regulation of its expression. *Eur Cytokine Netw.* 1993; 4: 99-110.

- [139] Kumar SN, Boss JM. Site A of the MCP-1 distal regulatory region functions as a transcriptional modulator through the transcription factor NF1. *Mol. Immunol.* 2000; 37: 623-32.
- [140] Weber M, Uguccioni M, Ochensberger B, Baggiolini M, Clark-Lewis I, Dahinden CA. Monocyte chemotactic protein MCP-2 activates human basophil and eosinophil leukocytes similar to MCP-3. *J. Immunol.* 1995; 154: 4166-72.
- [141] Garcia-Zepeda EA, Combadiere C, Rothenberg ME, Sarafi MN, Lavigne F, Hamid Q, et al. Human monocyte chemoattractant protein (MCP)-4 is a novel CC chemokine with activities on monocytes, eosinophils, and basophils induced in allergic and nonallergic inflammation that signals through the CC chemokine receptors (CCR)-2 and -3. *J. Immunol.* 1996; 157: 5613-26.
- [142] Allen JA, Roth BL. Strategies to discover unexpected targets for drugs active at G protein-coupled receptors. *Annu. Rev. Pharmacol. Toxicol.* 2011; 51: 117-44.
- [143] Pease JE, Williams TJ. Chemokines and their receptors in allergic disease. *J. Allergy Clin. Immunol.* 2006; 118: 305-18; quiz 19-20.
- [144] Balkwill F. Cancer and the chemokine network. *Nat. Rev. Cancer.* 2004; 4: 540-50.
- [145] Shin WS, Szuba A, Rockson SG. The role of chemokines in human cardiovascular pathology: enhanced biological insights. *Atherosclerosis.* 2002; 160: 91-102.
- [146] Tucci M, Quatraro C, Frassanito MA, Silvestris F. Deregulated expression of monocyte chemoattractant protein-1 (MCP-1) in arterial hypertension: role in endothelial inflammation and atheromasia. *J. Hypertens.* 2006; 24: 1307-18.
- [147] Gerard C, Rollins BJ. Chemokines and disease. *Nat. Immunol.* 2001; 2: 108-15.
- [148] Gu L, Okada Y, Clinton SK, Gerard C, Sukhova GK, Libby P, et al. Absence of monocyte chemoattractant protein-1 reduces atherosclerosis in low density lipoprotein receptor-deficient mice. *Mol. Cell.* 1998; 2: 275-81.
- [149] Aiello RJ, Bourassa PA, Lindsey S, Weng W, Natoli E, Rollins BJ, et al. Monocyte chemoattractant protein-1 accelerates atherosclerosis in apolipoprotein E-deficient mice. *Arterioscler. Thromb. Vasc. Biol.* 1999; 19: 1518-25.
- [150] Distler JH, Akhmetshina A, Schett G, Distler O. Monocyte chemoattractant proteins in the pathogenesis of systemic sclerosis. *Rheumatology (Oxford).* 2009; 48: 98-103.
- [151] Choi ES, Jakubzick C, Carpenter KJ, Kunkel SL, Evanoff H, Martinez FJ, et al. Enhanced monocyte chemoattractant protein-3/CC chemokine ligand-7 in usual interstitial pneumonia. *Am. J. Respir. Crit. Care. Med.* 2004; 170: 508-15.

References

- [152] Maddaluno M, Di Lauro M, Di Pascale A, Santamaria R, Guglielmotti A, Grassia G, et al. Monocyte chemotactic protein-3 induces human coronary smooth muscle cell proliferation. *Atherosclerosis*. 2011; 217: 113-9.
- [153] Pliska V. Partial agonism: mechanisms based on ligand-receptor interactions and on stimulus-response coupling. *J. Recept. Signal. Transduct. Res.* 1999; 19: 597-629.
- [154] Berchiche YA, Gravel S, Pelletier ME, St-Onge G, Heveker N. Different effects of the different natural CC chemokine receptor 2b ligands on β -arrestin recruitment, G α i signaling, and receptor internalization. *Mol. Pharmacol.* 2011; 79: 488-98.
- [155] Park PS, Lodowski DT, Palczewski K. Activation of G protein-coupled receptors: beyond two-state models and tertiary conformational changes. *Annu. Rev. Pharmacol. Toxicol.* 2008; 48: 107-41.
- [156] Costa T, Herz A. Antagonists with negative intrinsic activity at delta opioid receptors coupled to GTP-binding proteins. *Proc. Natl. Acad. Sci. U S A.* 1989; 86: 7321-5.
- [157] Lefkowitz RJ, Cotecchia S, Samama P, Costa T. Constitutive activity of receptors coupled to guanine nucleotide regulatory proteins. *Trends Pharmacol. Sci.* 1993; 14: 303-7.
- [158] Shukla AK, Violin JD, Whalen EJ, Gesty-Palmer D, Shenoy SK, Lefkowitz RJ. Distinct conformational changes in β -arrestin report biased agonism at seven-transmembrane receptors. *Proc. Natl. Acad. Sci. U S A.* 2008; 105: 9988-93.
- [159] Rajagopal S, Bassoni DL, Campbell JJ, Gerard NP, Gerard C, Wehrman TS. Biased agonism as a mechanism for differential signaling by chemokine receptors. *J. Biol. Chem.* 2013; 288: 35039-48.
- [160] Urban JD, Clarke WP, von Zastrow M, Nichols DE, Kobilka B, Weinstein H, et al. Functional selectivity and classical concepts of quantitative pharmacology. *J. Pharmacol. Exp. Ther.* 2007; 320: 1-13.
- [161] Kahsai AW, Xiao K, Rajagopal S, Ahn S, Shukla AK, Sun J, et al. Multiple ligand-specific conformations of the beta2-adrenergic receptor. *Nat. Chem. Biol.* 2011; 7: 692-700.
- [162] Klein Herenbrink C, Sykes DA, Donthamsetti P, Canals M, Coudrat T, Shonberg J, et al. The role of kinetic context in apparent biased agonism at GPCRs. *Nat. Commun.* 2016; 7: 10842.
- [163] Gurwitz D, Haring R, Heldman E, Fraser CM, Manor D, Fisher A. Discrete activation of transduction pathways associated with acetylcholine m1 receptor by several muscarinic ligands. *Eur. J. Pharmacol.* 1994; 267: 21-31.
- [164] Shonberg J, Lopez L, Scammells PJ, Christopoulos A, Capuano B, Lane JR. Biased agonism at G protein-coupled receptors: the promise and the challenges--a medicinal chemistry perspective. *Med. Res. Rev.* 2014; 34: 1286-330.

- [165] Sternini C, Spann M, Anton B, Keith DE, Jr., Bunnett NW, von Zastrow M, et al. Agonist-selective endocytosis of mu opioid receptor by neurons in vivo. *Proc. Natl. Acad. Sci. U S A.* 1996; 93: 9241-6.
- [166] Keith DE, Murray SR, Zaki PA, Chu PC, Lissin DV, Kang L, et al. Morphine activates opioid receptors without causing their rapid internalization. *J. Biol. Chem.* 1996; 271: 19021-4.
- [167] Wisler JW, DeWire SM, Whalen EJ, Violin JD, Drake MT, Ahn S, et al. A unique mechanism of β -blocker action: carvedilol stimulates β -arrestin signaling. *Proc. Natl. Acad. Sci. U S A.* 2007; 104: 16657-62.
- [168] Stallaert W, Dorn JF, van der Westhuizen E, Audet M, Bouvier M. Impedance responses reveal $\beta(2)$ -adrenergic receptor signaling pluridimensionality and allow classification of ligands with distinct signaling profiles. *PLoS One.* 2012; 7: e29420.
- [169] Newman-Tancredi A, Martel JC, Assie MB, Buritova J, Laressergues E, Cosi C, et al. Signal transduction and functional selectivity of F15599, a preferential post-synaptic 5-HT_{1A} receptor agonist. *Br. J. Pharmacol.* 2009; 156: 338-53.
- [170] Berg KA, Maayani S, Goldfarb J, Scaramellini C, Leff P, Clarke WP. Effector pathway-dependent relative efficacy at serotonin type 2A and 2C receptors: evidence for agonist-directed trafficking of receptor stimulus. *Mol. Pharmacol.* 1998; 54: 94-104.
- [171] Urban JD, Clarke WP, von Zastrow M, Nichols DE, Kobilka B, Weinstein H, et al. Functional selectivity and classical concepts of quantitative pharmacology. *J Pharmacol Exp Ther.* 2007; 320: 1-13.
- [172] Urban JD, Vargas GA, von Zastrow M, Mailman RB. Aripiprazole has functionally selective actions at dopamine D₂ receptor-mediated signaling pathways. *Neuropsychopharmacology.* 2007; 32: 67-77.
- [173] Nickolls SA, Fleck B, Hoare SR, Maki RA. Functional selectivity of melanocortin 4 receptor peptide and nonpeptide agonists: evidence for ligand-specific conformational states. *J. Pharmacol. Exp. Ther.* 2005; 313: 1281-8.
- [174] Ahn S, Shenoy SK, Wei H, Lefkowitz RJ. Differential kinetic and spatial patterns of β -arrestin and G protein-mediated ERK activation by the angiotensin II receptor. *J. Biol. Chem.* 2004; 279: 35518-25.
- [175] Wei H, Ahn S, Shenoy SK, Karnik SS, Hunyady L, Luttrell LM, et al. Independent β -arrestin 2 and G protein-mediated pathways for angiotensin II activation of extracellular signal-regulated kinases 1 and 2. *Proc. Natl. Acad. Sci. U S A.* 2003; 100: 10782-7.

References

- [176] Kohout TA, Nicholas SL, Perry SJ, Reinhart G, Junger S, Struthers RS. Differential desensitization, receptor phosphorylation, β -arrestin recruitment, and ERK1/2 activation by the two endogenous ligands for the CC chemokine receptor 7. *J. Biol. Chem.* 2004; 279: 23214-22.
- [177] Corbisier J, Gales C, Huszagh A, Parmentier M, Springael JY. Biased signaling at chemokine receptors. *J. Biol. Chem.* 2015; 290: 9542-54.
- [178] Oppermann M, Mack M, Proudfoot AE, Olbrich H. Differential effects of CC chemokines on CC chemokine receptor 5 (CCR5) phosphorylation and identification of phosphorylation sites on the CCR5 carboxyl terminus. *J. Biol. Chem.* 1999; 274: 8875-85.
- [179] Huttner WB. Tyrosine sulfation and the secretory pathway. *Annu. Rev. Physiol.* 1988; 50: 363-76.
- [180] Beisswanger R, Corbeil D, Vannier C, Thiele C, Dohrmann U, Kellner R, et al. Existence of distinct tyrosylprotein sulfotransferase genes: molecular characterization of tyrosylprotein sulfotransferase-2. *Proc. Natl. Acad. Sci. U S A.* 1998; 95: 11134-9.
- [181] Ouyang Y, Lane WS, Moore KL. Tyrosylprotein sulfotransferase: purification and molecular cloning of an enzyme that catalyzes tyrosine O-sulfation, a common posttranslational modification of eukaryotic proteins. *Proc. Natl. Acad. Sci. U S A.* 1998; 95: 2896-901.
- [182] Moore KL. The biology and enzymology of protein tyrosine O-sulfation. *J. Biol. Chem.* 2003; 278: 24243-6.
- [183] Mishiro E, Sakakibara Y, Liu MC, Suiko M. Differential enzymatic characteristics and tissue-specific expression of human TPST-1 and TPST-2. *J. Biochem.* 2006; 140: 731-7.
- [184] Stone MJ, Chuang S, Hou X, Shoham M, Zhu JZ. Tyrosine sulfation: an increasingly recognised post-translational modification of secreted proteins. *N. Biotechnol.* 2009; 25: 299-317.
- [185] Ludeman JP, Stone MJ. The structural role of receptor tyrosine sulfation in chemokine recognition. *Brit. J. Pharmacol.* 2014; 171: 1167-79.
- [186] Bundgaard JR, Vuust J, Rehfeld JF. New consensus features for tyrosine O-sulfation determined by mutational analysis. *J. Biol. Chem.* 1997; 272: 21700-5.
- [187] Huttner WB. Sulphation of tyrosine residues-a widespread modification of proteins. *Nature.* 1982; 299: 273-6.
- [188] Kehoe JW, Bertozzi CR. Tyrosine sulfation: a modulator of extracellular protein-protein interactions. *Chem. Biol.* 2000; 7: R57-61.
- [189] Pouyani T, Seed B. PSGL-1 recognition of P-selectin is controlled by a tyrosine sulfation consensus at the PSGL-1 amino terminus. *Cell.* 1995; 83: 333-43.

- [190] Sako D, Comess KM, Barone KM, Camphausen RT, Cumming DA, Shaw GD. A sulfated peptide segment at the amino terminus of PSGL-1 is critical for P-selectin binding. *Cell*. 1995; 83: 323-31.
- [191] Farzan M, Mirzabekov T, Kolchinsky P, Wyatt R, Cayabyab M, Gerard NP, et al. Tyrosine sulfation of the amino terminus of CCR5 facilitates HIV-1 entry. *Cell*. 1999; 96: 667-76.
- [192] Fong AM, Alam SM, Imai T, Haribabu B, Patel DD. CX3CR1 tyrosine sulfation enhances fractalkine-induced cell adhesion. *J. Biol. Chem*. 2002; 277: 19418-23.
- [193] Choe H, Moore MJ, Owens CM, Wright PL, Vasilieva N, Li W, et al. Sulphated tyrosines mediate association of chemokines and Plasmodium vivax Duffy binding protein with the Duffy antigen/receptor for chemokines (DARC). *Mol. Microbiol*. 2005; 55: 1413-22.
- [194] Szpakowska M, Fievez V, Arumugan K, van Nuland N, Schmit JC, Chevigne A. Function, diversity and therapeutic potential of the N-terminal domain of human chemokine receptors. *Biochem. Pharmacol*. 2012; 84: 1366-80.
- [195] Gozansky EK, Louis JM, Caffrey M, Clore GM. Mapping the binding of the N-terminal extracellular tail of the CXCR4 receptor to stromal cell-derived factor-1 α . *J. Mol. Biol*. 2005; 345: 651-8.
- [196] Love M, Sandberg JL, Ziarek JJ, Gerarden KP, Rode RR, Jensen DR, et al. Solution structure of CCL21 and identification of a putative CCR7 binding site. *Biochemistry*. 2012; 51: 733-5.
- [197] Hemmerich S, Paavola C, Bloom A, Bhakta S, Freedman R, Grunberger D, et al. Identification of residues in the monocyte chemotactic protein-1 that contact the MCP-1 receptor, CCR2. *Biochemistry*. 1999; 38: 13013-25.
- [198] Choe H, Farzan M. Chapter 7. Tyrosine sulfation of HIV-1 coreceptors and other chemokine receptors. *Methods Enzymol*. 2009; 461: 147-70.
- [199] Simpson LS, Zhu JZ, Widlanski TS, Stone MJ. Regulation of chemokine recognition by site-specific tyrosine sulfation of receptor peptides. *Chem. Biol*. 2009; 16: 153-61.
- [200] Jen CH, Leary JA. A competitive binding study of chemokine, sulfated receptor, and glycosaminoglycan interactions by nano-electrospray ionization mass spectrometry. *Anal Biochem*. 2010; 407: 134-40.
- [201] Tan JH, Ludeman JP, Wedderburn J, Canals M, Hall P, Butler SJ, et al. Tyrosine sulfation of chemokine receptor CCR2 enhances interactions with both monomeric and dimeric forms of the chemokine monocyte chemoattractant protein-1 (MCP-1). *J. Biol. Chem*. 2013; 288: 10024-34.

References

- [202] Gutierrez J, Kremer L, Zaballos A, Goya I, Martinez AC, Marquez G. Analysis of post-translational CCR8 modifications and their influence on receptor activity. *J. Biol. Chem.* 2004; 279: 14726-33.
- [203] Colvin RA, Campanella GS, Manice LA, Luster AD. CXCR3 requires tyrosine sulfation for ligand binding and a second extracellular loop arginine residue for ligand-induced chemotaxis. *Mol. Cell Biol.* 2006; 26: 5838-49.
- [204] Gao J-m, Xiang R-l, Jiang L, Li W-h, Feng Q-p, Guo Z-j, et al. Sulfated tyrosines 27 and 29 in the N-terminus of human CXCR3 participate in binding native IP-10. *Acta. Pharmacol. Sin.* 2009; 30: 193-201.
- [205] Farzan M, Babcock GJ, Vasilieva N, Wright PL, Kiprilov E, Mirzabekov T, et al. The role of post-translational modifications of the CXCR4 amino terminus in stromal-derived factor 1 α association and HIV-1 entry. *J. Biol. Chem.* 2002; 277: 29484-9.
- [206] Ziarek JJ, Heroux MS, Veldkamp CT, Peterson FC, Volkman BF. Sulfotyrosine recognition as marker for druggable sites in the extracellular space. *Int. J. Mol. Sci.* 2011; 12: 3740-56.
- [207] Veldkamp CT, Seibert C, Peterson FC, De la Cruz NB, Haugner JC, 3rd, Basnet H, et al. Structural basis of CXCR4 sulfotyrosine recognition by the chemokine SDF-1/CXCL12. *Sci. Signal.* 2008; 1: ra4.
- [208] Scholten DJ, Canals M, Wijtmans M, de Munnik S, Nguyen P, Verzijl D, et al. Pharmacological characterization of a small-molecule agonist for the chemokine receptor CXCR3. *Brit. J. Pharmacol.* 2012; 166: 898-911.
- [209] Smith PK, Krohn RI, Hermanson GT, Mallia AK, Gartner FH, Provenzano MD, et al. Measurement of Protein Using Bicinchoninic Acid. *Anal. Biochem.* 1985; 150: 76-85.
- [210] Zweemer AJ, Nederpelt I, Vrieling H, Hafith S, Doornbos ML, de Vries H, et al. Multiple binding sites for small-molecule antagonists at the CC chemokine receptor 2. *Mol. Pharm.* 2013; 84: 551-61.
- [211] Ayoub MA, Zhang Y, Kelly RS, See HB, Johnstone EKM, McCall EA, et al. Functional Interaction between Angiotensin II Receptor Type 1 and Chemokine (C-C Motif) Receptor 2 with Implications for Chronic Kidney Disease. *PLoS One.* 2015; 10.
- [212] Black JW, Leff P, Shankley NP, Wood J. An operational model of pharmacological agonism: the effect of E/[A] curve shape on agonist dissociation constant estimation. *Brit. J. Pharmacol.* 1985; 84: 561-71.
- [213] Kenakin T, Watson C, Muniz-Medina V, Christopoulos A, Novick S. A simple method for quantifying functional selectivity and agonist bias. *ACS Chem. Neurosci.* 2012; 3: 193-203.

- [214] Cheng Y, Prusoff WH. Relationship between Inhibition Constant (K₁) and Concentration of Inhibitor Which Causes 50 Per Cent Inhibition (I₅₀) of an Enzymatic-Reaction. *Biochem. Pharmacol.* 1973; 22: 3099-108.
- [215] Christopoulos A. Assessing the distribution of parameters in models of ligand-receptor interaction: to log or not to log. *Trends Pharmacol. Sci.* 1998; 19: 351-7.
- [216] Steen A, Larsen O, Thiele S, Rosenkilde MM. Biased and G protein-independent signaling of chemokine receptors. *Front. Immunol.* 2014; 5: 277.
- [217] Yoshie O. Chemokine receptors as therapeutic targets. *Nihon Rinsho Meneki Gakkai Kaishi.* 2013; 36: 189-96.
- [218] O'Hayre M, Salanga CL, Handel TM, Hamel DJ. Emerging concepts and approaches for chemokine-receptor drug discovery. *Expert. Opin. Drug Discov.* 2010; 5: 1109-22.
- [219] Wan Y, Jakway JP, Qiu H, Shah H, Garlisi CG, Tian F, et al. Identification of full, partial and inverse CC chemokine receptor 3 agonists using [³⁵S]GTPγS binding. *Eur. J. Immunol.* 2002; 456: 1-10.
- [220] Martinelli R, Sabroe I, LaRosa G, Williams TJ, Pease JE. The CC chemokine eotaxin (CCL11) is a partial agonist of CC chemokine receptor 2B. *J. Biol. Chem.* 2001; 276: 42957-64.
- [221] Rajagopal S, Ahn S, Rominger DH, Gowen-MacDonald W, Lam CM, Dewire SM, et al. Quantifying ligand bias at seven-transmembrane receptors. *Mol. Pharm.* 2011; 80: 367-77.
- [222] Zidar DA. Endogenous ligand bias by chemokines: implications at the front lines of infection and leukocyte trafficking. *Endocr. Metab. Immune Disord. Drug Targets.* 2011; 11: 120-31.
- [223] Monteclaro FS, Charo IF. The amino-terminal extracellular domain of the MCP-1 receptor, but not the RANTES/MIP-1α receptor, confers chemokine selectivity. Evidence for a two-step mechanism for MCP-1 receptor activation. *J. Biol. Chem.* 1996; 271: 19084-92.
- [224] Kenakin T. Biased agonism. *F1000 Biol. Rep.* 2009; 1: 87.
- [225] Struyf S, Van Collie E, Paemen L, Put W, Lenaerts JP, Proost P, et al. Synergistic induction of MCP-1 and -2 by IL-1β and interferons in fibroblasts and epithelial cells. *J. Leukoc. Biol.* 1998; 63: 364-72.
- [226] Qiu B, Frait KA, Reich F, Komuniecki E, Chensue SW. Chemokine expression dynamics in mycobacterial (type-1) and schistosomal (type-2) antigen-elicited pulmonary granuloma formation. *Am. J. Pathol.* 2001; 158: 1503-15.
- [227] Zheng H, Loh HH, Law PY. Agonist-selective signaling of G protein-coupled receptor: mechanisms and implications. *IUBMB Life.* 2010; 62: 112-9.

References

- [228] Shenoy SK, Drake MT, Nelson CD, Houtz DA, Xiao K, Madabushi S, et al. β -arrestin-dependent, G protein-independent ERK1/2 activation by the β 2 adrenergic receptor. *J. Biol. Chem.* 2006; 281: 1261-73.
- [229] Zheng H, Chu J, Qiu Y, Loh HH, Law PY. Agonist-selective signaling is determined by the receptor location within the membrane domains. *Proc. Natl. Acad. Sci. U S A.* 2008; 105: 9421-6.
- [230] Mohan ML, Vasudevan NT, Gupta MK, Martelli EE, Naga Prasad SV. G-protein coupled receptor resensitization-appreciating the balancing act of receptor function. *Curr. Mol. Pharmacol.* 2012.
- [231] Neel NF, Schutyser E, Sai J, Fan GH, Richmond A. Chemokine receptor internalization and intracellular trafficking. *Cytokine Growth Factor Rev.* 2005; 16: 637-58.
- [232] Seger R, Krebs EG. The MAPK signaling cascade. *FASEB J.* 1995; 9: 726-35.
- [233] Ashida N, Arai H, Yamasaki M, Kita T. Differential signaling for MCP-1-dependent integrin activation and chemotaxis. *Ann. N. Y. Acad. Sci.* 2001; 947: 387-9.
- [234] Ashida N, Arai H, Yamasaki M, Kita T. Distinct signaling pathways for MCP-1-dependent integrin activation and chemotaxis. *J. Biol. Chem.* 2001; 276: 16555-60.
- [235] Kenakin T. Quantifying biological activity in chemical terms: a pharmacology primer to describe drug effect. *ACS Chem. Biol.* 2009; 4: 249-60.
- [236] Black JW, Gerskowitch VP, Leff P, Shankley NP. Pharmacological analysis of β -adrenoceptor-mediated agonism in the guinea-pig, isolated, right atrium. *Br. J. Pharmacol.* 1985; 84: 779-85.
- [237] Jarnagin K, Grunberger D, Mulkins M, Wong B, Hemmerich S, Paavola C, et al. Identification of surface residues of the monocyte chemotactic protein 1 that affect signaling through the receptor CCR2. *Biochemistry.* 1999; 38: 16167-77.
- [238] Crump MP, Gong JH, Loetscher P, Rajarathnam K, Amara A, Arenzana-Seisdedos F, et al. Solution structure and basis for functional activity of stromal cell-derived factor-1; dissociation of CXCR4 activation from binding and inhibition of HIV-1. *EMBO J.* 1997; 16: 6996-7007.
- [239] Nesselova IV, Ermakova E, Daragan VA, Pang M, Menendez M, Lagartera L, et al. Lactose binding to galectin-1 modulates structural dynamics, increases conformational entropy, and occurs with apparent negative cooperativity. *J. Mol. Biol.* 2010; 397: 1209-30.
- [240] Chen C, Li J, Bot G, Szabo I, Rogers TJ, Liu-Chen LY. Heterodimerization and cross-desensitization between the μ -opioid receptor and the chemokine CCR5 receptor. *Eur. J. Pharmacol.* 2004; 483: 175-86.
- [241] Mueller A, Mahmoud NG, Goedecke MC, McKeating JA, Strange PG. Pharmacological characterization of the chemokine receptor, CCR5. *Brit. J. Pharmacol.* 2002; 135: 1033-43.

- [242] Pease JE, Wang J, Ponath PD, Murphy PM. The N-terminal extracellular segments of the chemokine receptors CCR1 and CCR3 are determinants for MIP-1 α and eotaxin binding, respectively, but a second domain is essential for efficient receptor activation. *J. Biol. Chem.* 1998; 273: 19972-6.
- [243] Skelton NJ, Quan C, Reilly D, Lowman H. Structure of a CXC chemokine-receptor fragment in complex with interleukin-8. *Structure.* 1999; 7: 157-68.
- [244] Blanpain C, Doranz BJ, Bondué A, Govaerts C, De Leener A, Vassart G, et al. The core domain of chemokines binds CCR5 extracellular domains while their amino terminus interacts with the transmembrane helix bundle. *J. Biol. Chem.* 2003; 278: 5179-87.
- [245] Mirzadegan T, Diehl F, Ebi B, Bhakta S, Polsky I, McCarley D, et al. Identification of the binding site for a novel class of CCR2b chemokine receptor antagonists: binding to a common chemokine receptor motif within the helical bundle. *J. Biol. Chem.* 2000; 275: 25562-71.
- [246] Govaerts C, Blanpain C, Deupi X, Ballet S, Ballesteros JA, Wodak SJ, et al. The TXP motif in the second transmembrane helix of CCR5. A structural determinant of chemokine-induced activation. *J. Biol. Chem.* 2001; 276: 13217-25.
- [247] Kofuku Y, Yoshiura C, Ueda T, Terasawa H, Hirai T, Tominaga S, et al. Structural basis of the interaction between chemokine stromal cell-derived factor-1/CXCL12 and its G-protein-coupled receptor CXCR4. *J. Biol. Chem.* 2009; 284: 35240-50.
- [248] Rodriguez-Frade JM, Vila-Coro AJ, de Ana AM, Albar JP, Martinez AC, Mellado M. The chemokine monocyte chemoattractant protein-1 induces functional responses through dimerization of its receptor CCR2. *Proc. Natl. Acad. Sci. U S A.* 1999; 96: 3628-33.
- [249] Berkhout TA, Blaney FE, Bridges AM, Cooper DG, Forbes IT, Gribble AD, et al. CCR2: characterization of the antagonist binding site from a combined receptor modeling/mutagenesis approach. *J. Med. Chem.* 2003; 46: 4070-86.
- [250] Zheng Y, Qin L, Zacarias NV, de Vries H, Han GW, Gustavsson M, et al. Structure of CC chemokine receptor 2 with orthosteric and allosteric antagonists. *Nature.* 2016; 540: 458-61.
- [251] Oswald C, Rappas M, Kean J, Dore AS, Errey JC, Bennett K, et al. Intracellular allosteric antagonism of the CCR9 receptor. *Nature.* 2016; 540: 462-5.
- [252] Ballesteros JA, Weinstein H. Integrated methods for the construction of three-dimensional models and computational probing of structure-function relations in G protein-coupled receptors. In: Sealfon SC, editor. *Methods in Neurosciences.* San Diego: Academic Press; 1995. p. 366-428.

References

- [253] Roumen L, Scholten DJ, de Kruijf P, de Esch IJ, Leurs R, de Graaf C. C(X)CR in silico: Computer-aided prediction of chemokine receptor-ligand interactions. *Drug Discov. Today Technol.* 2012; 9: e281-91.
- [254] Wescott MP, Kufareva I, Paes C, Goodman JR, Thaker Y, Puffer BA, et al. Signal transmission through the CXC chemokine receptor 4 (CXCR4) transmembrane helices. *Proc. Natl. Acad. Sci. U S A.* 2016; 113: 9928-33.
- [255] Hall SE, Mao A, Nicolaidou V, Finelli M, Wise EL, Nedjai B, et al. Elucidation of binding sites of dual antagonists in the human chemokine receptors CCR2 and CCR5. *Mol. Pharmacol.* 2009; 75: 1325-36.
- [256] O'Hayre M, Salanga CL, Kipps TJ, Messmer D, Dorrestein PC, Handel TM. Elucidating the CXCL12/CXCR4 signaling network in chronic lymphocytic leukemia through phosphoproteomics analysis. *PLoS One.* 2010; 5: e11716.
- [257] Gong JH, Clark-Lewis I. Antagonists of monocyte chemoattractant protein 1 identified by modification of functionally critical NH₂-terminal residues. *J. Exp. Med.* 1995; 181: 631-40.
- [258] Jin H, Shen X, Baggett BR, Kong X, LiWang PJ. The human CC chemokine MIP-1 β dimer is not competent to bind to the CCR5 receptor. *J. Biol. Chem.* 2007; 282: 27976-83.
- [259] Nasser MW, Raghuwanshi SK, Grant DJ, Jala VR, Rajarathnam K, Richardson RM. Differential activation and regulation of CXCR1 and CXCR2 by CXCL8 monomer and dimer. *J. Immunol.* 2009; 183: 3425-32.
- [260] Drury LJ, Ziarek JJ, Gravel S, Veldkamp CT, Takekoshi T, Hwang ST, et al. Monomeric and dimeric CXCL12 inhibit metastasis through distinct CXCR4 interactions and signaling pathways. *Proc. Natl. Acad. Sci. U S A.* 2011; 108: 17655-60.
- [261] Ravindran A, Sawant KV, Sarmiento J, Navarro J, Rajarathnam K. Chemokine CXCL1 dimer is a potent agonist for the CXCR2 receptor. *J. Biol. Chem.* 2013; 288: 12244-52.
- [262] Ravindran A, Joseph PR, Rajarathnam K. Structural basis for differential binding of the interleukin-8 monomer and dimer to the CXCR1 N-domain: role of coupled interactions and dynamics. *Biochemistry.* 2009; 48: 8795-805.
- [263] Ziarek JJ, Getschman AE, Butler SJ, Taleski D, Stephens B, Kufareva I, et al. Sulfopeptide probes of the CXCR4/CXCL12 interface reveal oligomer-specific contacts and chemokine allostery. *ACS Chem. Biol.* 2013; 8: 1955-63.
- [264] Tan Q, Zhu Y, Li J, Chen Z, Han GW, Kufareva I, et al. Structure of the CCR5 chemokine receptor-HIV entry inhibitor maraviroc complex. *Science.* 2013; 341: 1387-90.

- [265] Wu B, Chien EY, Mol CD, Fenalti G, Liu W, Katritch V, et al. Structures of the CXCR4 chemokine GPCR with small-molecule and cyclic peptide antagonists. *Science*. 2010; 330: 1066-71.
- [266] Park SH, Das BB, Casagrande F, Tian Y, Nothnagel HJ, Chu M, et al. Structure of the chemokine receptor CXCR1 in phospholipid bilayers. *Nature*. 2012; 491: 779-83.
- [267] Arimont M, Sun SL, Leurs R, Smit M, de Esch IJ, de Graaf C. Structural Analysis of Chemokine Receptor-Ligand Interactions. *J. Med. Chem.* 2017.
- [268] Mayer MR, Stone MJ. Identification of receptor binding and activation determinants in the N-terminal and N-loop regions of the CC chemokine eotaxin. *J. Biol. Chem.* 2001; 276: 13911-6.
- [269] Clark-Lewis I, Schumacher C, Baggiolini M, Moser B. Structure-activity relationships of interleukin-8 determined using chemically synthesized analogs. Critical role of NH₂-terminal residues and evidence for uncoupling of neutrophil chemotaxis, exocytosis, and receptor binding activities. *J. Biol. Chem.* 1991; 266: 23128-34.
- [270] Hebert CA, Vitangcol RV, Baker JB. Scanning mutagenesis of interleukin-8 identifies a cluster of residues required for receptor binding. *J. Biol. Chem.* 1991; 266: 18989-94.
- [271] Moser B, Dewald B, Barella L, Schumacher C, Baggiolini M, Clark-Lewis I. Interleukin-8 antagonists generated by N-terminal modification. *J. Biol. Chem.* 1993; 268: 7125-8.
- [272] Manglik A, Kim TH, Masureel M, Altenbach C, Yang Z, Hilger D, et al. Structural Insights into the Dynamic Process of β 2-Adrenergic Receptor Signaling. *Cell*. 2015; 161: 1101-11.
- [273] Moukhametzianov R, Warne T, Edwards PC, Serrano-Vega MJ, Leslie AG, Tate CG, et al. Two distinct conformations of helix 6 observed in antagonist-bound structures of a beta1-adrenergic receptor. *Proc. Natl. Acad. Sci. U S A.* 2011; 108: 8228-32.
- [274] Yao X, Parnot C, Deupi X, Ratnala VR, Swaminath G, Farrens D, et al. Coupling ligand structure to specific conformational switches in the β 2-adrenoceptor. *Nat. Chem. Biol.* 2006; 2: 417-22.
- [275] Florian S, Sonneck K, Czerny M, Hennersdorf F, Hauswirth AW, Buhring HJ, et al. Detection of novel leukocyte differentiation antigens on basophils and mast cells by HLDA8 antibodies. *Allergy*. 2006; 61: 1054-62.
- [276] Han KH, Tangirala RK, Green SR, Quehenberger O. Chemokine receptor CCR2 expression and monocyte chemoattractant protein-1-mediated chemotaxis in human monocytes. A regulatory role for plasma LDL. *Arterioscler. Thromb. Vasc. Biol.* 1998; 18: 1983-91.
- [277] Wain JH, Kirby JA, Ali S. Leucocyte chemotaxis: Examination of mitogen-activated protein kinase and phosphoinositide 3-kinase activation by Monocyte Chemoattractant Proteins-1, -2, -3 and -4. *Clin. Exp. Immunol.* 2002; 127: 436-44.

References

Appendices

Appendix I

A table showing common and systematic names of the chemokines used in this thesis.

Appendix II

Supplementary material of “NMR characterization of cooperativity: fast ligand binding coupled to protein dimerisation” (Chapter 3)

[**Huma Z.E.**, Ludeman J.P., Wilkinson B.L., Payne R.J., Stone M.J., NMR Characterisation of Cooperativity: fast ligand binding coupled to slow protein dimerisation. *Chem Sci.* 2014; 5: 2783-8, DOI: 10.1039/c4sc00131a.

Appendix III

Oligonucleotides for chemokine chimeras and receptor mutants

Appendix IV

Protein and nucleotide sequences of the chimeras

Appendix V

SDS-PAGE gels showing all chimeras, MCP-1(P8A) and wild type MCP-3

Appendix I

Common names	Systematic names
Gro- α	CXCL1
Gro- β	CXCL2
Gro- γ	CXCL3
Platelet factor 4	CXCL4
ENA78	CXCL5
GCP-2	CXCL6
IL-8	CXCL8
SDF-1	CXCL12
MCP-1	CCL2
MIP-1 α	CCL3
MIP-1 β	CCL4
RANTES	CCL5
MCP-3	CCL7
MCP-2	CCL8
Eotaxin-1	CCL11
MCP-4	CCL13
HCC-1	CCL14
ELC	CCL19
SLC	CCL21
Eotaxin-2	CCL24
Eotaxin-3	CCL26
Fractalkine	CX ₃ CL1
Lymphotactin	XCL1

Electronic Supplementary Material (ESI) for Chemical Science.
This journal is © The Royal Society of Chemistry 2014

Appendix II

S1

Supporting Information for:

NMR Characterization of Cooperativity: Fast Ligand Binding Coupled to Slow Protein Dimerization.

Zil E Huma, Justin P. Ludeman, Brendan L. Wilkinson, Richard J. Payne, Martin J. Stone

Proteins and Peptide Preparation. MCP-1 was expressed and purified as described by Tan *et al* (*J. Biol. Chem.* 2012, 287(18), 14692). Briefly, an N-terminal His₆-tagged form of MCP-1 was expressed in *E.coli* using minimal media to allow ¹⁵N-enrichment. Inclusion bodies containing the fusion protein were isolated and dissolved in denaturing buffer and then purified by Ni²⁺-affinity chromatography. The fusion protein was refolded by drop wise dilution into native buffer, the His₆-tag was removed using human α-thrombin and the protein was further purified by cation exchange chromatography. The CCR2 sulfopeptides **1** and **2** were prepared by solid-phase synthesis and purified as described (Taleski *et al*, *Chem. Asian J.* 2011 6, 1316-1320).

NMR Measurements. Samples for NMR spectroscopy (150 μL in Norell thick-walled 5 mm NMR tubes) contained 50 μM wild type MCP-1 alone or in the presence of 10, 20, 35, 50, 80 or 150 μM peptide (**1** or **2**) in NMR buffer (20 mM sodium acetate-d₄, 5% D₂O, 0.02% NaN₃, pH 7.0). NMR experiments were conducted at 25 °C on a Bruker Avance 600 MHz NMR spectrometer equipped with a triple-resonance cryoprobe. Chemical shifts were referenced to 4, 4-dimethyl-4-silapentane-1-sulfonic acid (DSS). For each sample a ¹⁵N-heteronuclear single quantum coherence (HSQC) spectrum was recorded using 48 and 1024 complex points and spectral widths of 24 and 12 ppm in ¹⁵N and ¹H dimensions, respectively, and 276 scans per FID (experiment time: 8hrs 45 min). The NMR data were processed using Bruker Topspin 3.0.

NMR Spectra Analysis. NMR spectra were analyzed using Sparky (T. D. Goddard and D. G. Kneller, University of California, San Francisco, CA). Weighted changes in NH chemical shift for resolved monomer and dimer peaks (*m* and *d*, respectively) were determined according to the formula: $\Delta\delta_{\text{NH}}$

= $|\Delta\delta_H| + 0.2|\Delta\delta_N|$. The standard errors in chemical shift measurements were estimated by analysis of peaks that did not shift monotonically with peptide concentration. Relative intensities of monomer and dimer peaks (r_{MD}) were calculated from the heights of corresponding monomer and dimer peaks; peak volumes could not be determined with sufficient precision or accuracy due to spectral noise and overlap. The standard errors in the peak heights were assumed to be equal to the standard deviation of the base plane noise level. Average values of m , d and r_{MD} (and their standard errors) were calculated for the five NH groups showing resolving monomer and dimer peaks at all concentrations of peptide used: K19, L25, I42, F43 and C52.

Data Fitting Procedures. Global fitting of the NMR data to the coupled thermodynamic model were performed using a home-written Perl script. Briefly, the script performs a series of increasingly focused grid searches to find values of K_{MD} , K_{ML} and K_{DL} in closest agreement with the observed m , d and r_{MD} values (each at several concentrations of ligand); typically K_{MD} was held constant at the value corresponding to the observed value of r_{MD} in the absence of ligand ($K_{MD} = 7.0 \mu\text{M}$). For each set of K_{MD} , K_{ML} and K_{DL} values, the simulation algorithm shown schematically in Figure S1 was used to simulate the values of m/m_{max} , d/d_{max} and r_{MD} at each ligand concentration used and then grid searches were used to determine the best fit values of m_{max} and d_{max} . The agreement between the resulting simulated values of m , d and r_{MD} and the corresponding experimental values was evaluated using the target function χ^2 , defined as:

$$\chi^2 = \sum_{L_t} \left[\left(\frac{m_{sim} - m_{expt}}{m_{expt}} \right)^2 + \left(\frac{d_{sim} - d_{expt}}{d_{expt}} \right)^2 + \left(\frac{r_{MD,sim} - r_{MD,expt}}{r_{MD,expt}} \right)^2 \right]$$

in which the subscripts “sim” and “expt” refer to simulated and experimentally determined values, respectively, and the sum extends over all values of total ligand concentration (L_t) used in the experiments. The precision of the resulting fitted values of K_{MD} , K_{ML} and K_{DL} was determined using Monte-Carlo (M-C) simulations. For each M-C simulation, input values of m , d and r_{MD} at each value of L_t were generated randomly accordingly to a Gaussian distribution defined by the average and

standard error of the measured parameter. The fitting procedure was then applied to obtain fitted values of the equilibrium constants. For each data set, 500 M-C simulations were performed, of which the best 95% (475, based on χ^2 values) were used to determine the final values and errors of equilibrium constants and cooperativity. Conventional fits of the *m* and *d* data were performed using the methods described previously (Tan *et al.*, *J. Biol. Chem.* 2012, 287(18), 14692).

Figure S1. ^{15}N -HSQC Chemical Shifts for Monomeric and Dimeric forms of Residue Cys-52 with peptides 1 and 2. A detailed region (Cys-52 NH resonances) of the ^{15}N -HSQC spectrum is shown for 50 μM MCP-1 alone (red) and in the presence of 20 μM (cyan), 50 μM (orange) and 150 μM (blue) of CCR2 sulfopeptides: (a) **1** and (b) **2**. For each peptide the ratio of monomer to dimer peak intensities (r_{MD}) increases over the titration course. For sulfopeptide **2**, all resonances were substantially weaker in the final titration point compared to the earlier points.

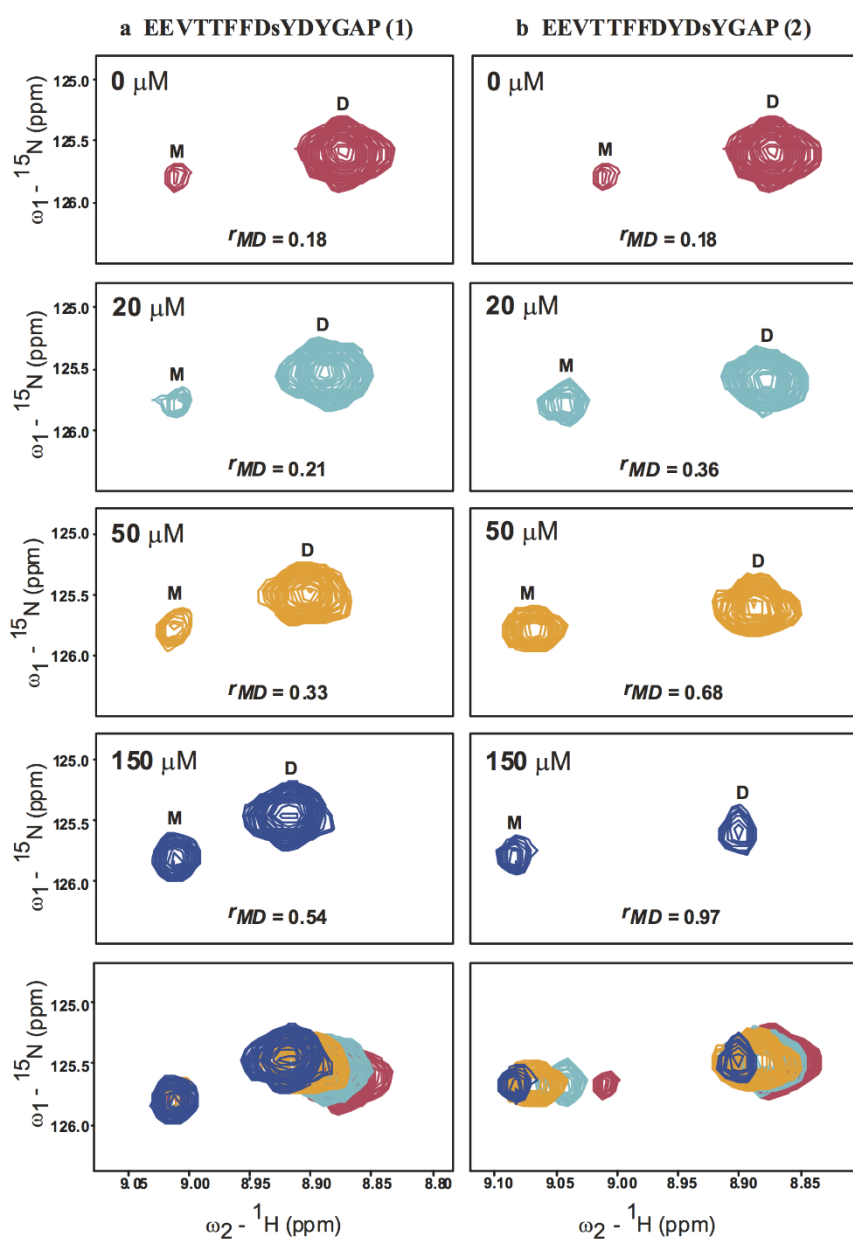


Figure S2. Algorithm for Simulation of Measurable Parameters from Equilibrium Constants in the Coupled Thermodynamic Model. Concentrations of species are adjusted iteratively until the calculated values of equilibrium constants (K_{MD} , K_{ML} , K_{DL} and K_{MDL}) are in close agreement with the input (target) values of equilibrium constants are represented as ($*K_{MD}$, $*K_{ML}$, $*K_{DL}$ and $*K_{MDL}$). Once this condition is satisfied, the species concentrations are used to calculate the values of m/m_{max} , d/d_{max} and r_{MD} .

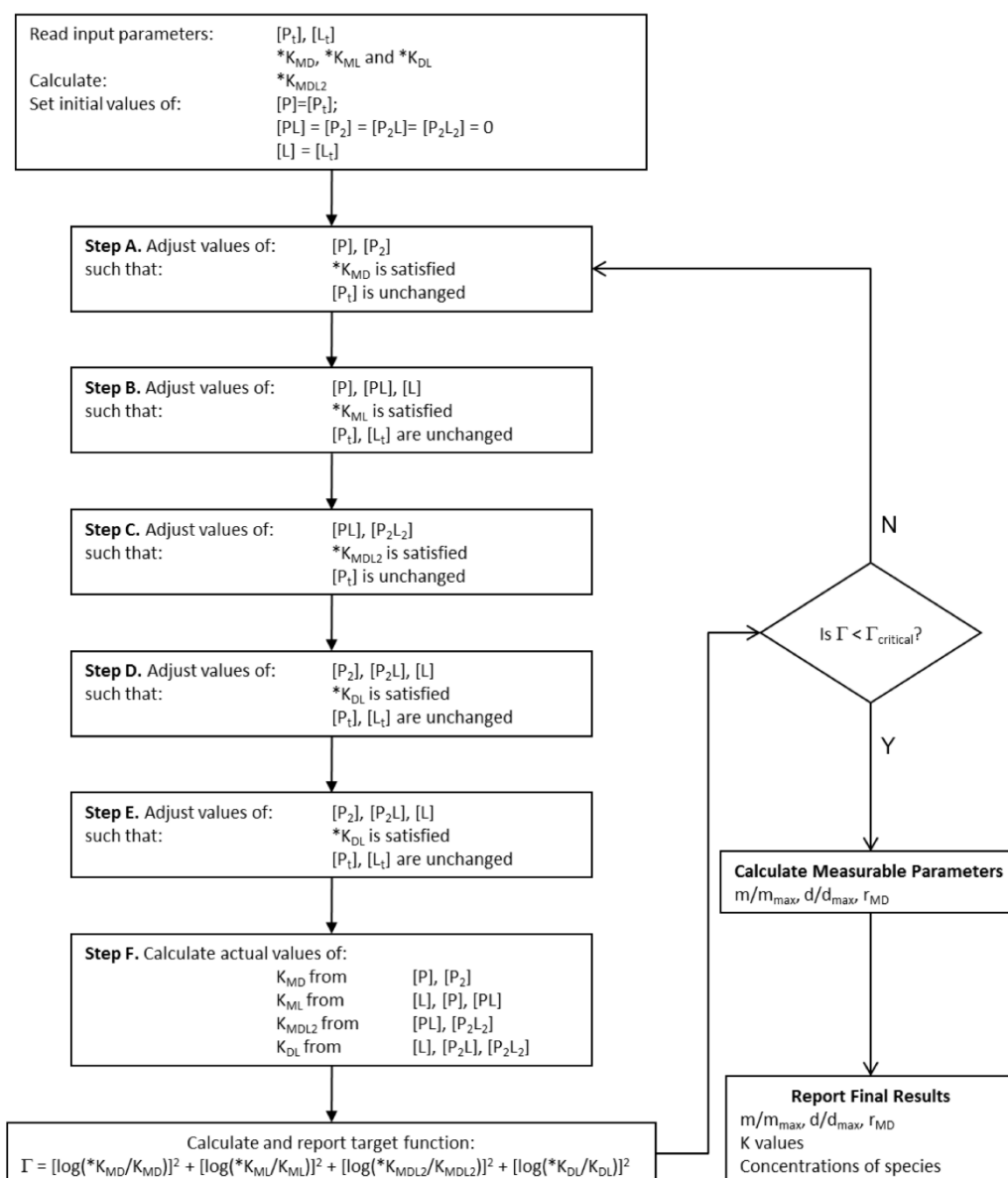
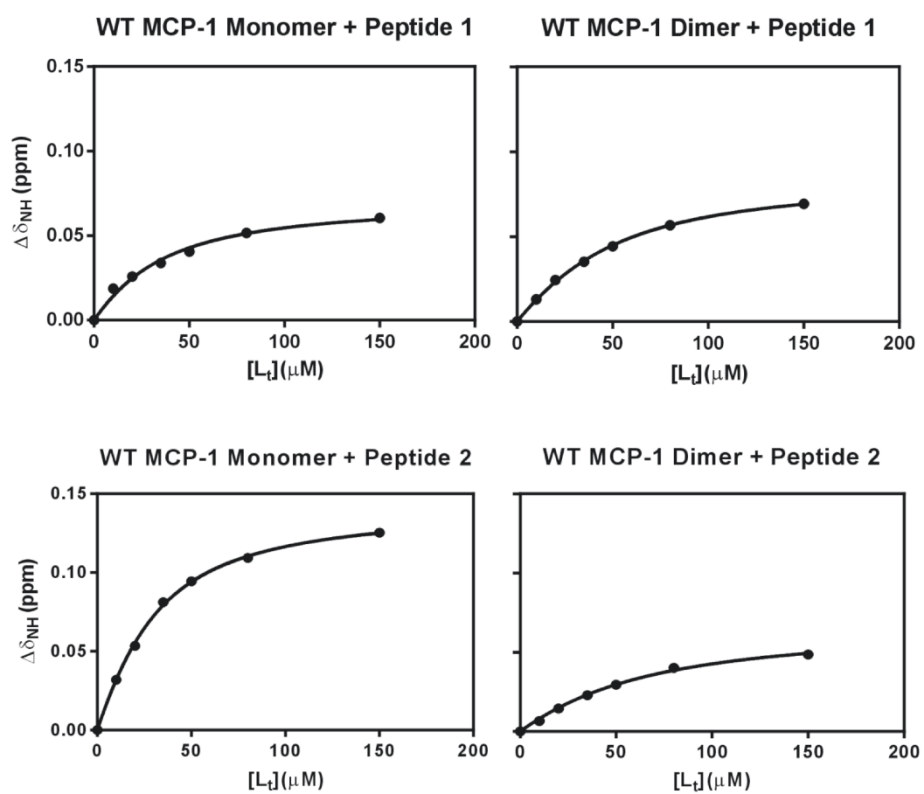


Figure S3. Results of Conventional Fits of WT MCP-1 Monomer and Dimer with Peptides 1 and 2.



Appendix III

Oligonucleotide Primers used for Chimeras and Mutants

A. Oligonucleotide list for all the chimeras

Oligo Label	Description	Oligo sequence
ZH-14-01A	Oligo for recursive PCR to synthesise genes encoding chimeras of MCP-1 and MCP-3 in an MCP-1 background. This oligo encodes: His6 tag, modified thrombin cleavage site (LVPR/QP) and MCP-1 N-terminus. Includes NcoI site (NcoI used for cloning into pET28a vector)	5'ACCGAGATACCATGGGAC ACCATCATCATCATCATCTG GTGCCGCGCCAGCCGGACGC AATCAACGCTGCAGTTAC 3'
ZH-14-01B	Oligo for recursive PCR to synthesise genes encoding chimeras of MCP-1 and MCP-3 in an MCP-1 background. This oligo encodes: His6 tag, modified thrombin cleavage site (LVPR/QP) and MCP-3 N-terminus. Includes NcoI site (NcoI used for cloning into pET28a vector)	5'ACCGAGATACCATGGGAC ACCATCATCATCATCATCTG GTGCCGCGCCAGCCGGTTGG CATCAATACCAGTACCACC 3'
ZH-14-02A	Oligo for recursive PCR to synthesise genes encoding chimeras of MCP-1 and MCP-3 in an MCP-1 background. This oligo includes: MCP-1 N-terminus and N-loop	5'CGGACGCAATCAACGCTGC AGTTACCTGCTGTTACAAC TCACTAACCGTAAAATCTCT GTCCAACGGCTGGCGTCCTA C 3'
ZH-14-02B	Oligo for recursive PCR to synthesise genes encoding chimeras of MCP-1 and MCP-3 in an MCP-1 background. This oligo includes: N-terminus of MCP-1 and chimeric N-loop of MCP-1/MCP-3	5'CGGACGCAATCAACGCTG CAGTTACCTGCTGTTACCGC TTTATTAACAAAAAATCCC GGTCCAACGGCTGGCGTCCT AC 3'
ZH-14-02C	Oligo for recursive PCR to synthesise genes encoding chimeras of MCP-1 and MCP-3 in an MCP-1 background. This Oligo includes: N-terminus of MCP-3 and N-loop of MCP-1	5'CGGTTGGCATCAATACCAG TACCACCTGCTGTTACAAC TCACTAACCGTAAAATCTCT GTCCAACGGCTGGCGTCCTA C 3'

Appendix III

ZH-14-02D	Oligo for recursive PCR to synthesise genes encoding chimeras of MCP-1 and MCP-3 in an MCP-1 background. This Oligo includes: N-terminus of MCP-3 and chimeric N-loop of MCP-1/MCP-3	5'CGGTTGGCATCAATACCAG TACCACCTGCTGTTACCGAT TTATTAACAAAAAATCCCG GTCCAACGGCTGGCGTCCTA C 3'
ZH-14-03	Oligo for recursive PCR to synthesise genes encoding chimeras of MCP-1 and MCP-3 in an MCP-1 background. This Oligo includes MCP-1 sequence.	5'GTCCAACGGCTGGCGTCCT ACCGGCGCATTACAAGTTCA AAATGCCCGAAGGAAGCGG TTATCTTC 3'
ZH-14-04A	Oligo for recursive PCR to synthesise genes encoding chimeras of MCP-1 and MCP-3 in an MCP-1 background. This Oligo includes MCP-1 sequence	5'CCCACTTCTGTTTCGGATC TGCGCAGATTTCTTTAGCCA CAATGGTTTTGAAGATAACC GCTTCCTTCGGGC 3'
ZH-14-04B	Oligo for recursive PCR to synthesise genes encoding chimeras of MCP-1 and MCP-3 in an MCP-1 background. This Oligo includes: MCP-1 sequence with chimeric MCP-1/MCP-3 β 2/ β 3 turn sequence	5'CCCACTTCTGTTTCGGATC TGCGCAGATTTCTTTGTCCA GAATGGTTTTGAAGATAACC GCTTCCTTCGGGC 3'
ZH-14-05	Oligo for recursive PCR to synthesise genes encoding chimeras of MCP-1 and MCP-3 in an MCP-1 background. This Oligo includes MCP-1 sequence	5' CTGGGTCTGTTTATCCAGGT GGTCCATTGAGTCCTGAACC CACTTCTGTTTCGGATCTGC GC 3'
ZH-14-06	Oligo for recursive PCR to synthesise genes encoding chimeras of MCP-1 and MCP-3 in an MCP-1 background. This Oligo includes: MCP-1 sequence, Includes XhoI site (XhoI used for cloning into pET28a vector)	5'GGTACCGGATCCCTCGAGT CATTAGGTTTTTCGGAGTCTG GGTCTGTTTATCCAGGTGGT CC 3'
ZH-14-07A	Oligo for recursive PCR to synthesise genes encoding chimeras of MCP-1 and MCP-3 in an MCP-3 background. This oligo encodes: His6 tag, modified thrombin cleavage site (LVPR/QP) and MCP-3 N-terminus. Includes NcoI site (NcoI used for cloning into pET28a vector)	5'ACCGAGATACCATGGGTC ACCACCATCATCACCATCTG GTTCCGCGTCAGCCGGTTGG CATTAATACCAGCACCACC 3'

ZH-14-07B	<p>Oligo for recursive PCR to synthesise genes encoding chimeras of MCP-1 and MCP-3 in an MCP-1 background. This oligo encodes: His6 tag, modified thrombin cleavage site (LVPR/QP) and MCP-1 N-terminus. Includes NcoI site (NcoI used for cloning into pET28a vector)</p>	<p>5'ACCGAGATACCATGGGAC ATCATCATCATCACCATCTG GTTCCGCGTCAGCCGGATGC TATCAACGCTGCAGTTACC 3'</p>
ZH-14-08A	<p>Oligo for recursive PCR to synthesise genes encoding chimeras of MCP-1 and MCP-3 in an MCP-3 background. This Oligo includes: MCP-3 N-terminus and N-loop</p>	<p>5'CGGTTGGCATTAAATACCAG CACCACCTGTTGTTATCGCT TTATTAACAAAAAATCCCG AACAGCGCCTGGAGAGCT ATCG 3'</p>
ZH-14-08B	<p>Oligo for recursive PCR to synthesise genes encoding chimeras of MCP-1 and MCP-3 in an MCP-3 background. This Oligo includes: N-terminus of MCP-3 and chimeric N-loop of MCP-3/MCP-1</p>	<p>5'CGGTTGGCATTAAATACCAG CACCACCTGTTGTTATAACT TACTAACCGTAAAATCTCT AACAGCGCCTGGAGAGCT ATCG 3'</p>
ZH-14-08C	<p>Oligo for recursive PCR to synthesise genes encoding chimeras of MCP-1 and MCP-3 in an MCP-3 background. This Oligo includes: N-terminus of MCP-1 and N-loop of MCP-3</p>	<p>5'CGGATGCTATCAACGCTGC AGTTACCTGTTGTTATCGCTT TATTAACAAAAAATCCCGA AACAGCGCCTGGAGAGCTAT CG 3'</p>
ZH-14-08D	<p>Oligo for recursive PCR to synthesise genes encoding chimeras of MCP-1 and MCP-3 in an MCP-1 background. This Oligo includes: N-terminus of MCP-1 and chimeric N-loop of MCP-3/MCP-1</p>	<p>5'CGGATGCTATCAACGCTGC AGTTACCTGTTGTTATAACT TACTAACCGTAAAATCTCT AACAGCGCCTGGAGAGCT ATCG 3'</p>
ZH-14-09	<p>Oligo for recursive PCR to synthesise genes encoding chimeras of MCP-1 and MCP-3 in an MCP-3 background. This Oligo includes MCP-3 sequence.</p>	<p>5'CAGCGCCTGGAGAGCTAT CGTCGTACCACCAGTAGCCA TTGTCCGCGTGAAGCAGTGA TCTTCAAAC 3'</p>
ZH-14-10A	<p>Oligo for recursive PCR to synthesise genes encoding chimeras of MCP-1 and MCP-3 in an MCP-3 background. This Oligo includes MCP-3 sequence</p>	<p>5'CCCATTTCTGTGTCGGATC TGCACAGATTTCTTGTCCA GTTTGGTTTTGAAGATCACT GCTTCACGCGG 3'</p>
ZH-14-10B	<p>Oligo for recursive PCR to synthesise genes encoding chimeras of MCP-1 and MCP-3 in an MCP-3 background. This Oligo includes: MCP-3 sequence with chimeric MCP-3/MCP-1 β2/β3 turn sequence</p>	<p>5'CCCATTTCTGTGTCGGATC TGCACAAATTTCTTAGCCA CTTTGGTTTTGAAGATCACT GCTTCACGCGG 3'</p>

Appendix III

ZH-14-11	Oligo for recursive PCR to synthesise genes encoding chimeras of MCP-1 and MCP-3 in an MCP-3 background. This Oligo includes MCP-3 sequence	5'CTGGGTCTTCTTGTCCAGG TGCTTCATAAAAATCCTGAAC CCATTTCTGTGTCGGATCTG CAC 3'
ZH-14-12	Oligo for recursive PCR to synthesise genes encoding chimeras of MCP-1 and MCP-3 in an MCP-3 background. This Oligo includes: MCP-3 sequence, Includes BamH1 site (BamH1 used for cloning into pET28a vector)	5' GGCCACTCGGGATCCTTATT ACAGTTTCGGGGTCTGGGTC TTCTTGTCCAGGTGCTTC 3'

B. Oligonucleotide list for all the receptor mutants

Oligonucleotide Label	Description	Oligonucleotide sequence
ZH-15-07	Oligo for the QC mutagenesis of CCR2 for K34A mutation	5' CAT AAA TTT GAC GTG GCG CAA ATT GGG GCC CAA CTC 3'
ZH-15-08	Oligo for the QC mutagenesis of CCR2 for K34A mutation	5' GAGTTGGGCCCAATTTGCGCCACGTCAA ATTTATG 3'
ZH-15-09	Oligo for the QC mutagenesis of CCR2 for Y120F mutation	5' GCAATGTGCAAATTATTCACAGGGCTGTT TCACATCGGTTATTTTGGC 3'
ZH-15-10	Oligo for the QC mutagenesis of CCR2 for Y120F mutation	5' GCCAAAATAACCGATGTGAAACAGCCCT GTGAATAATTTGCACATTGC 3'
ZH-15-13	Oligo for the QC mutagenesis of CCR2 for V187A/V189A mutation	5' CAGAAAGAAGATTCTGCTTATGCCTGTGG CCCTTATTTCCACGAGGATGG 3'
ZH-15-14	Oligo for the QC mutagenesis of CCR2 for V187A/V189A mutation	5' CCATCCTCGTGGAAAATAAGGGCCACAG GCATAAGCAGAATCTTCTTTCTG 3'

ZH-15-15	Oligo for the QC mutagenesis of CCR2 for N199A/T203A mutation	5' CCTTATTTTCCACGAGGATGGGCTAATTT CCACGCAATAATGAGGAACATTTTGGGG 3'
ZH-15-16	Oligo for the QC mutagenesis of CCR2 for N199A/T203A mutation	5' – CCCCAAAATGTTCCCTCATTATTGCGTGGA AATTAGCCCATCCTCGTGGAATAAAGG 3'
ZH-15-17	Oligo for the QC mutagenesis of CCR2 for R206A mutation	5' GGATGGAATAATTTCCACACAATAATGGC GAACATTTTGGGGCTGGGG 3'
ZH-15-18	Oligo for the QC mutagenesis of CCR2 for R206A mutation	5' CCCAGCCCCAAAATGTTCCGCCATTATTG TGTGGAAATTATTCATCC 3'
ZH-15-19	Oligo for the QC mutagenesis of CCR2 for Y259F mutation	5' CTCTTCTGGACTCCCTTTAATATTGTCATT CTC 3'
ZH-15-20	Oligo for the QC mutagenesis of CCR2 for Y259F mutation	5' GAGAATGACAATATTAAGGGAGTCCAG AAGAG 3'
ZH-15-21	Oligo for the QC mutagenesis of CCR2 for I263A/N266A mutation	5' CTCTTCTGGACTCCCTATAATATTGTCGCT CTCCTAGCCACCTTCCAGGAATTCTTCGG C 3'
ZH-15-22	Oligo for the QC mutagenesis of CCR2 for I263A/N266A mutation	5' GCCGAAGAATTCCTGGAAGGTGGCTAGG AGAGCGACAATATTATAGGGAGTCCAGA AGAG 3'
ZH-15-23	Oligo for the QC mutagenesis of CCR2 for E270A/F272A mutation	5' CTCCTGAACACCTTCCAAGCATTGCGCGG CCTGAGTAACTGTGAAAGCACC 3'
ZH-15-24	Oligo for the QC mutagenesis of CCR2 for E270A/F272A mutation	5' GGTGCTTTCACAGTTACTCAGGCCGGCAA ATGCTTGGAAGGTGTTTCAGGAG 3'

Appendix III

ZH-15-25	Oligo for the QC mutagenesis of CCR2 for D284A mutation	5' GAAAGCACCAGTCAACTAGCCCAAGCCA CGCAGGTG 3'
ZH-15-26	Oligo for the QC mutagenesis of CCR2 for D284A mutation	5' CACCTGCGTGGCTTGGGCTAGTTGACTGG TGCTTTC 3'
ZH-15-27	Oligo for the QC mutagenesis of CCR2 for E291A mutation	5' GCCACGCAGGTGACAGCTACTCTTGGGAT GACTCAC 3'
ZH-15-28	Oligo for the QC mutagenesis of CCR2 for E291A mutation	5' GTGAGTCATCCCAAGAGTAGCTGTCACCT GCGTGGC 3'

Appendix IV**Protein and nucleotide sequence of all chimeras**

The protein and the nucleotide sequences of all uncleaved chimeras are given below. The residues which have been mutated are underlined in both protein and nucleotide sequences of each chimera.

MCP1-311**MGHHHHHHLVPR**

**QPVGINTSTTCCYNFTNRKISVQRLASYRRITSSKCPKEAVIFKTIVAKEICADPKQKWVQDSMDH
LDKQTQTPKT**

ACCGAGATACCATGGGACACCATCATCATCATCATCTGGTGCCGCGCCAGCCGGTTGGCATCAATA
CCAGTACCACCTGCTGTTACAACTTCACTAACCGTAAAATCTCTGTCCAACGGCTGGCGTCCTACC
GGCGCATTACAAGTTCAAAATGCCCGAAGGAAGCGGTTATCTTCAAAACCATTGTGGCTAAAGAAA
TCTGCGCAGATCCGAAACAGAAGTGGGTTCAGACTCAATGGACCACCTGGATAAACAGACCCAGA
CTCCGAAAACCTAATGACTCGAGGGATCCGGTACC

MCP1-131**MGHHHHHHLVPR**

**QPDAINAAVTCCYRFINKKIPVQRLASYRRITSSKCPKEAVIFKTIVAKEICADPKQKWVQDSMDH
LDKQTQTPKT**

ACCGAGATACCATGGGACACCATCATCATCATCATCTGGTGCCGCGCCAGCCGGACGCAATCAACG
CTGCAGTTACCTGCTGTTACCGCTTTATTAACAAAAAAATCCCGGTCCAACGGCTGGCGTCCTACC
GGCGCATTACAAGTTCAAAATGCCCGAAGGAAGCGGTTATCTTCAAAACCATTGTGGCTAAAGAAA
TCTGCGCAGATCCGAAACAGAAGTGGGTTCAGACTCAATGGACCACCTGGATAAACAGACCCAGA
CTCCGAAAACCTAATGACTCGAGGGATCCGGTACC

MCP1-113**MGHHHHHHLVPR**

**QPDAINAAVTCCYNFTNRKISVQRLASYRRITSSKCPKEAVIFKTILDKEICADPKQKWVQDSMDH
LDKQTQTPKT**

ACCGAGATACCATGGGACACCATCATCATCATCATCTGGTGCCGCGCCAGCCGGACGCAATCAACG
CTGCAGTTACCTGCTGTTACAACTTCACTAACCGTAAAATCTCTGTCCAACGGCTGGCGTCCTACC
GGCGCATTACAAGTTCAAAATGCCCGAAGGAAGCGGTTATCTTCAAAACCATTCTGGACAAAGAAA
TCTGCGCAGATCCGAAACAGAAGTGGGTTCAGACTCAATGGACCACCTGGATAAACAGACCCAGA
CTCCGAAAACCTAATGACTCGAGGGATCCGGTACC

MCP1-133

MGHHHHHHLVPR

**QPDAINAAVTCCYRFINKKIPVQRLASYRRITSSKCPKEAVIFKTILDKEICADPKQKWVQDSMDH
LDKQTQTPKT**

ACCGAGATACCATGGGACACCATCATCATCATCATCTGGTGCCGCGCCAGCCGGACGCAATCAACG
CTGCAGTTACCTGCTGTTACCGCTTTATTAACAAAAAATCCCGGTCCAACGGCTGGCGTCTTACC
GGCGCATTACAAGTTCAAAATGCCCGAAGGAAGCGTTATCTTCAAACCATCTGGACAAAGAAA
TCTGCGCAGATCCGAAACAGAAGTGGGTTCAGGACTCAATGGACCACCTGGATAAACAGACCCAGA
CTCCGAAAACCTAATGACTCGAGGGATCCCGTACC

MCP1-333

MGHHHHHHLVPR

**QPVGINTSTTCCYRFINKKIPVQRLASYRRITSSKCPKEAVIFKTILDKEICADPKQKWVQDSMDH
LDKQTQTPKT**

ACCGAGATACCATGGGACACCATCATCATCATCATCTGGTGCCGCGCCAGCCGGTTGGCATCAATA
CCAGTACCACCTGCTGTTACCGATTTATTAACAAAAAATCCCGGTCCAACGGCTGGCGTCTTACC
GGCGCATTACAAGTTCAAAATGCCCGAAGGAAGCGTTATCTTCAAACCATCTGGACAAAGAAA
TCTGCGCAGATCCGAAACAGAAGTGGGTTCAGGACTCAATGGACCACCTGGATAAACAGACCCAGA
CTCCGAAAACCTAATGACTCGAGGGATCCCGTACC

MCP3-133

MGHHHHHHLVPR

**QPDAINAAVTCCYRFINKKIPKQRLASYRRITSSHCPREAVIFKTKLDKEICADPTQKWVQDFMKH
LDKKTQTPKL**

ACCGAGATACCATGGGACATCATCATCATCACCATCTGGTCCGCGTCAGCCGGATGCTATCAACG
CTGCAGTTACCTGTTGTTATCGCTTTATTAACAAAAAATCCCGAAACAGCGCCTGGAGAGCTATC
GTCGTACCACAGTAGCCATTGTCCGCGTGAAGCAGTGATCTTCAAACCAAACCTGGACAAGGAAA
TCTGTGCAGATCCGACACAGAAATGGGTTCAGGATTTTATGAAGCACCTGGACAAGAAGACCCAGA
CCCCGAAACTGTAATAAGGATCCCGAGTGCC

MCP3-313

MGHHHHHHLVPR

**QPVGINTSTTCCYNFTNRKISKQRLESYRRTTSSHCPREAVIFKTKLDKEICADPTQKWVQDFMKH
LDKKTQTPKL**

ACCGAGATACCATGGGTCACCACCATCATCACCATCTGGTTC CGCGTCAGCCGGTTGGCATT AATA
CCAGCACCACCTGTTGTTATAACTTTACTAACCGTAAAATCTCTAAACAGCGCCTGGAGAGCTATC
GTCGTACCACCAGTAGCCATTGTCCGCGTGAAGCAGTGATCTTCAAACCAAAGTGGACAAGGAAA
TCTGTGCAGATCCGACACAGAAATGGGTT CAGGATTTTATGAAGCACCTGGACAAGAAGACCCAGA
CCCCGAAACTGTAATAAGGATCCCGAGTGGCC

MCP3-331

MGHHHHHHLVPR

**QPVGINTSTTCCYRFINKKIPKQRLESYRRTTSSHCPREAVIFKTKVAKEICADPTQKWVQDFMKH
LDKKTQTPKL**

ACCGAGATACCATGGGTCACCACCATCATCACCATCTGGTTC CGCGTCAGCCGGTTGGCATT AATA
CCAGCACCACCTGTTGTTATCGCTTTATTAACAAAAAATCCCCGAAACAGCGCCTGGAGAGCTATC
GTCGTACCACCAGTAGCCATTGTCCGCGTGAAGCAGTGATCTTCAAACCAAAGTGGCTAAGGAAA
TTTGTGCAGATCCGACACAGAAATGGGTT CAGGATTTTATGAAGCACCTGGACAAGAAGACCCAGA
CCCCGAAACTGTAATAAGGATCCCGAGTGGCC

MCP3-311

MGHHHHHHLVPR

**QPVGINTSTTCCYNFTNRKISKQRLESYRRTTSSHCPREAVIFKTKVAKEICADPTQKWVQDFMKH
LDKKTQTPKL**

ACCGAGATACCATGGGTCACCACCATCATCACCATCTGGTTC CGCGTCAGCCGGTTGGCATT AATA
CCAGCACCACCTGTTGTTATAACTTTACTAACCGTAAAATCTCTAAACAGCGCCTGGAGAGCTATC
GTCGTACCACCAGTAGCCATTGTCCGCGTGAAGCAGTGATCTTCAAACCAAAGTGGCTAAGGAAA
TTTGTGCAGATCCGACACAGAAATGGGTT CAGGATTTTATGAAGCACCTGGACAAGAAGACCCAGA
CCCCGAAACTGTAATAAGGATCCCGAGTGGCC

MCP3-111

MGHHHHHHLVPR

**QPDAINAAVTCCYNFTNRKISKQRLESYRRTTSSHCPREAVIFKTKVAKEICADPTQKVVQDFMKH
LDKKTQTPKL**

ACCGAGATACCATGGGACATCATCATCACCATCTGGTTC CGCGTCAGCCGGATGCTATCAACG
CTGCAGTTACCTGTTGTTATAACTTTACTAACCGTAAAATCTCTAAACAGCGCCTGGAGAGCTATC
GTCGTACCACCAGTAGCCATTGTCCGCGTGAAGCAGTGATCTTCAAACCAAAGTGGCTAAGGAAA
TTTGTGCAGATCCGACACAGAAATGGGTT CAGGATTTTATGAAGCACCTGGACAAGAAGACCCAGA
CCCCGAAACTGTAATAAGGATCCCGAGTGGCC

Appendix V

SDS PAGE gels showing the two set of chimeras under the non-reducing conditions

